

*NISTIR 6737*

# **Analysis of Samples Removed from a Damaged Pipeline**

*Paul E. Stutzman*



**NIST**

**National Institute of Standards and Technology**  
Technology Administration, U.S. Department of Commerce

**NISTIR 6737**

---

---

**Analysis of Samples Removed from a Damaged Pipeline**

Paul E. Stutzman

Building and Fire Research Laboratory

April 2001



U.S. Department of Commerce  
*Donald L. Evans, Secretary*

National Institute of Standards and Technology  
*Karen H. Brown, Acting Director*

## Abstract

A section of a 40.6 cm diameter gasoline pipeline showed signs of mechanical gouging and had experienced a rupture in service. The gouges were partly filled with a partially indurated material of undetermined origin. A set of specimens adhered to a pipe, provided by National Safety Transportation Board (NTSB), were sampled for microstructure evaluation. The Building Materials Division of the National Institute of Standards and Technology was contacted by NTSB to assist in characterizing the material and to determine if it was a portland cement-based material. If the sampled materials were determined to be portland cement based, the study would further characterize the specimens to determine if they were related to concrete used in construction subsequent to the installation of the gasoline pipeline.

- The specimens removed from the pipe are not portland cement-based materials. They do not exhibit compositional or microstructural features typical of a portland cement paste, mortar, or concrete. The specimens appear to be comprised of soil containing sandy mono- and poly-mineralic grains, clay, and mica cemented by calcium carbonate that appears to be in the form of the mineral calcite. The calcite is irregularly distributed with some regions extensively filled and some containing only isolated masses. Iron-bearing mineral inclusions were common in the extensively cemented areas and appear to be either corrosion products from the pipe or secondary mineralization of pyrite, or a natural degradation product of pyrite, melanterite.
- The backfill material contains a well-graded sand and dense, uniform clay matrix. These features make this material unique from the others examined in this study. Two of the specimens (I and J) removed from the gouges contain some fragments that appear similar in texture and composition to the backfill material.
- The microstructure of two concrete samples extracted from nearby construction contains a portland cement paste comprised of phases that are typically found in hardened cement pastes in concrete. In addition, an entrained air-void system is present and is unique to this subset of specimens. The air void system is a network of bubbles ranging in size from about 1 mm to about 10  $\mu\text{m}$  that serves to protect the concrete from freeze-thaw cycling damage.

## TABLE OF CONTENTS

<b>1.0 INTRODUCTION</b>	<b>1</b>
<b>2.0 CONCRETE SPECIMENS</b>	<b>4</b>
<b>3.0 BACKFILL</b>	<b>11</b>
<b>4.0 SOIL E</b>	<b>16</b>
<b>5.0 SAMPLE F</b>	<b>19</b>
<b>6.0 SAMPLES H, I, AND J</b>	<b>26</b>
<b>7.0 SUMMARY</b>	<b>45</b>
<b>Appendix A. Imaging and X-ray Microanalysis of Selected Specimens Fill, I, and J</b>	<b>46</b>
Fill material	46
Specimens I and J	49

## List of Figures

- Figure 1. Pipe section showing the location of the gaping crack (G) and crack origin (O) after removal from the field. North and south ends are indicated by “N” and “S”, respectively. Pipe was cut in the field in the area indicated by arrows “Z” ..... 1
- Figure 2. Close-up photograph (left) of the north end of the pipe showing two exposed diagonal gouge marks. Specimen labeled “E” was removed from the gouge mark located at the upper left corner of the photograph..... 3
- Figure 3. Close-up photograph of three gouge marks between arrows “H”, “I” and “J”. Samples removed from these gouge marks were labeled with the same letter designation, respectively..... 3
- Figure 4. Low-magnification backscattered SEM image of the “Main Thrust Block” concrete sample. This exhibits a typical concrete microstructure with aggregate (A), hardened cement paste (CP), and the cross sections of air bubbles incorporated into the concrete microstructure for freeze-thaw resistance (AV). Field Width: 4.9 mm..... 6
- Figure 5. The hardened cement paste microstructure showing residual cement (C), calcium-silicate-hydrate (CSH), and porosity (P). Field Width: 144  $\mu\text{m}$ ..... 6
- Figure 6. Energy-dispersive X-ray spectra provides chemical analyses from a residual calcium aluminoferrite cement grain (upper) and calcium-silicate-hydrate (lower). The x in the image window denotes the location of the analyses..... 7
- Figure 7. OPL concrete sample showing a typical concrete microstructure with aggregate (A), hardened cement paste (CP), and air void system (AV). Field width: 4.9 mm..... 8
- Figure 8. Hardened cement paste showing residual cement (C), calcium-silicate-hydrate (CSH), calcium hydroxide (CH), secondary ettringite in the entrained air voids (AFT), and a fly ash grain (FA). Field Width: 144  $\mu\text{m}$ ..... 8
- Figure 9. X-ray powder diffraction pattern of hardened cement paste from the 'Main Thrust Block' shows a distinct set of peaks for calcium hydroxide (blue stick figures) and is typical for a cement paste. Other phases identified include quartz (green, most likely from the aggregate) and calcite (purple, a common carbonation product) and feldspar (dark red, most likely from the aggregate)..... 9
- Figure 10. Stereo microscope images of fresh-fracture surfaces of the backfill material with a field width of 7 mm for the upper and 1 mm for the lower image..... 12

Figure 11. Scanning electron microscope backscattered electron image of an epoxy-impregnated, polished cross section of the back fill with uniform sand grading. Field Width: 4.9 mm..... 13

Figure 12. Scanning electron microscope backscattered electron image of an epoxy-impregnated, polished cross section of the back fill exhibiting a uniform-textured matrix distinct from that of the portland cement concrete. Field Width: 144  $\mu\text{m}$ ..... 13

Figure 13. Energy-dispersive X-ray spectrum of the fill matrix showing strong silicon and aluminum and intermediate-intensity magnesium and iron peaks. XRD analysis suggests chlorite – an aluminum magnesium hydroxide silicate which may occur as both a clay mineral and as a more coarse-grained rock-forming mineral..... 14

Figure 14. X-ray powder diffraction patterns of the whole-sample (black) and fines (red) show it to be comprised primarily of quartz (Q), mica (M), and clays chlorite (C) and kaolinite (K) ..... 15

Figure 15. SEM image showing a polished cross section of soil microstructure is heterogeneous with irregularly-shaped air voids, poly-mineralic large and fine grains, and a fine-grained matrix. Field Width: 4.9 mm..... 16

Figure 16. E-soil specimen exhibits a heterogeneous matrix with the upper image field width of 475  $\mu\text{m}$ , and the lower 144  $\mu\text{m}$ . The platy grains showing apparently good basal cleavage are probably a mica, or micaceous mineral..... 17

Figure 17. X-ray powder diffraction pattern of soil shows the presence of quartz, calcite, clays chlorite (C) and kaolinite (K), and mica (M) ..... 18

Figure 18. Optical microscope image of sample F, with a 7 mm field (upper) and 1 mm field (lower) width image of F showing sandy, dark texture of the fragment surface.20

Figure 19. X-ray powder diffraction pattern of sample F shows the presence of quartz, calcite, and peaks that may be from either portlandite or melanterite, and iron sulfide hydroxide. The latter phase diffraction peaks coincide with peaks of portlandite making identification difficult. The calcite peaks are relatively stronger than with other patterns suggesting an increased abundance.....21

Figure 20. Expanded view of the specimen 'F' powder diffraction pattern shows that the relative intensities for portlandite at 2- $\theta$  positions 18.1°, 28.65°, and 34.1° do not agree with the powder diffraction reference in the database and no portlandite was observed in microscope examination. Bright regions identified as iron -bearing make the identification of melanterite a possibility.....22

Figure 21. Sample F grain showing two distinct textures typical of these fragments, a) a dense, light-shaded material and b) a darker more porous material. Field Width: 3.5 mm.....23

Figure 22. SEM/BE image of the dense, light-appearing material with bright inclusions. X-ray microanalysis indicates the light material to likely be a calcium carbonate (calcite) and the bright grains are high in iron, possibly a pipe corrosion product. Field Width: 500  $\mu\text{m}$ ..... 23

Figure 23. X-ray microanalysis of the dense material (upper spectra) indicates that it probably is calcite, with high calcium and relatively strong carbon peaks. The bright inclusions (lower spectra) show strong iron spectra.....24

Figure 24. Close up SEM image of the more porous region of specimen F shows the fine-grained texture. Spot X-ray microanalysis indicates the presence of aluminum, silicon, calcium, chlorine, magnesium, and iron. Field Width: 475  $\mu\text{m}$ .....25

Figure 25. Specimen H at 7 mm (upper) and 2 mm (lower) field width is a brown to yellow, sandy, friable material.....27

Figure 26. SEM images of specimen H with a 2.5 mm (upper) and 480  $\mu\text{m}$  (lower) field widths shows sand grains encased in a calcium carbonate cement. No portland cement microstructural features or residual portland cement was seen. The bright spots in the lower image are common and appear to be iron oxide or iron sulfide.....28

Figure 27. Spot X-ray microanalysis of dense matrix cementing product shows calcium, magnesium, and probably carbon, typical of a calcium carbonate while the bright grains strong sulfur and iron suggest the iron sulfide pyrite. None of these features or chemical spectra is similar to that of a portland cement hydration product or portland cement.29

Figure 28. Secondary electron image of the surface texture and spot x-ray microanalysis of the surface of a specimen of sample H show it is composed of calcium and carbon and is probably the calcite, as observed in the XRD and HCL tests. The gold and palladium peaks are from the conductive coating necessary for imaging insulating specimens..30

Figure 29. Sample H at 4.7 mm shows two typical textures, one of a calcium carbonate-cemented sandy material (a) and the other of a fine-grained rounded material that appears to be a shale (b).....30

Figure 30. X-ray powder diffraction pattern of specimen H (black), I (red), and J (blue) shows the similarity to each other with quartz, calcite, mica (M), and clays kaolinite (K) and chlorite (C).....31

Figure 31. Specimen I with 7 mm (upper) and 1 mm (lower) field width appear similar in coloration and texture to H.....32

Figure 32. Specimen I at 6 mm (upper) and 2.5 mm (lower) field width shows cementation of the sand grains with a calcium carbonate cement. No portland cement hydration products or residual cement were observed.....33

Figure 33. Specimen I at 3 mm (upper) and 490  $\mu\text{m}$  (lower) field width shows a more uniform sand size distribution but a heterogeneous distribution of porous sandy and calcium carbonate-cemented sandy regions.....34

Figure 34. Another specimen from sample location I at 6 mm (upper) and 475  $\mu\text{m}$  (lower) field width shows the heterogeneous phase distribution and microstructure distinctly different from that of the concretes.....35

Figure 35. Specimen J at 7 mm (upper) and 1 mm (lower) field widths appears similar to that of H and I.....36

Figure 36. Specimen J at 3 mm (upper) and 490  $\mu\text{m}$  (lower) field widths has a sandy, calcite-cemented microstructure. The dark region with bright inclusions appears to be a coating with pigment and perhaps is the black coating from the pipe.....37

Figure 37. Specimen J at 3 mm (upper) and 490  $\mu\text{m}$  (lower) field widths showing a wide range of sand sizes and heterogeneous distribution of the calcium carbonate cement. This fragment appears to be a soil.....38

Figure 38. Specimen J fragment exhibits a more uniform sand size and a matrix similar in texture to that of the fill material and also shows evidence of the heterogeneously-distributed calcium carbonate. Upper image 3 mm and lower image 490  $\mu\text{m}$  field width.....39

Figure 39. SEM image (upper, 150  $\mu\text{m}$  field width) shows a uniformity and texture of the matrix similar to that of the backfill. Spot EDS spectra from specimen J (left image, red spectra), and backfill (right image, blue spectra) appear similar as well.....40

Figure 40. Specimen J fragment II showing a microstructure similar to that of the backfill material. Uniform sand size and matrix appear similar to the backfill. Upper image 5 mm and lower image 2.5 mm field widths.....41

Figure 41. Fragment III of specimen J showing microstructure similar to that of the backfill material with a uniform-textured matrix. Upper image 490  $\mu\text{m}$  and lower image 150  $\mu\text{m}$  field widths.....42

Figure 42. Specimen J exhibiting a microstructure similar to that of the backfill and also a band of secondary calcium carbonate around part of its perimeter and irregularly distributed within the fragment matrix. Upper image 5 mm and lower image 2.5 mm field widths.....43

Figure 43. High-magnification SEM images of specimen J showing the calcite cement around the edge and the uniform-textured matrix. This texture is similar to that of the backfill material. Upper image 490  $\mu\text{m}$  and lower image 150  $\mu\text{m}$  field widths.....44



Figure 44. Four separate, arbitrarily-selected fields of the backfill microstructure at 1.2 mm field width each show the uniformity of the sand and matrix.....46

Figure 45. Higher magnification images of the matrix show the uniform-texture and the cracking both features that serve to distinguish the fill from the soil specimens. ....47

Figure 46. Spot X-ray microanalysis of the matrix indicates a magnesium - aluminum - silicate composition with minor iron, calcium, sodium, and potassium. A set of three spectra provided the following peak intensities that will be used for comparison. The ratio of the magnesium and aluminum peaks to silicon were about 0.10 and 0.57, respectively. The values of the replicate spectra were Mg : 0.11,0 .09,0 .11 and Al: 0.57, 0.56, and 0.59.....48

Figure 47. Fragments from specimen I in images appear consistent with the soil.....49

Figure 48. Additional fragments from specimen I appear consistent with the soil. Image field width: 1.2 mm.....50

Figure 49. Fragment 15 of Specimen I appears consistent with the backfill. Part of the fragment (images A, B, C, and F) exhibits the same matrix homogeneity and cracking, as well as the chemical signature that is consistent with that of the backfill. There does appear to be some calcite cement, similar to that found in the soils. Images D and E from the other side of the fragment have more porous regions that appear consistent with the soil.....51

Figure 50. Comparison of the x-ray microanalysis spectra of I-15 matrix (blue) to that of the backfill material matrix (red) illustrates the similarity in composition.....52

Figure 51. Specimen J fragments 1 - 4 appear to be consistent with the soil as they have a porous matrix and calcite cement.....53

Figure 52. Specimen J fragment 7 appears similar to that of the backfill but the matrix texture and chemical composition are different.....54

Figure 53. Specimen J, fragment 9 is consistent with the backfill with respect to matrix texture and spot X-ray microanalysis composition.....55

Figure 54. Image texture and spot X-ray microanalysis of the matrix material from specimen J (blue) plotted against that from the backfill material matrix (red). Fragment 7 matrix (A) is not consistent, while fragment 9 (B) appears consistent with the backfill material with respect to texture and chemical composition.....56

## 1.0 Introduction

A section of a 40.6 cm (16 in) diameter gasoline pipeline showed signs of mechanical gouging and had experienced a rupture in service (Figs. 1-3). The gouges were partly filled with a partially indurated material of undetermined origin. The National Safety Transportation Board (NTSB) provided a set of specimens that were adhered to a pipe for microstructure evaluation. NTSB staff contacted the Building Materials Division of the National Institute of Standards and Technology to assist in characterizing the material and to determine if it was a portland cement-based material. If these materials were determined to be portland cement based, they would be characterized to see if they were related to concrete used in any construction subsequent to the installation of the gasoline pipeline.

The following specimens were provided by NTSB personnel for analysis:

- A sample of an imported backfill that surrounded a 183 cm (72 in) diameter water main line that crossed above the gasoline pipeline south of the rupture.
- A sample of concrete labeled “24-inch Main Thrust Block” that was removed from a thrust block poured on the 61 cm (24 in) water line tee installed near the rupture.
- A second sample of concrete labeled “OPL Over Pour” that was removed from a chunk of concrete found above the rupture.
- Materials found within and bonded to the gouges in the pipe, labeled “F”, “H”, “I”, and “J”, and a soil sample labeled “E”. The letter designation for these samples corresponds to the letter designation of the gouge marks in the pipe. The identification marks were established in NTSB Materials Laboratory Factual Report No 00-157.

A series of optical and scanning electron microscope images, supplemented by chemical information using X-ray microanalysis, and X-ray powder diffraction, are presented to illustrate the specimens. These instrumental methods are complementary in petrographic studies with the X-ray powder diffraction providing a direct means for phase analysis and microscopy a direct means for textural examination. Together, these methods can be used to characterize, identify, and compare materials. The microstructure of the two concrete specimens are presented first to illustrate their unique microstructural features. The backfill material is presented next, followed by the soil sample, and finally specimens removed from the gouges.

The following conclusions were made after the laboratory examination:

1. The specimens removed from the pipe are not portland cement-based materials. They do not exhibit compositional or microstructural features typical of a portland cement paste, mortar, or concrete.
2. The specimens removed from the pipe appear to be comprised of soil containing sandy mono- and poly-mineralic grains, clay, and mica cemented

by calcium carbonate that appears to be in the form of the mineral calcite. This form of cementation appears to be natural resulting from the precipitation of calcium carbonate. The calcite is irregularly distributed with some regions extensively filled and some containing only isolated masses. Iron-bearing minerals were common in the extensively cemented areas and appear to be either corrosion products from the pipe, the naturally occurring mineral pyrite or melanterite, possibly a natural product of pyrite decomposition.

3. Specimens I and J contain some fragments that appear similar to the backfill.
4. The backfill material contains a well-graded sand and dense, uniform clay matrix. These features make this specimen unique from the others examined in this study,
5. The microstructure of the concrete samples contains a portland cement paste comprised of calcium-silicate-hydrate gel, calcium hydroxide, ettringite, and residual cement grains comprised primarily of calcium aluminoferrite, or  $\text{Ca}_2(\text{Fe,Al})_2\text{O}_5$ . These phases are typically found in concrete pastes and serve as indicators of the presence of a portland cement-based material. In addition, an entrained air-void system is present and is unique to this subset of specimens. The air void system is a mass of bubbles ranging in size from about 1 mm to about 10  $\mu\text{m}$  that serves to protect the concrete from freeze-thaw cycling damage and improve the flow properties of the plastic concrete. None of these microstructural features were observed in any of the other specimens.



Figure 1. Pipe section showing the location of the gaping crack (G) and crack origin (O) after removal from the field. North and south ends are indicated by “N” and “S”, respectively. Pipe was cut in the field in the area indicated by arrows “Z”.



Figure 2. Close-up photograph (left) of the north end of the pipe showing two exposed diagonal gouge marks. Specimen labeled “E” was removed from the gouge mark located at the upper left corner of the photograph.



Figure 3. Close-up photograph of three gouge marks between arrows “H”, “I” and “J”. Samples removed from these gouge marks were labeled with the same letter designation, respectively.

Portland cement concrete is a composite material comprised of hardened cement paste, residual cement, sand, and coarse aggregate. Portland cement is made by firing a finely-ground mixture of shale, limestone, and waste materials in a kiln to temperatures of about 1500 °C. The resulting product is cooled and then ground with about 5 % gypsum to produce portland cement. Portland cement contains phases: alite ( $\text{Ca}_3\text{SiO}_5$ ), belite ( $\text{Ca}_2\text{SiO}_4$ ), aluminate ( $\text{Ca}_3\text{Al}_2\text{O}_6$ ), ferrite ( $\text{Ca}_4(\text{Al},\text{F})_2\text{O}_5$ ), periclase ( $\text{MgO}$ ), and gypsum ( $\text{Ca}_2\text{SO}_4 \cdot 2\text{H}_2\text{O}$ ) and is the cementing agent in portland cement concrete[1]. The process of setting, or hardening, is brought about by a series of complex chemical reactions between the water and cement after mixing known as hydration.

Concrete is an important building material because of its relatively low cost, ease of placement, and resistance to most environmental conditions. For most concretes, the identification of residual cement grains and a hydration product known as portlandite, or calcium hydroxide ( $\text{Ca}(\text{OH})_2$ ) are diagnostic of the material containing a portland cement. These materials may be identified using X-ray powder diffraction and scanning electron microscopy. An entrained air void system comprised of air bubbles sized from 5  $\mu\text{m}$  to 1200  $\mu\text{m}$ , and ideally spaced about 0.2 mm apart within the paste, is often incorporated into concrete expected to encounter freezing and thawing conditions, and often for facilitating concrete flow and consolidation. This entrained air void system is a distinct feature in portland cement concrete and, while not sufficient in itself, is helpful in identifying a material as a portland cement concrete.

## 2.0 Concrete Specimens

The scanning electron microscope (SEM) provides images of the specimen microstructure. The SEM scans a focused beam of electrons across the specimen and measures any of several signals resulting from the electron beam interaction with the specimen. The advantages lie in its ability to provide detailed images of microstructure, to perform chemical analyses and image element distribution, and in image processing and analysis.

Secondary electrons (SE) are low energy electrons used to image topographic features on fracture surfaces. Backscattered electrons (BE) are high-energy beam electrons scattered by the specimen. BE imaging of polished surfaces is most useful for observing phase distribution. Image contrast is generated by different phases' compositions relative to their average atomic number ( $Z$ ). Chemical analysis capabilities may be used to carry out spot analyses for phase identification. Additionally, X-ray imaging and image processing may be employed to represent spatial distribution of selected elements and phases.

For BE imaging, an epoxy-impregnated polished surface is necessary [2]. The epoxy impregnation maintains the integrity of the microstructure during processing and also fills the voids with a low atomic number ( $Z$ ) material, facilitating the BE imaging of voids and cracks. The epoxy was cured at 60 °C for 20 h after which a sample was demolded, labeled, ground to expose a fresh surface, and polished to 0.25  $\mu\text{m}$  with diamond pastes. Each specimen was then cleaned using a dry lint-free cotton cloth and compressed air, and then a thin (100 nm) layer of carbon was evaporated on to the surface to provide a conductive path to dissipate excess beam charge. All specimens were stored in vacuum dessiccators.

Scanning electron microscope images of the Main Thrust Block and OPL concrete specimens along with spot chemical analyses for the hardened cement paste from the Main Thrust Block specimen are presented in Figs. 4 through 8. In Figs. 4 and 7, the overall composition and texture of the specimen is typical for a concrete where coarse and fine aggregate are cemented by a thin matrix of hardened portland cement paste. The dark circular objects within the cement paste are the entrained air voids and are a unique element found in both concrete samples, but in no other sample presented for study.

Higher-magnification images of the hardened cement paste in Figs. 5 and 8 show the hardened paste hydration products, calcium-silicate-hydrate and calcium hydroxide as well as the residual cement grains comprised primarily of calcium aluminoferrite. The ferrite phase exhibits a lower hydraulic reactivity and residual grains are often found in older concrete samples. The calcium-silicate-hydrate (C-S-H) products form the bulk of the hardened cement paste. C-S-H occurs into two forms, an inner-product considered to be formed in situ and often exhibiting the outline of the cement grain, and an outer-product C-S-H that was formed in the originally water-filled void space and exhibits a more heterogeneous, higher coarse-porosity. Calcium hydroxide can occur as either plates (cross-sections of the crystals) or as a massive (without form) and is slightly brighter than the C-S-H yet less bright than the ferrite.

Phase identification of cement hydration products was obtained using X-ray powder diffraction analysis. A paste concentrate was obtained by gently dis-aggregating the concrete and sieving through a 100  $\mu\text{m}$  screen. This minimizes the presence of aggregate and its diluting effect on the paste hydration products, calcium hydroxide. In some cases the diffraction pattern of residual ferrite may be detected. In this case, only that from calcium hydroxide was clearly discernable from the background and is shown in Fig. 9 denoted by blue stick figures. Other phases present include quartz and possibly feldspar, likely from the aggregates, and calcite, which may be a product of the carbonation of calcium hydroxide and of C-S-H.

The spot X-ray analyses presented in Fig. 6 show typical spectra of the ferrite phase and C-S-H. For the ferrite phase, the principal components are calcium, aluminum, and iron with minor amounts of silicon and magnesium. For C-S-H, calcium and silicon with minor sulfur and magnesium are typical. Fig. 6 shows the X-ray powder diffraction pattern of hardened cement paste from the Main Thrust Block concrete sample. X-ray powder diffraction patterns for Main Thrust Block and OPL were similar. These spectra will serve for comparison with features in the remaining specimens.

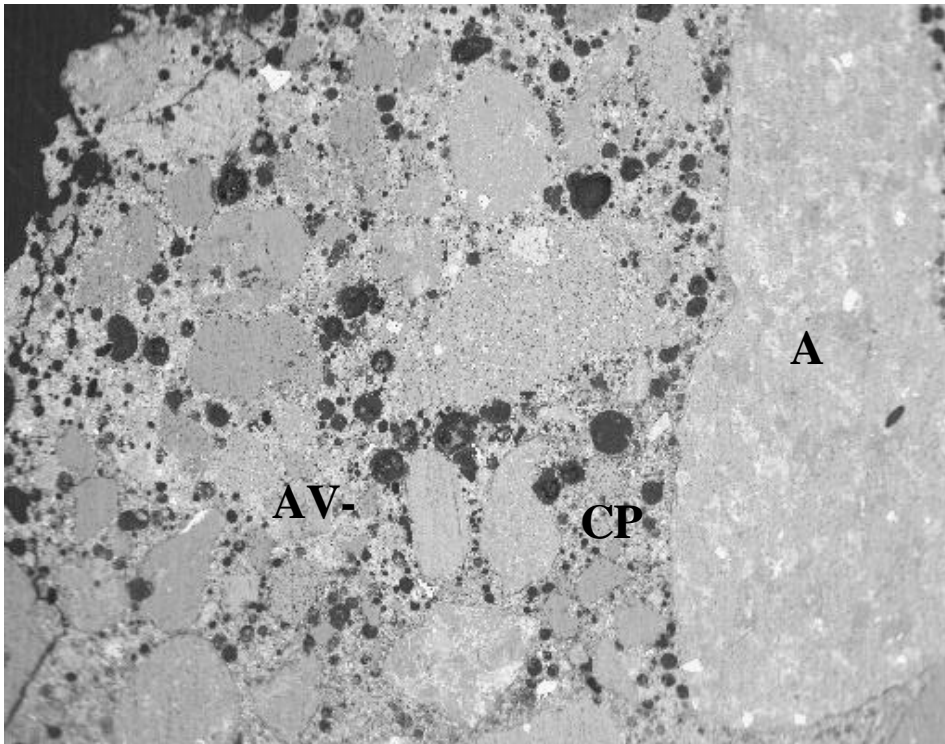


Figure 4. Low-magnification backscattered SEM image of the “Main Thrust Block” concrete sample. This exhibits a typical concrete microstructure with aggregate (A), hardened cement paste (CP), and the cross sections of air bubbles incorporated into the concrete microstructure for freeze-thaw resistance (AV). Field Width: 4.9 mm

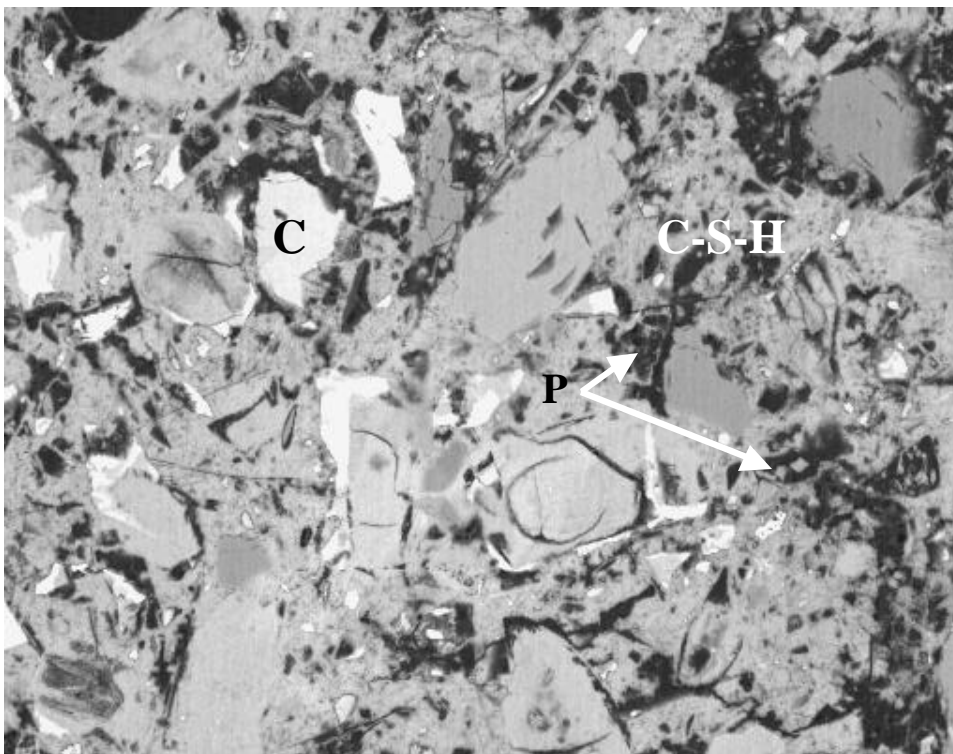


Figure 5. The hardened cement paste microstructure showing residual cement (C), calcium-silicate-hydrate (CSH), and porosity (P). Field Width: 144  $\mu$ m

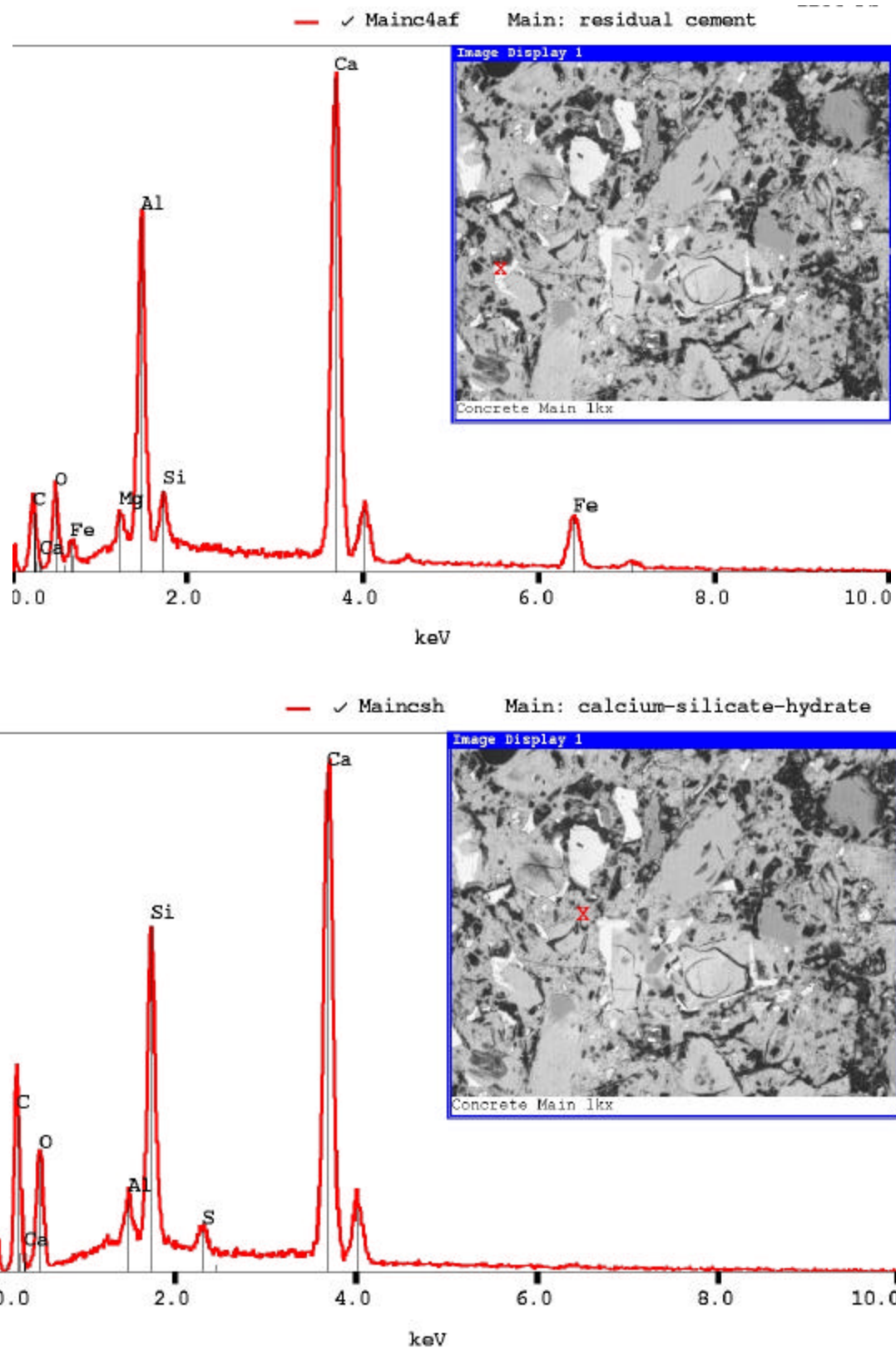


Figure 6. Energy-dispersive X-ray spectra provides chemical analyses from a residual calcium aluminoferrite cement grain (upper) and calcium-silicate-hydrate (lower). The x in the image window denotes the location of the analyses.



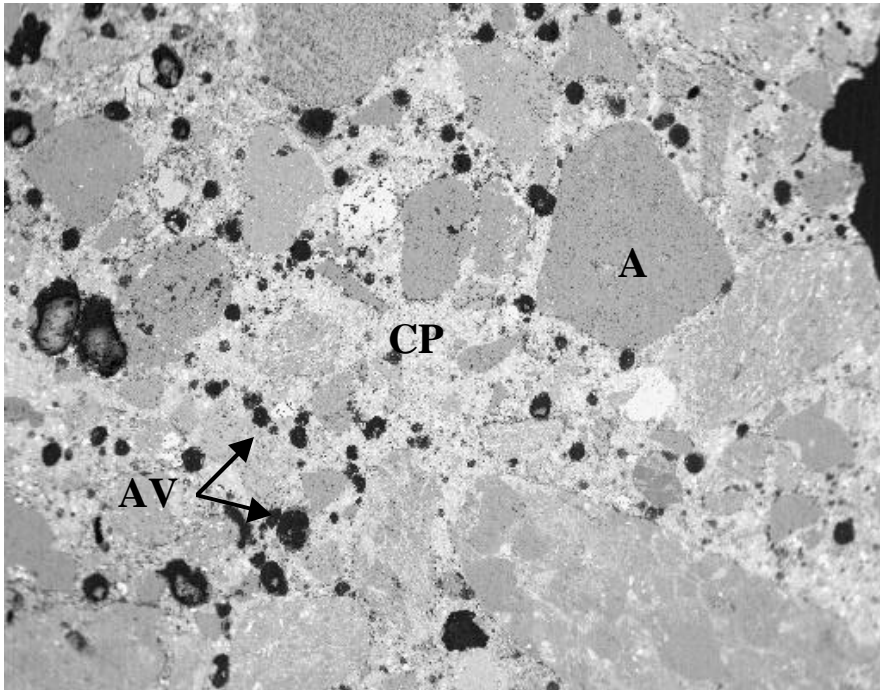


Figure 7. OPL concrete showing a typical concrete microstructure with aggregate (A), hardened cement paste (CP), and air void system (AV). Field width: 4.9 mm.

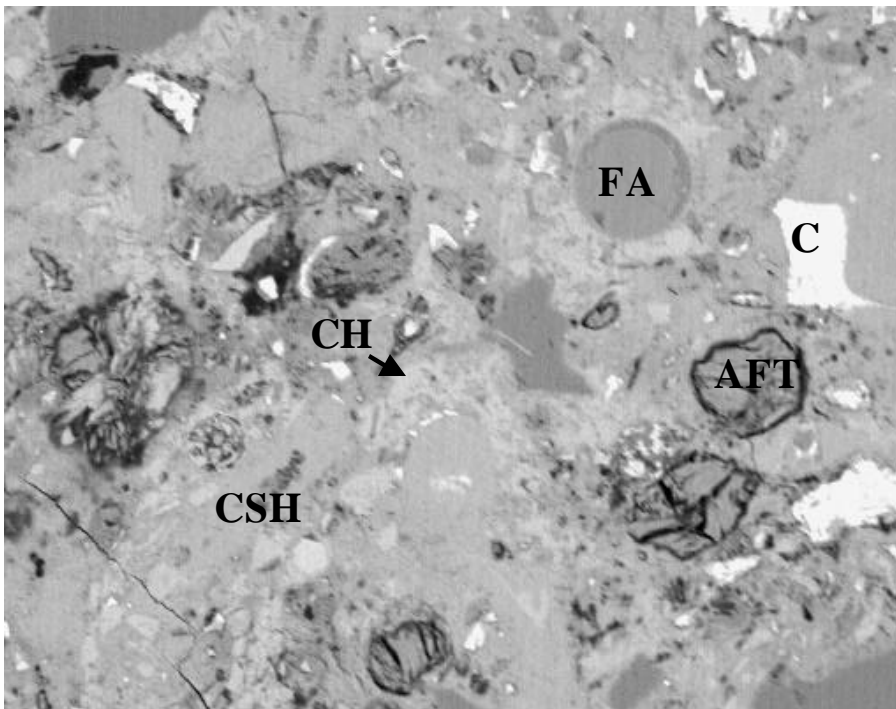
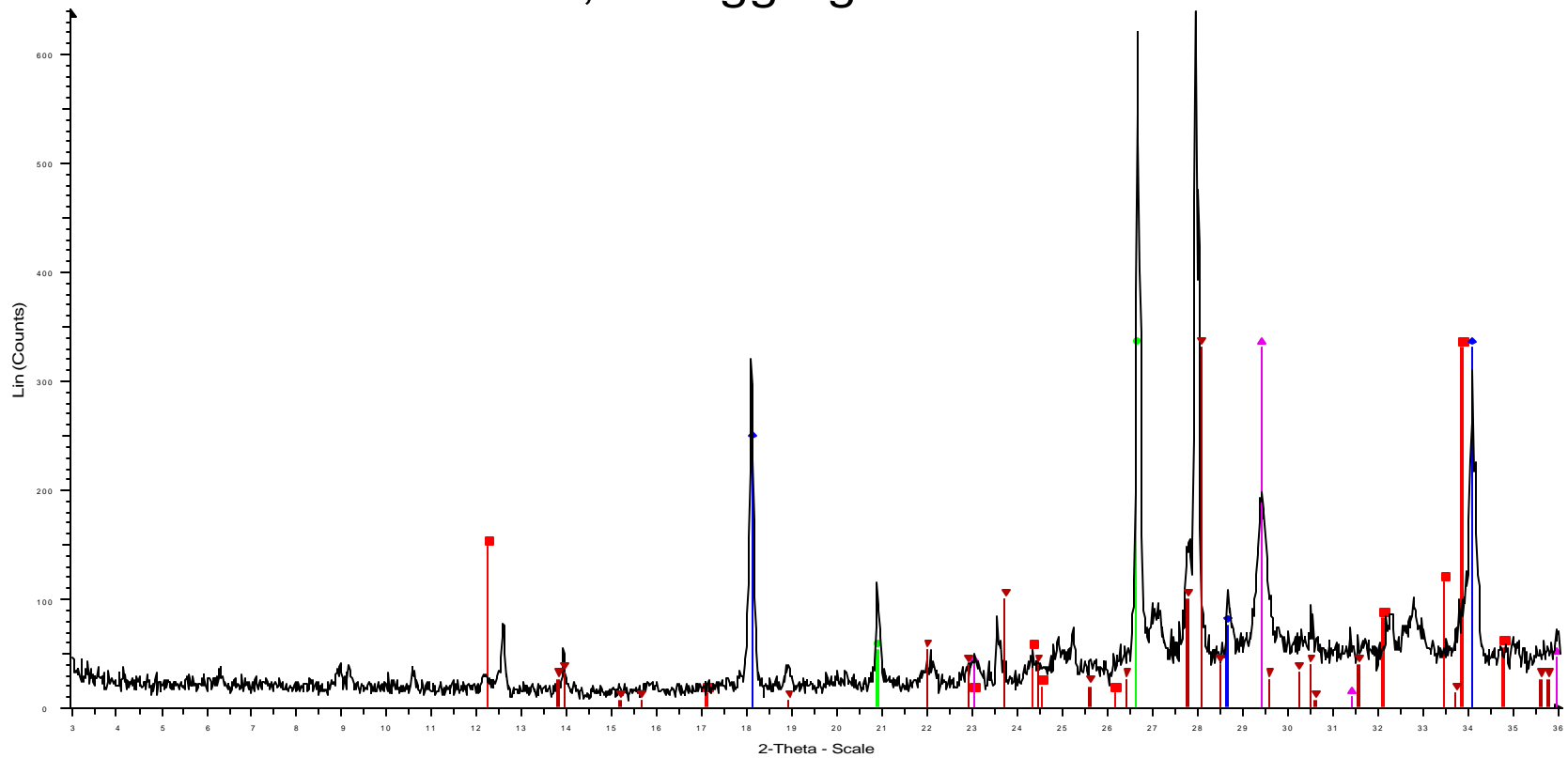


Figure 8. Hardened cement paste showing residual cement (C), calcium-silicate-hydrate (CSH), calcium hydroxide (CH), secondary ettringite in the entrained air voids (AFT), and a fly ash grain (FA). Field Width: 144  $\mu\text{m}$

# -125 Mesh, Disaggregated Main Paste



-125 Mesh, Disaggregated Main Paste - File: mainpaste.RAW - Type: 2Th/Th locked - Start: 2.973 ° - End: 37.974 ° - Step: 0.020 ° - Step time: 2. s - Temp.: 25 °C (Room) - Time Started: 0 s - 2-Theta: 2.973 ° - T  
 Operations: Displacement 0.052 | Displacement 0.104 | Import  
 30-0226 (\*) - Brownmillerite, syn -  $\text{Ca}_2(\text{Al,Fe})_2\text{O}_5$  - Y: 50.30 % - d x by: 1. - WL: 1.5406 - Orthorhombic - a 5.5672 - b 14.521 - c 5.349 - alpha 90.000 - beta 90.000 - gamma 90.000 - Primitive - Pcrn (62) - 4 - 4  
 04-0733 (l) - Portlandite, syn -  $\text{Ca}(\text{OH})_2$  - Y: 50.30 % - d x by: 1. - WL: 1.5406 - Hexagonal - a 3.593 - b 3.59300 - c 4.909 - alpha 90.000 - beta 90.000 - gamma 120.000 - Primitive - P-3m1 (164) - 1 - 54.8830 - l/  
 46-1045 (\*) - Quartz, syn -  $\text{SiO}_2$  - Y: 50.30 % - d x by: 1. - WL: 1.5406 - Hexagonal - a 4.91344 - b 4.91344 - c 5.40524 - alpha 90.000 - beta 90.000 - gamma 120.000 - Primitive - P3221 (154) - 3 - 113.010 - l/c  
 05-0586 (\*) - Calcite, syn -  $\text{CaCO}_3$  - Y: 50.30 % - d x by: 1. - WL: 1.5406 - Hexagonal (Rh) - a 4.989 - b 4.98900 - c 17.062 - alpha 90.000 - beta 90.000 - gamma 120.000 - Primitive - R-3c (167) - 6 - 367.780 - l/  
 10-0393 (\*) - Albite, disordered -  $\text{Na}(\text{Si}_3\text{Al})\text{O}_8$  - Y: 50.30 % - d x by: 1. - WL: 1.5406 - Triclinic - a 8.165 - b 12.872 - c 7.111 - alpha 93.45 - beta 116.4 - gamma 90.28 - Base-centred - C-1 (0) - 4 - 667.792 -

Figure 9. X-ray powder diffraction pattern of hardened cement paste from the 'Main Thrust Block' shows a distinct set of peaks for calcium hydroxide (blue stick figures) and is typical for a cement paste. Other phases identified include quartz (green, most likely from the aggregate) and calcite (purple, a common carbonation product) and feldspar (dark red, most likely from the aggregate).

### 3.0 Backfill

The backfill sample is dark, friable sand (Fig. 10) and was collected to serve as a reference for comparison with the gouge-fill materials.

SEM images of the backfill at low (Fig. 11) and high (Fig. 12) magnification illustrates the very uniform sand size and the interstitial voids filled almost completely with the clay. The uniform sand-size gradation and a matrix of dense clay are features unique to this specimen. X-ray microanalysis of the matrix (Fig. 13) indicates the presence of silicon, aluminum, magnesium and only minor amounts of iron, titanium, and calcium, based upon the peak heights and is distinctly different from that of hardened cement paste. X-ray powder diffraction analysis (Fig. 14) of the bulk (whole-sample) and fines after disaggregation and removal of the coarse sand indicate a phase composition of quartz and feldspar and clays composed of chlorite (aluminum magnesium silicate hydroxide) and possibly kaolinite (alumino-silicate). Additional images of the fill are provided in Appendix A.

SEM examination of the microstructure showed no evidence of any hydration products or residual cement that are characteristic of a portland cement concrete. Compared to the hardened cement paste matrix of the Main Thrust Block and OPL specimens, the backfill matrix is dense, very uniform, and exhibits what appear to be shrinkage cracks. Contact of the specimen with a dilute hydrochloric acid (approx. 10 %, by volume) resulted in no effervescence, a general field test for the presence of carbonate minerals.

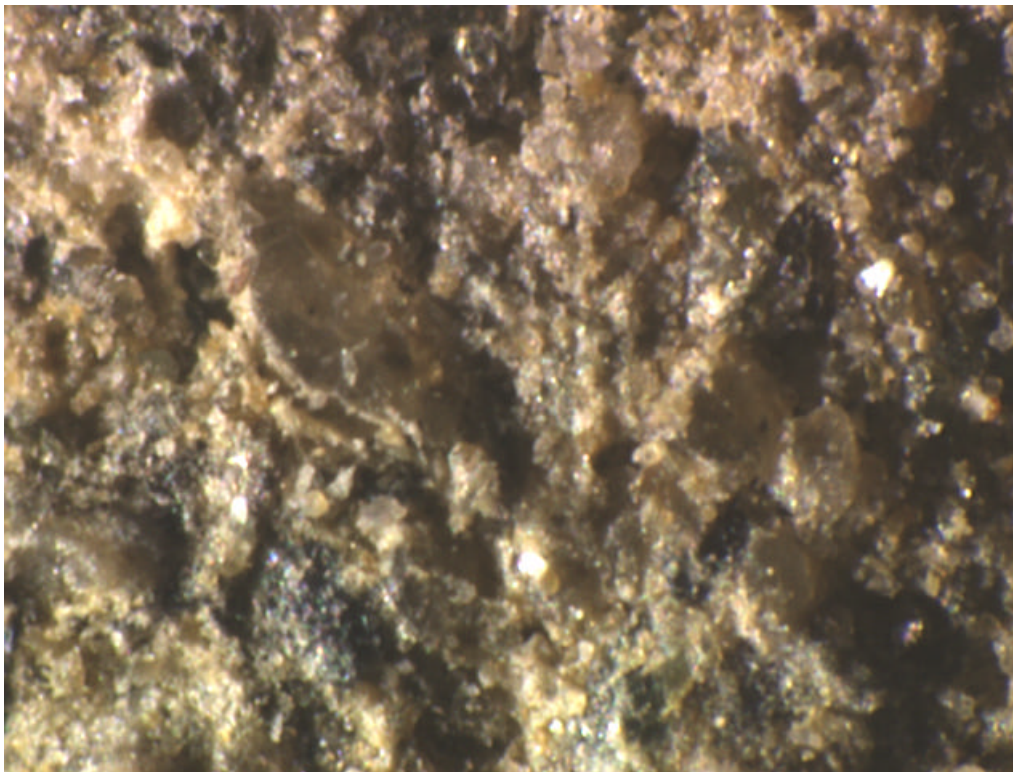
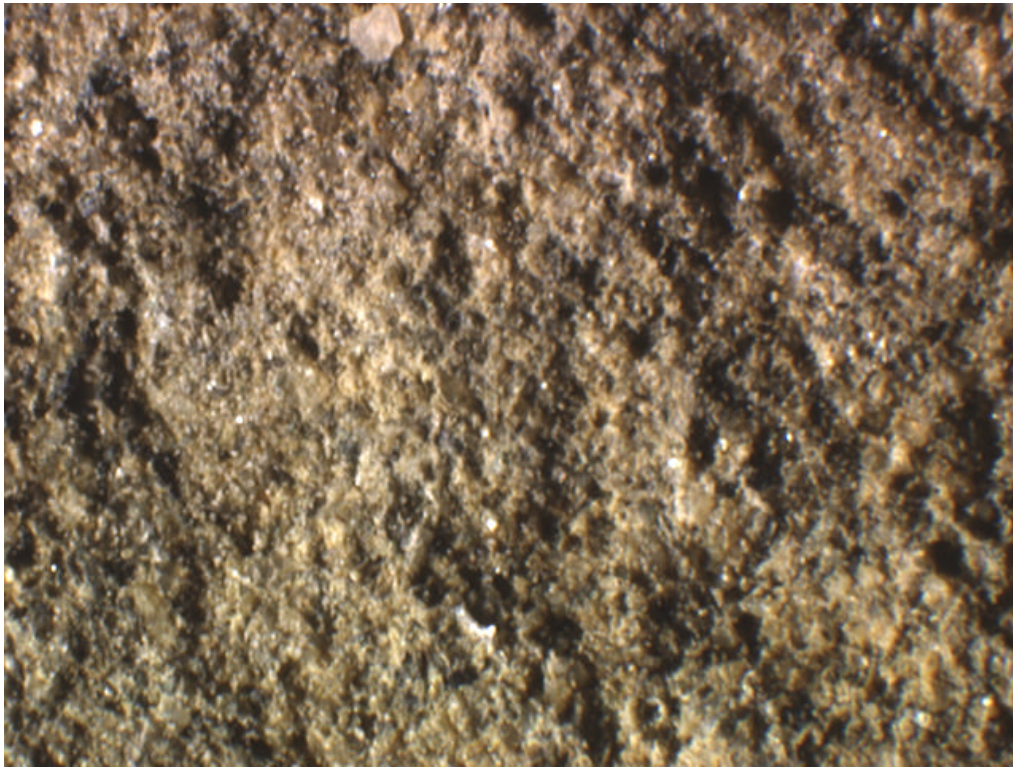


Figure 10. Stereo microscope images of fresh-fracture surfaces of the backfill material with a field width of 7 mm for the upper and 1 mm for the lower image.



Figure 11. Scanning electron microscope backscattered electron image of an epoxy-impregnated, polished cross section of the back fill with uniform sand grading. Field Width: 4.9 mm

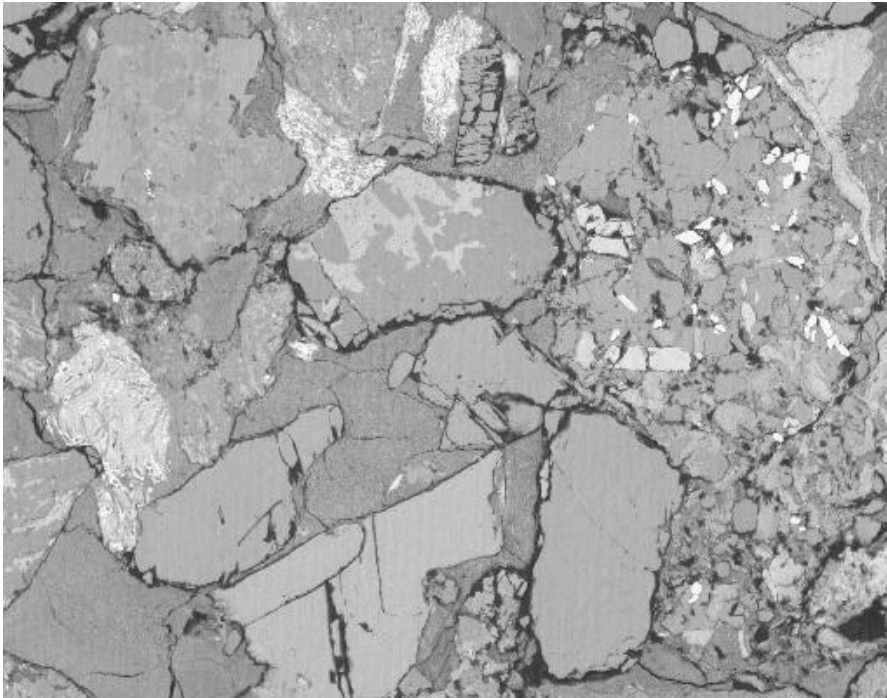


Figure 12. Scanning electron microscope backscattered electron image of an epoxy-impregnated, polished cross section of the back fill exhibiting a uniform-textured matrix distinct from that of the portland cement concrete. Field Width: 144  $\mu\text{m}$

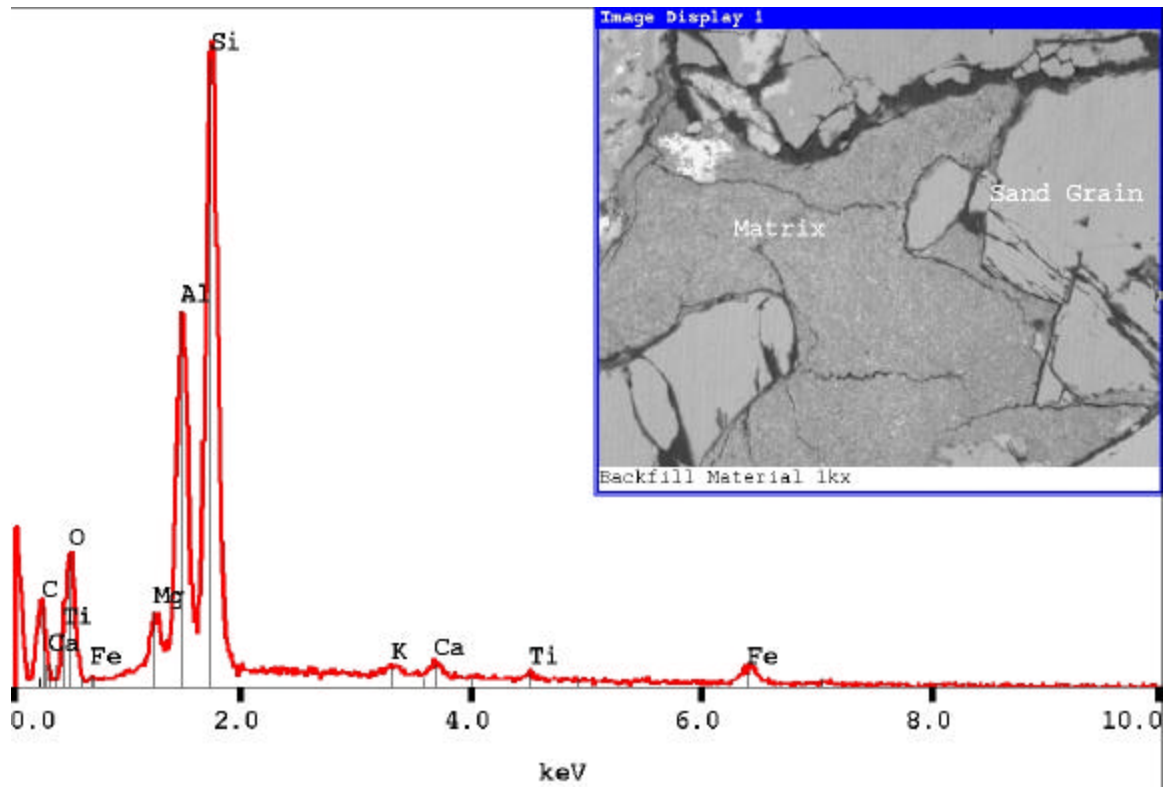


Figure 13. Energy-dispersive X-ray spectrum of the fill matrix showing strong silicon and aluminum and intermediate-intensity magnesium and iron peaks. XRD analysis suggests chlorite – an aluminum magnesium hydroxide silicate which may occur as both a clay mineral and as a more coarse-grained rock-forming mineral.

## Backfill Material - Bulk

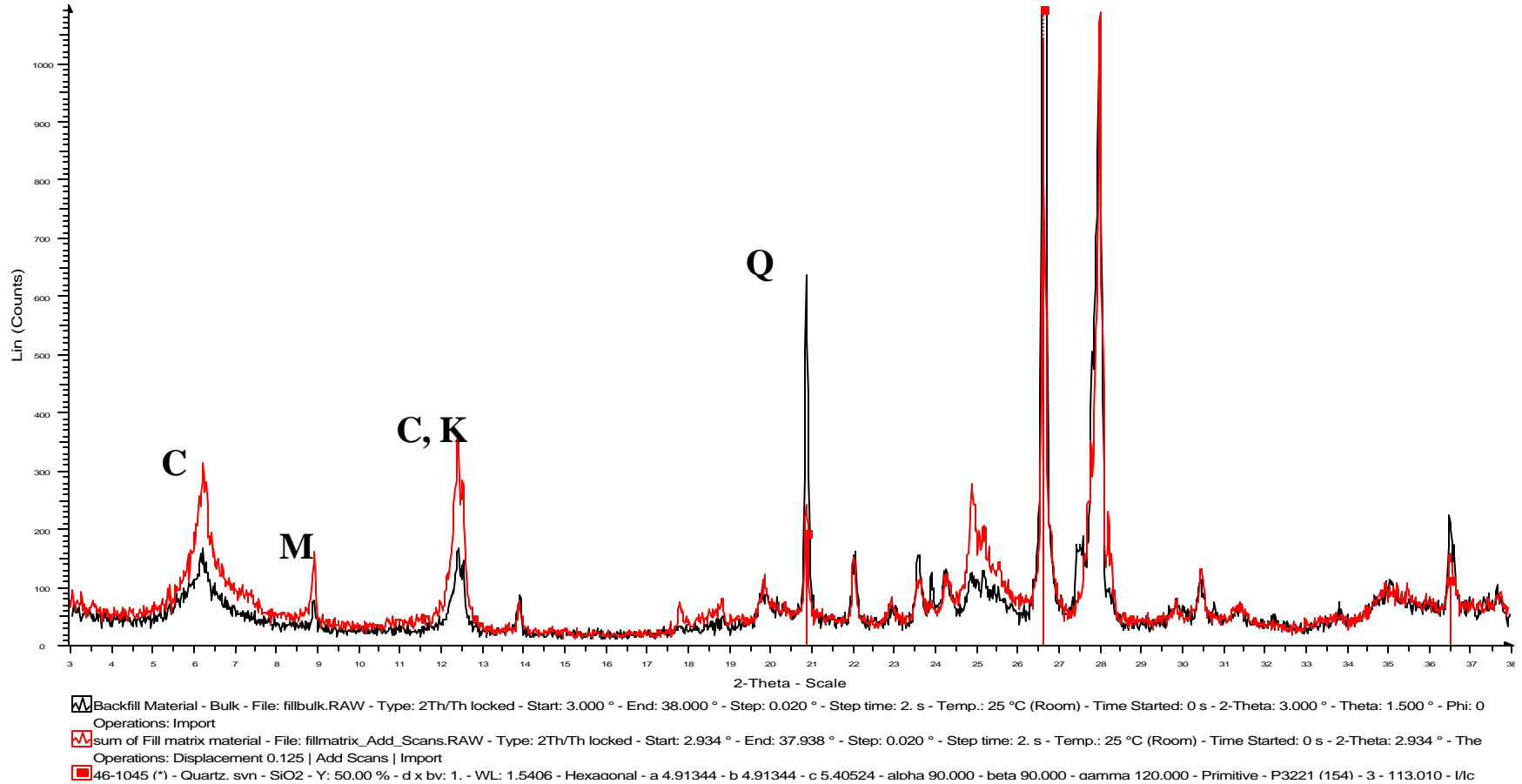


Figure 14. X-ray powder diffraction patterns of the whole-sample (black) and fines (red) show it to be comprised primarily of quartz (Q), mica (M), and clays chlorite (C) and kaolinite (K).

#### 4.0 Soil E

Specimen E was provided as a reference for local soils. SEM images show an abundance of coarse and fine-sized multi-phase aggregates (see Figs. 15 and 16). These aggregates are probably shale, given their fine texture. The matrix is fine-grained and heterogeneous and exhibits irregular-shaped voids, distinct from the hardened cement paste and the entrained air voids found in the concrete. The X-ray powder diffraction patterns in Fig. 17 indicated the presence of quartz, calcite, feldspar, mica, and clays. The HCL spot test was positive, indicating the presence of calcite (calcium carbonate).

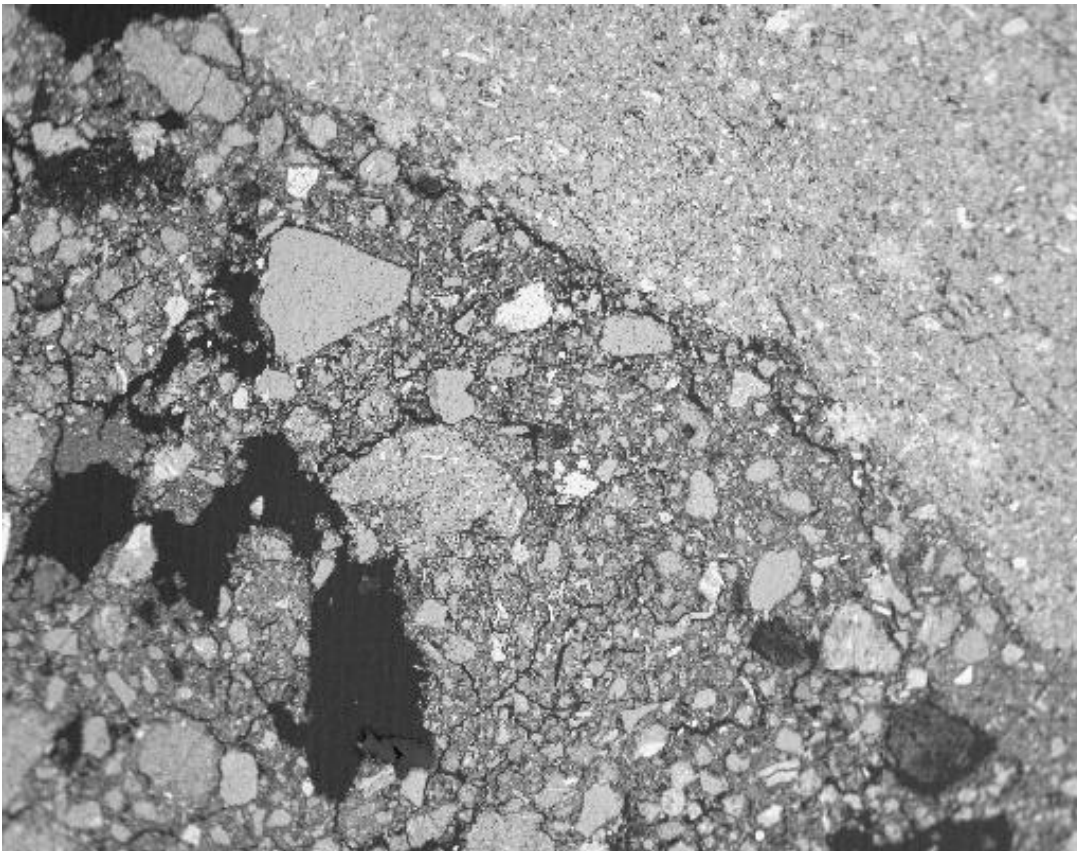


Figure 15. SEM image showing a polished cross section of soil microstructure is heterogeneous with irregularly-shaped air voids, poly-mineralic large and fine grains, and a fine-grained matrix. Field Width: 4.9 mm



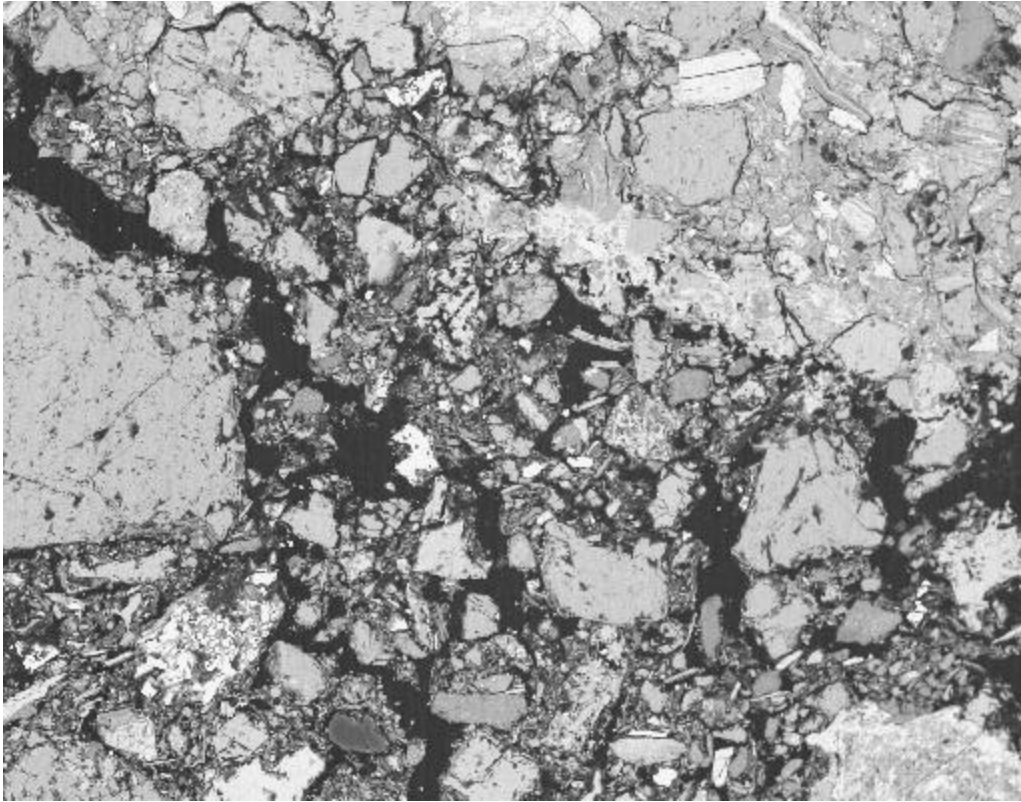
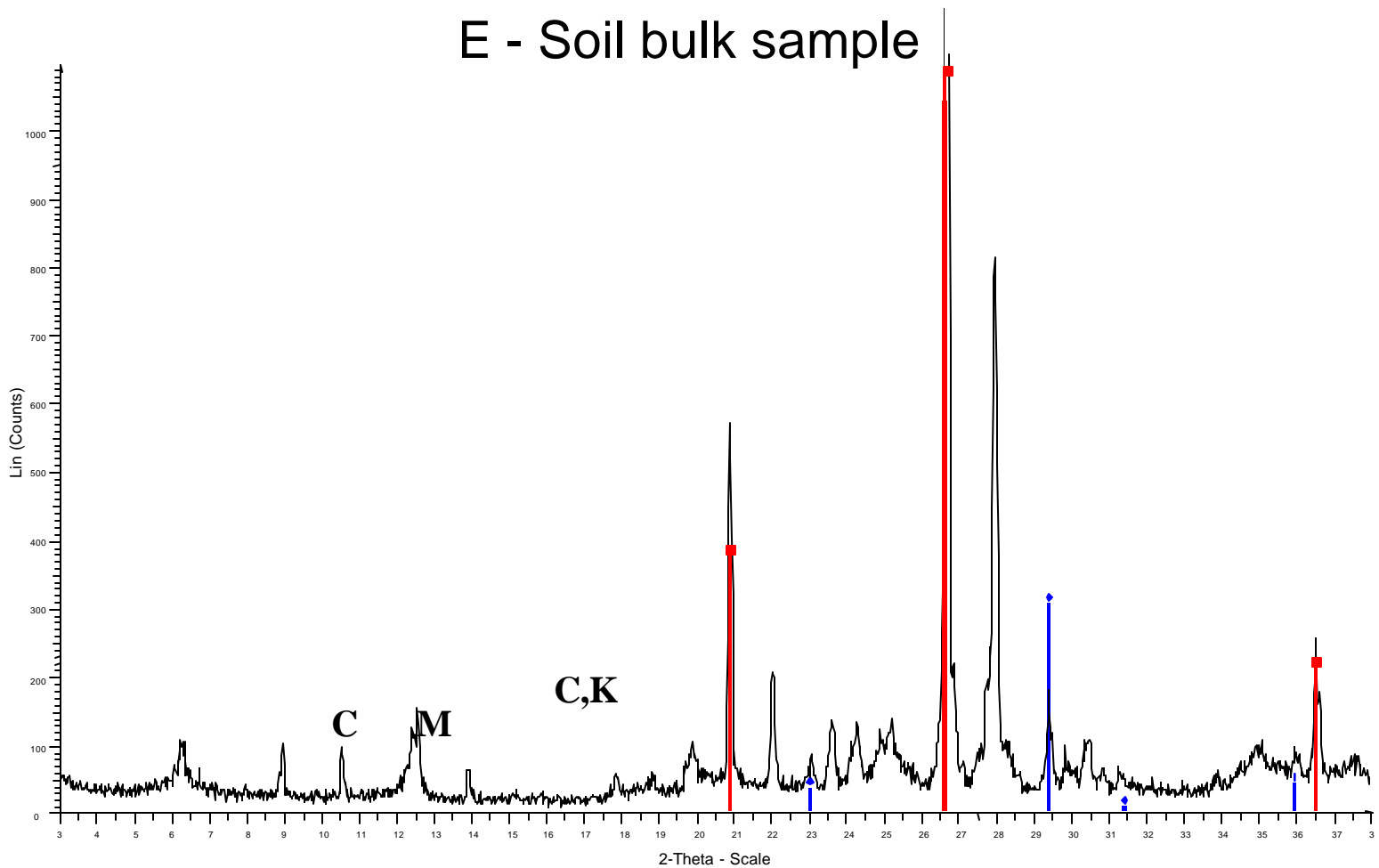


Figure 16. E-soil specimen exhibits a heterogeneous matrix with the upper image field width of 475  $\mu\text{m}$ , and the lower 144  $\mu\text{m}$ . The platy grains showing apparently good basal cleavage are probably a mica, or micaceous mineral.

# E - Soil bulk sample



E - Soil bulk sample - File: ebulk.RAW - Type: 2Th/Th locked - Start: 3.000 ° - End: 38.000 ° - Step: 0.020 ° - Step time: 2. s - Temp.: 25 °C (Room) - Time Started: 0 s - 2-Th Operations: Import  
 46-1045 (\*) - Quartz, syn - SiO<sub>2</sub> - Y: 95.83 % - d x by: 1. - WL: 1.5406 - Hexagonal - a 4.91344 - b 4.91344 - c 5.40524 - alpha 90.000 - beta 90.000 - gamma 120.000 - Prim  
 05-0586 (\*) - Calcite, syn - CaCO<sub>3</sub> - Y: 12.50 % - d x by: 1. - WL: 1.5406 - Hexagonal (Rh) - a 4.989 - b 4.98900 - c 17.062 - alpha 90.000 - beta 90.000 - gamma 120.000 - F

Figure 17. X-ray powder diffraction pattern of soil shows the presence of quartz, calcite, clays chlorite (C) and kaolinite (K), and mica (M).

## 5.0 Sample F

Examination of sample F using optical microscopy did not initially distinguish it from the other samples. It consisted of a dark, sandy, friable mass often exhibiting flat-appearing surfaces that were occasionally covered with a black film that may have been a protective coating on the pipe (Fig. 18). X-ray powder diffraction data (Figs. 19 and 20) showed a larger, broad calcite peak and what appears to be either a set of peaks for portlandite (calcium hydroxide) or possibly melanterite. The lack of a (311) diffraction peak for portlandite around  $28.7^\circ$  and a weak (101) peak at  $34.1^\circ$   $2\theta$  made the identification of portlandite doubtful. Portlandite is a principal crystalline hydration product of portland cement and, if present, may indicate the use of a portland cement. The lack of a principal diffraction peak necessitated additional investigation by scanning electron microscopy, where portlandite may be identified using textural and compositional characteristics. Melanterite is a secondary mineral formed from the decomposition of iron sulfides like pyrite and marcasite [3]. While pyrite was not clearly identified in this specimen, it was seen in specimen H, as will be discussed below.

SEM examination of polished cross sections showed a very heterogeneous, sandy material that appeared texturally similar to the soil reference sample but also had numerous occurrences of a calcium-rich cementing phase. The HCL test was positive, indicating the presence of calcite. Portlandite was not observed in the SEM imaging of sample F.

A typical example is shown in Figs. 21 and 22 with a specimen showing the dense calcium-cemented grains to the left and a more porous microstructure to the right. Closer examination of the dense region revealed it was a calcium carbonate (most likely calcite) cemented grains. Lack of any calcium silicate or calcium hydroxide hydration products, of any residual cement, or any relic textures of hardened cement paste indicates this specimen is not related to a portland cement-based material. Bright regions along a smooth surface were thought to be corrosion product from the pipe. X-ray microanalysis (Fig. 23) of these locations indicated the presence of iron. Another possibility is that these grains may be the melanterite identified in the powder diffraction data (Figs. 19 and 20) and appear to discount the possibility of portlandite being present within this specimen.

SEM images of the more porous region of the fragment (Fig. 24) show a microstructure similar to that of the soil, specimen "E".

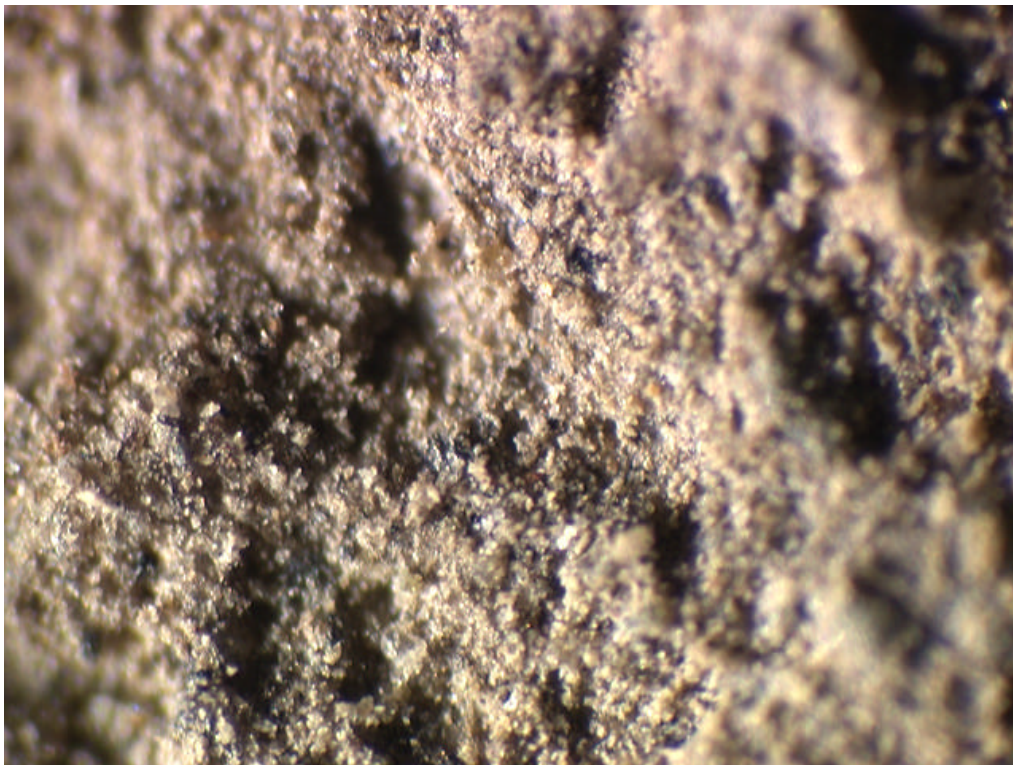
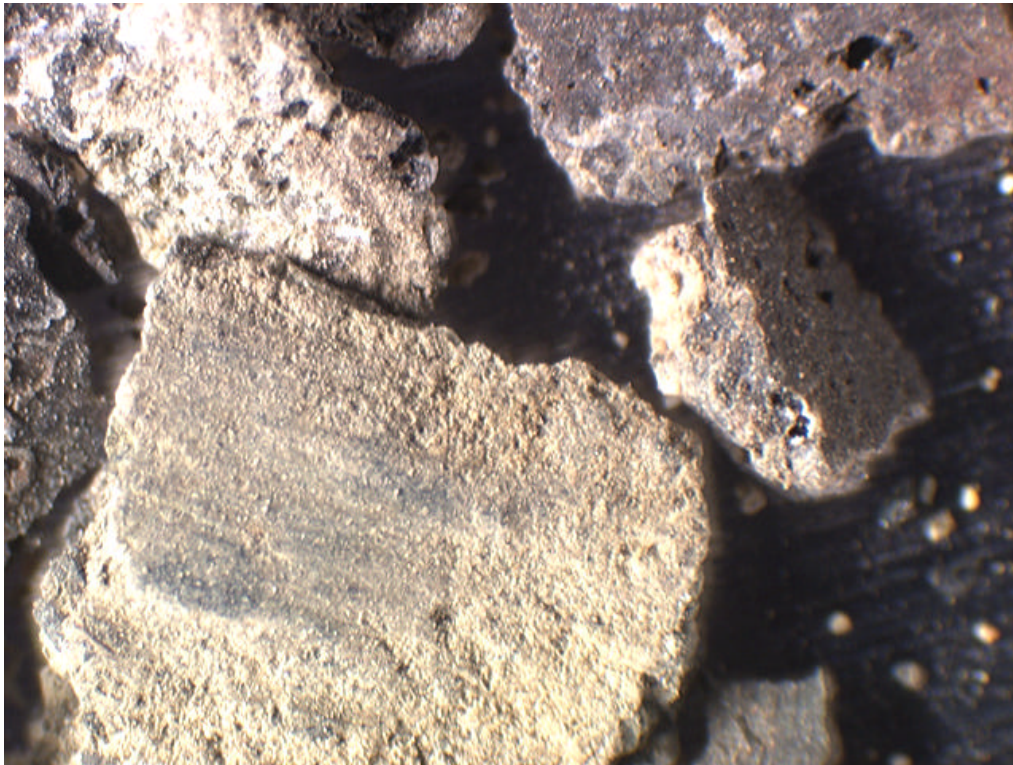


Figure 18. Optical microscope image of sample F, with a 7 mm field (upper) and 1 mm field (lower) width image of F showing sandy, dark texture of the fragment surface.

## F-bulk, on ZBP

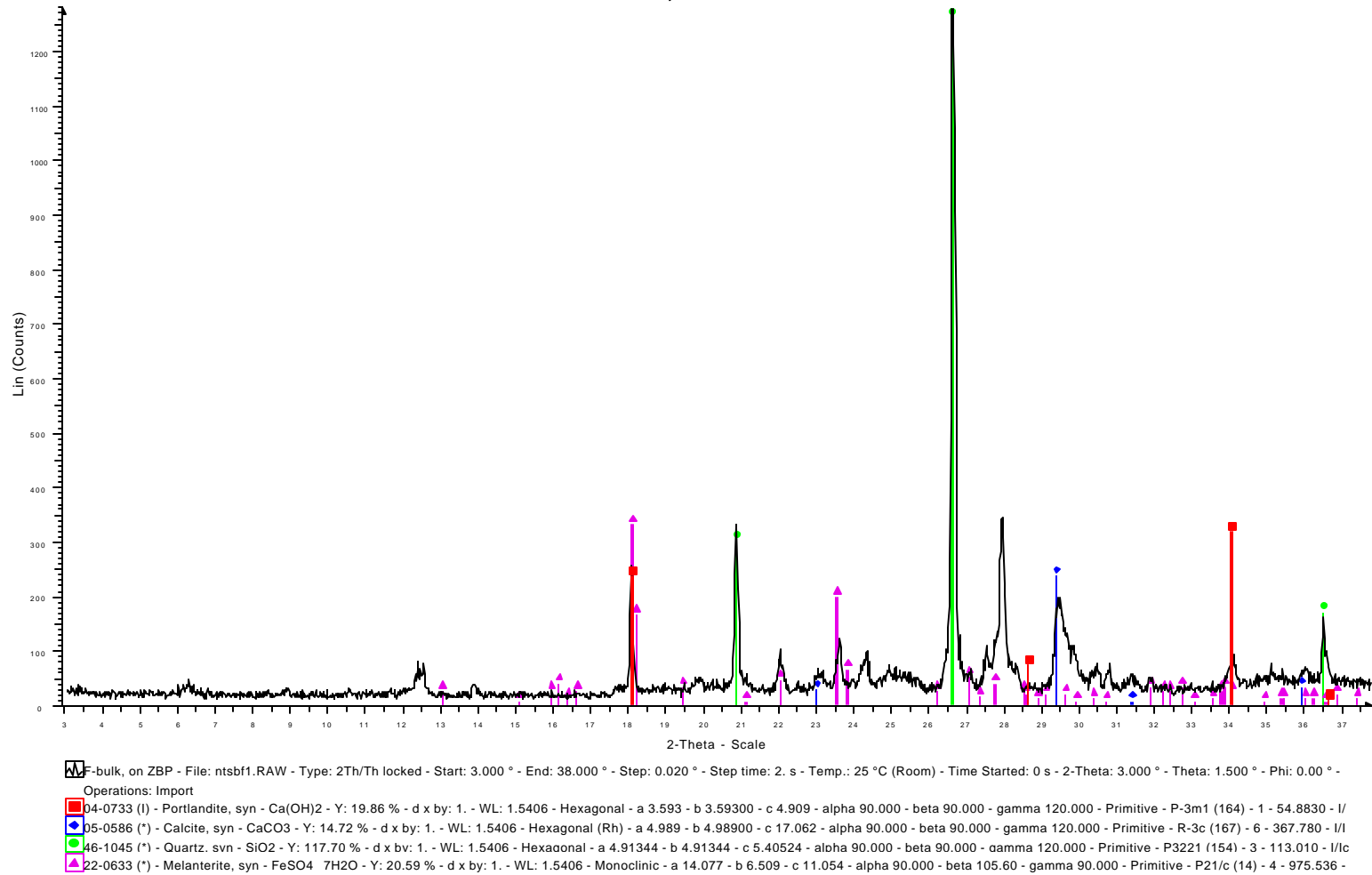


Figure 19. X-ray powder diffraction pattern of sample F shows the presence of quartz, calcite, and peaks that may be from either portlandite or melanterite, an iron sulfate hydrate. The latter phase diffraction peaks coincide with peaks of portlandite making identification difficult. The calcite peaks are relatively stronger than with other patterns suggesting an increased abundance.

## F-bulk, on ZBP

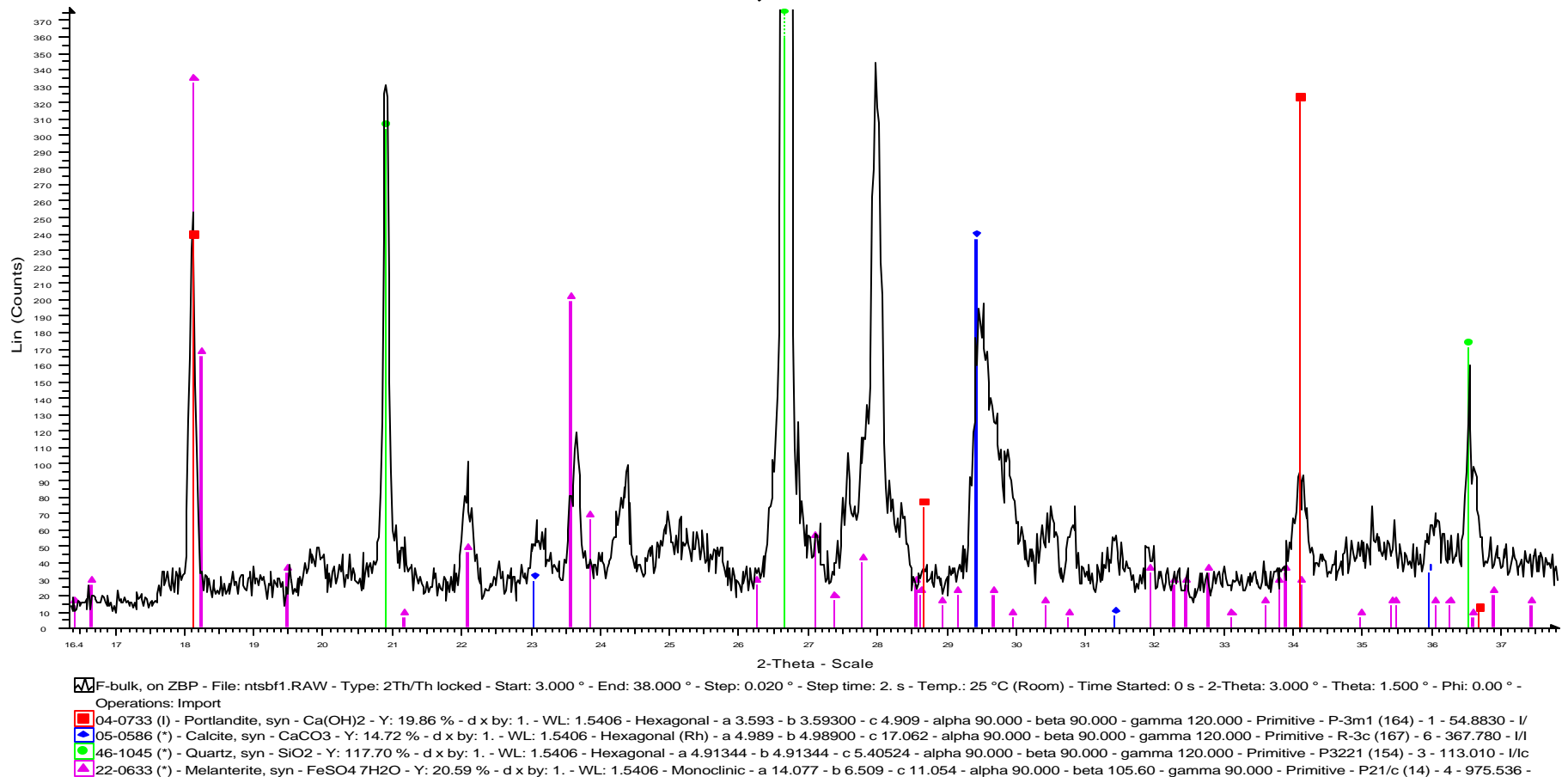


Figure 20. Expanded view of the specimen 'F' powder diffraction pattern shows that the relative intensities for portlandite at 2- $\theta$  positions 18.1°, 28.65°, and 34.1° do not agree with the powder diffraction reference in the database and no portlandite was observed in microscope examination. Bright regions identified as iron-bearing make the identification of melanterite a possibility.

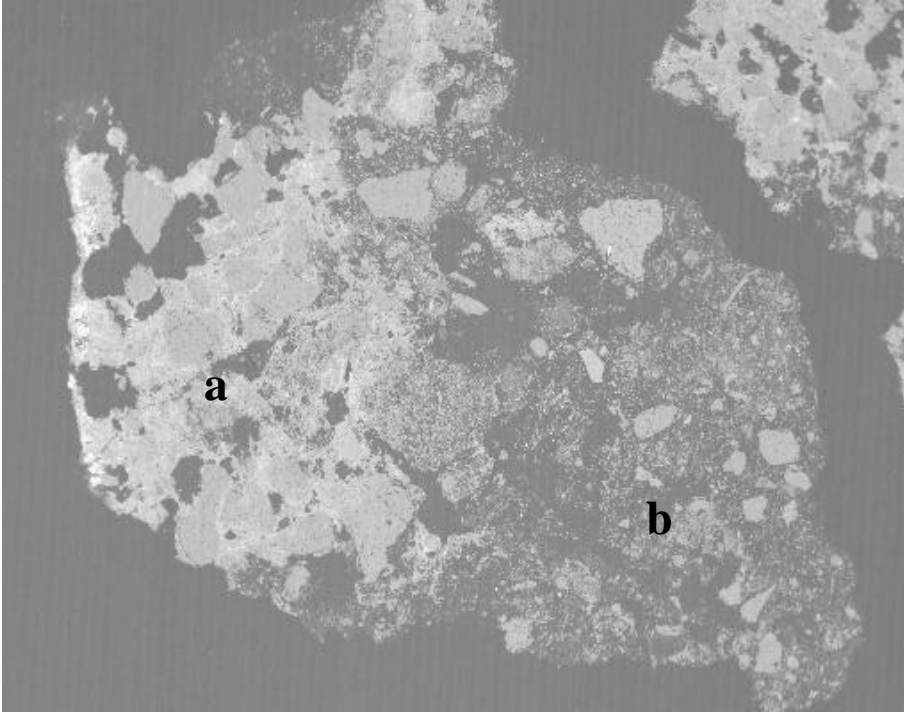


Figure 21. Sample F grain showing two distinct textures typical of these fragments, a) a dense, light-shaded material and b) a darker more porous material. Field Width: 3.5 mm.

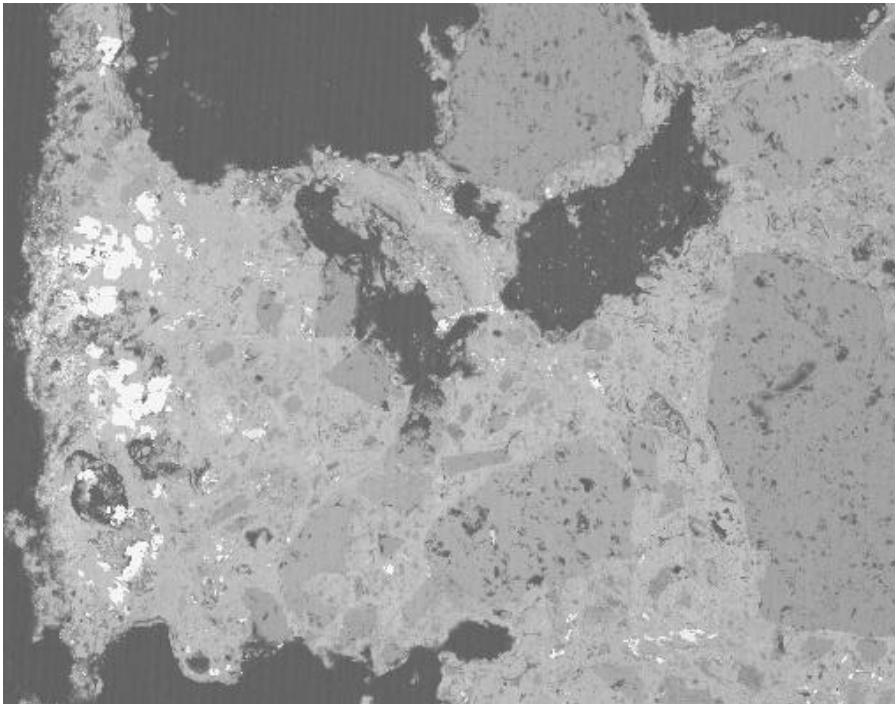


Figure 22. SEM/BE image of the dense, light-appearing material with bright inclusions. X-ray microanalysis indicates the light material to likely be a calcium carbonate (calcite) and the bright grains are high in iron, possibly a pipe corrosion product. Field Width: 500  $\mu\text{m}$

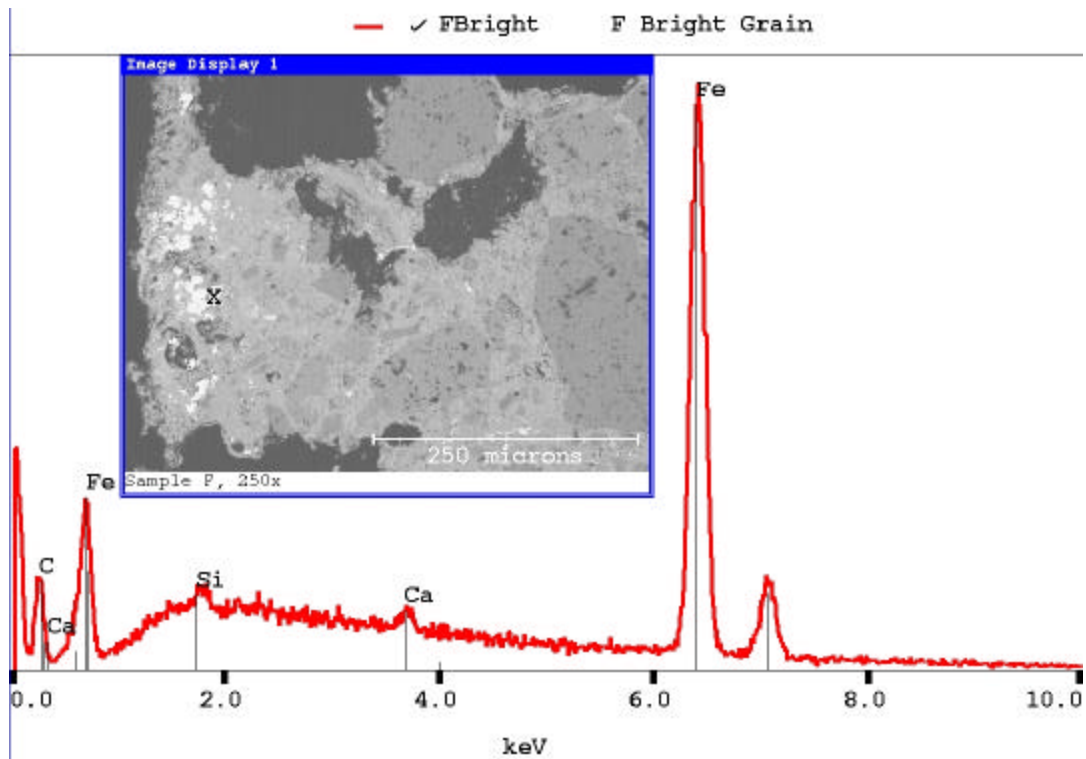
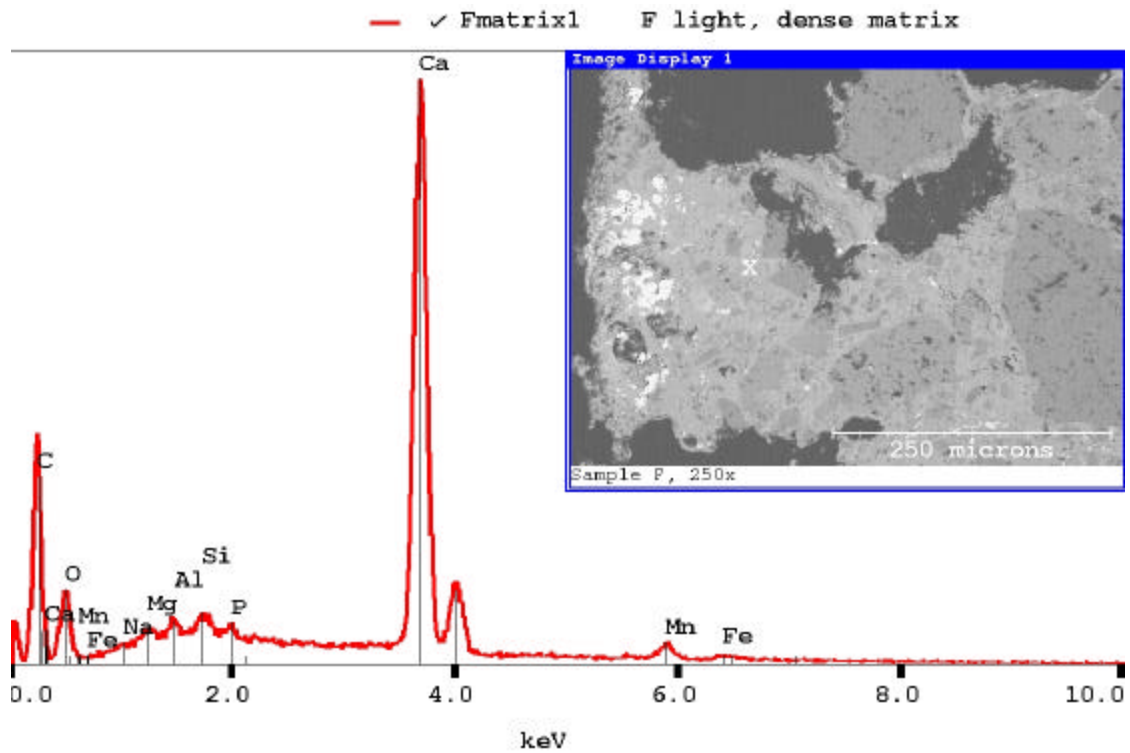


Figure 23. X-ray microanalysis of the dense material (upper spectra) indicates that it probably is calcite, with high calcium and relatively strong carbon peaks. The bright inclusions (lower spectra) show strong iron spectra.



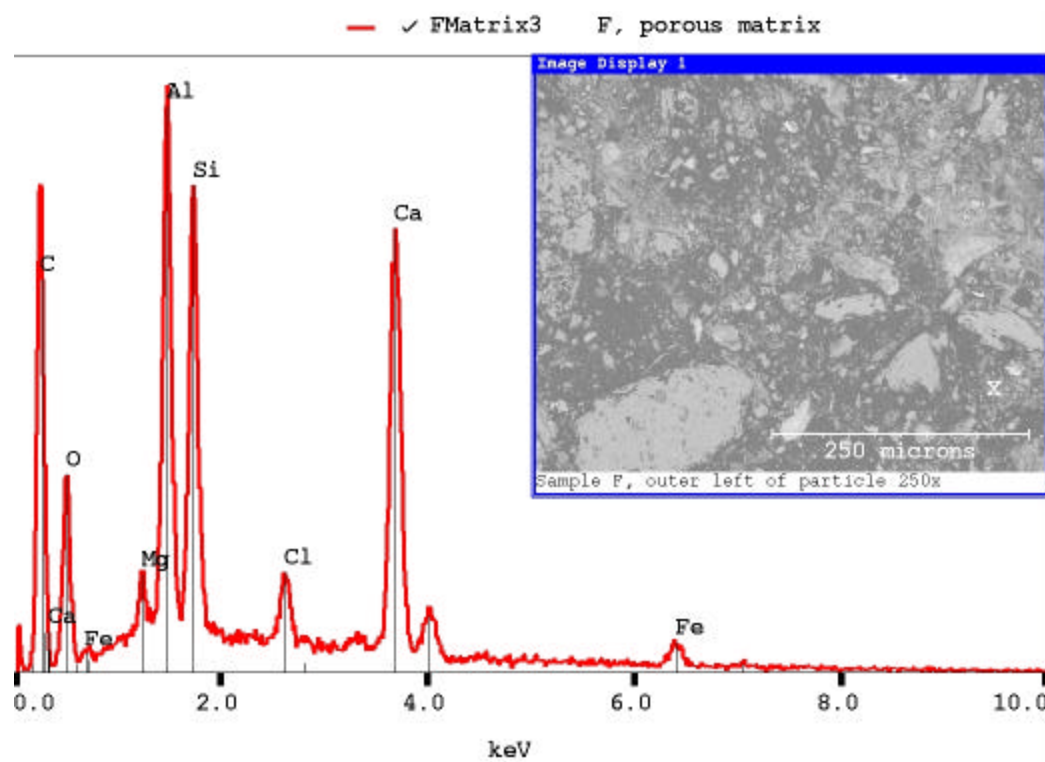
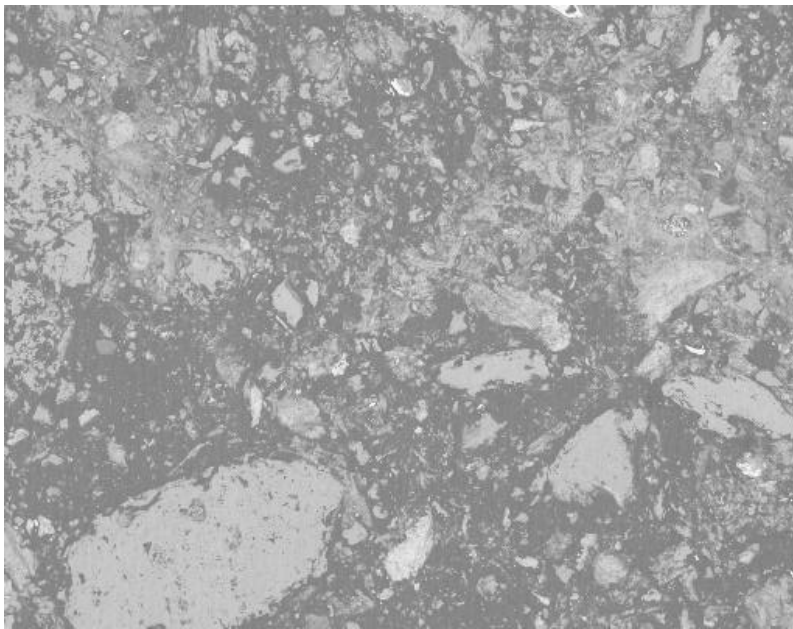


Figure 24. Close up SEM image of the more porous region of specimen F shows the fine-grained texture. Spot X-ray microanalysis indicates the presence of aluminum, silicon, calcium, chlorine, magnesium, and iron. Field Width: 475  $\mu\text{m}$ .

## 6.0 Samples H, I, and J

Samples H, I, and J are similar and appear to be shale particles and /or soil, partially cemented by calcium carbonate. A stereo microscope image of sample H is shown in Fig. 25. The overall appearances of these specimens are similar, as a light yellow-brown, sandy, friable material. In the SEM, massive calcite cement in specimen H appears to bind the sand grains together (Fig. 26). Close examination of the calcite cement showed no evidence of any portland cement hydration products or of any residual portland cement. X-ray spectra of the dense matrix indicated a calcium, carbon, and oxygen composition, probably calcite. The bright inclusions in the calcite are of two types, iron-rich which is probably a corrosion product, and iron and sulfur rich, probably being the iron sulfide, pyrite (Fig. 27). A secondary electron image of a selected fragment of H (Fig. 28), showing surface topography, and a corresponding X-ray spectra indicates a calcium, carbon, and oxygen composition that is probably calcite. A low-magnification SEM image of fragments using a polished section is shown in Fig. 29. Two distinct textured fragments are typically found; one of a calcite-cemented sandy material, and the other as darker, rounded multi-phase grains that appear to be a shale.

X-ray powder diffraction patterns of specimens H, I, and J (Fig. 30) appear similar and show the characteristic patterns of quartz, calcite, mica, and clays. No hydration products of portland cement were observed in the diffraction patterns.

The stereo microscope image of I appears similar to that of H and J with the slightly yellowish-brown color and sandy texture (Fig. 31). In Figure 32, the SEM backscattered electron images of one of the fragments shows a very heterogeneous sand size, calcite-cemented sand resembling the soil specimen. In contrast, Fig. 33 shows a fragment from specimen I that exhibits a much more uniform sand size distribution and heterogeneous calcite cement distribution. Another image set is given in Fig. 34 showing the extensive calcite cementation. This fragment appears similar to the backfill. No portland cement hydration products or textures were seen.

Figure 35 shows the optical microscope images of specimen J and, as noted earlier, it appears similar in color and texture to those of H and I. SEM images in Figure 36 show a sandy, calcite-cemented material with a darker region near the top of the image. This may be the coating from the pipe and the bright inclusions within the layer may be pigment or filler. Another fragment shown in Fig. 37 appears similar to that of the soil as it exhibits an irregular calcite cement distribution and irregular sand size. Figure 38 shows a SEM image of a microstructure similar to that of the fill material with a uniform sand size and homogeneous matrix but containing some calcite cement. Spot x-ray microanalysis of the matrix produces spectra similar to that of the fill. Additional SEM images of fragments from this specimen shown in Figs. 39 through 42 appear similar in texture to that of the fill. This specimen contained thirteen fragments that were larger than a few millimeters in cross section. Of these fragments, three appear similar in microstructure to that of the backfill specimen. Additional images of specimens I and J may be found in Appendix A.

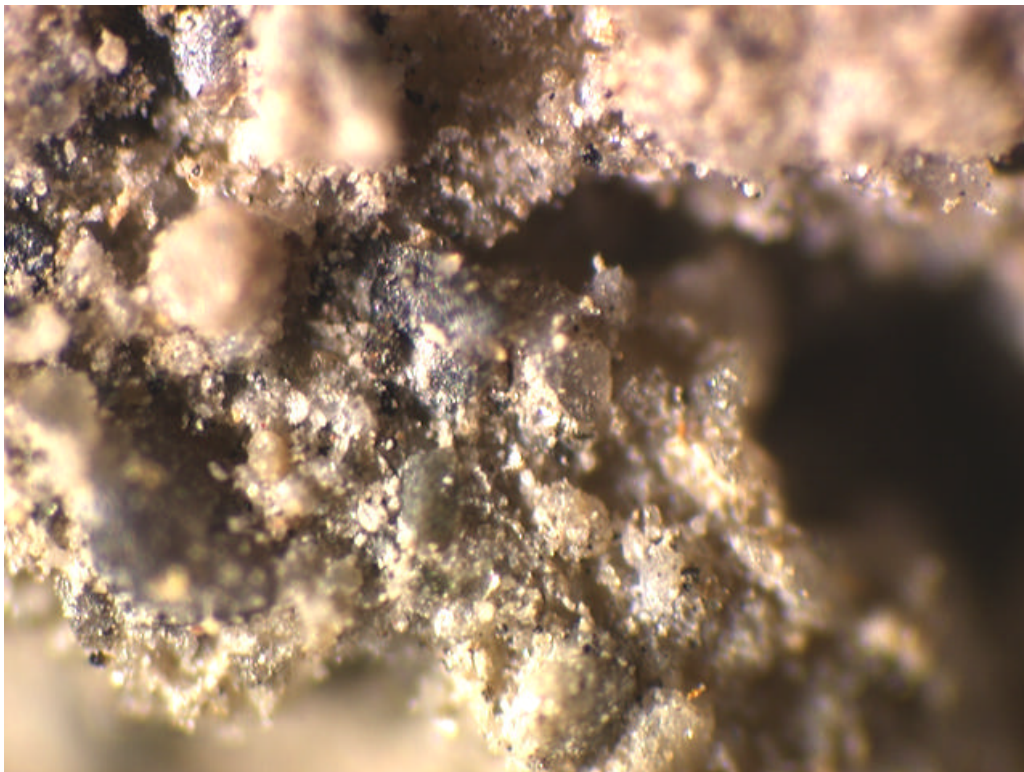


Figure 25. Specimen H at 7 mm (upper) and 2 mm (lower) field width is a brown to yellow, sandy, friable material.

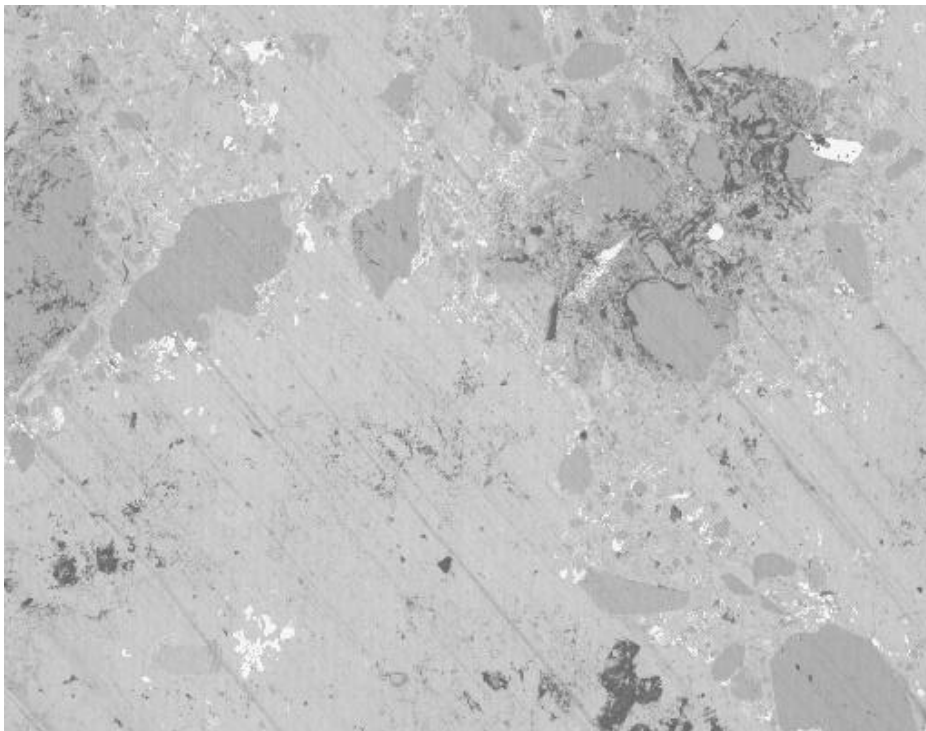
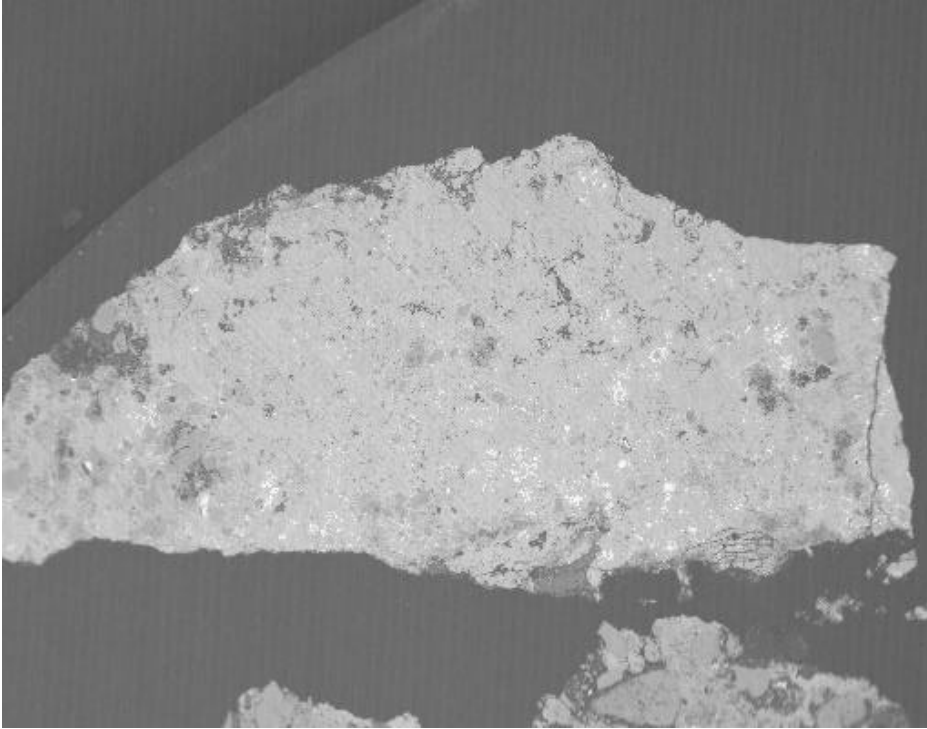


Figure 26. SEM images of specimen H with a 2.5 mm (upper) and 480  $\mu\text{m}$  (lower) field widths shows sand grains encased in a calcium carbonate cement. No portland cement microstructural features or residual portland cement was seen. The bright spots in the lower image are common and appear to be iron oxide or iron sulfide.

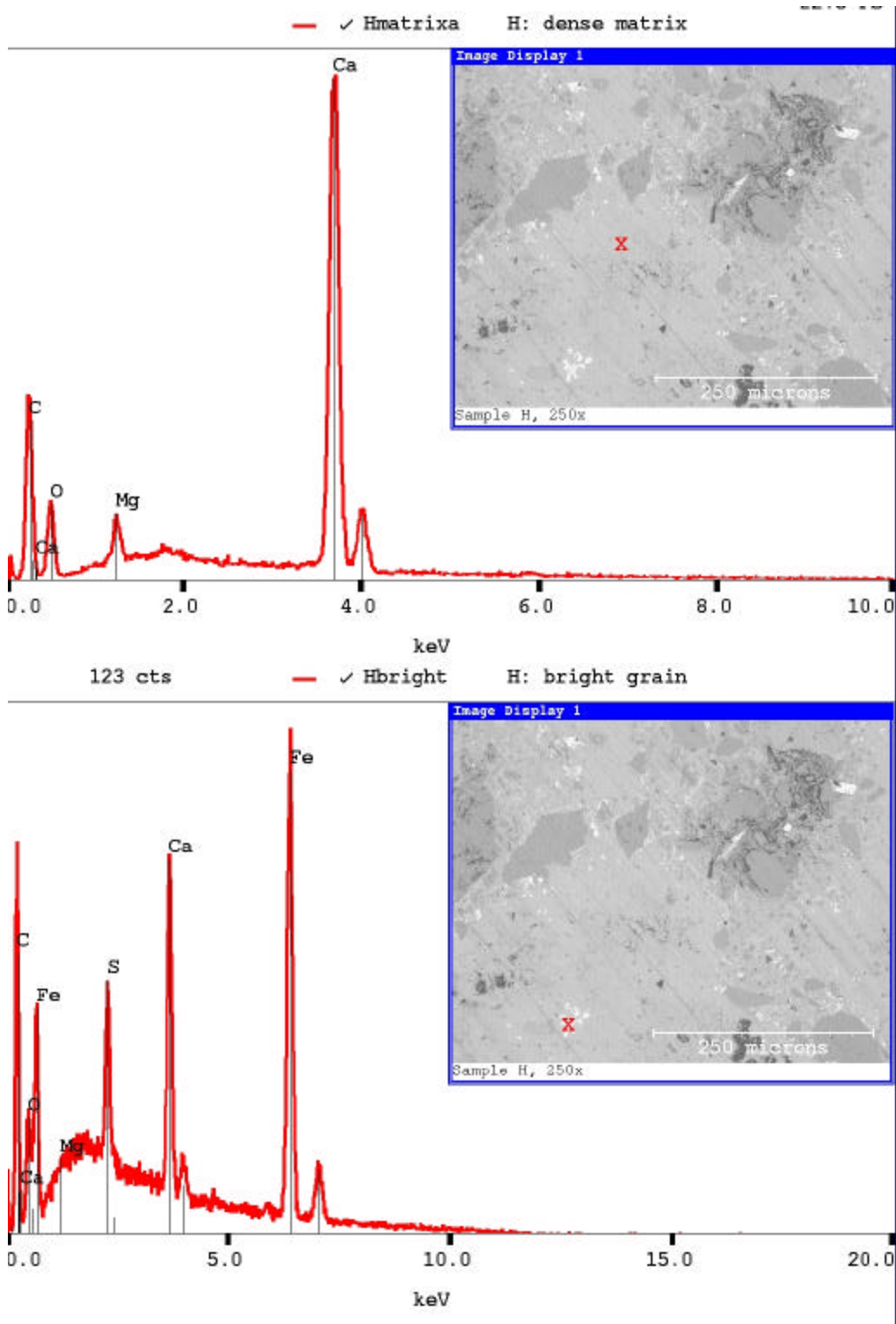


Figure 27. Spot X-ray microanalysis of dense matrix cementing product shows calcium, magnesium, and probably carbon, typical of a calcium carbonate while the bright grains strong sulfur and iron suggest the iron sulfide pyrite. None of these features or chemical spectra is similar to that of a portland cement hydration product or portland cement.

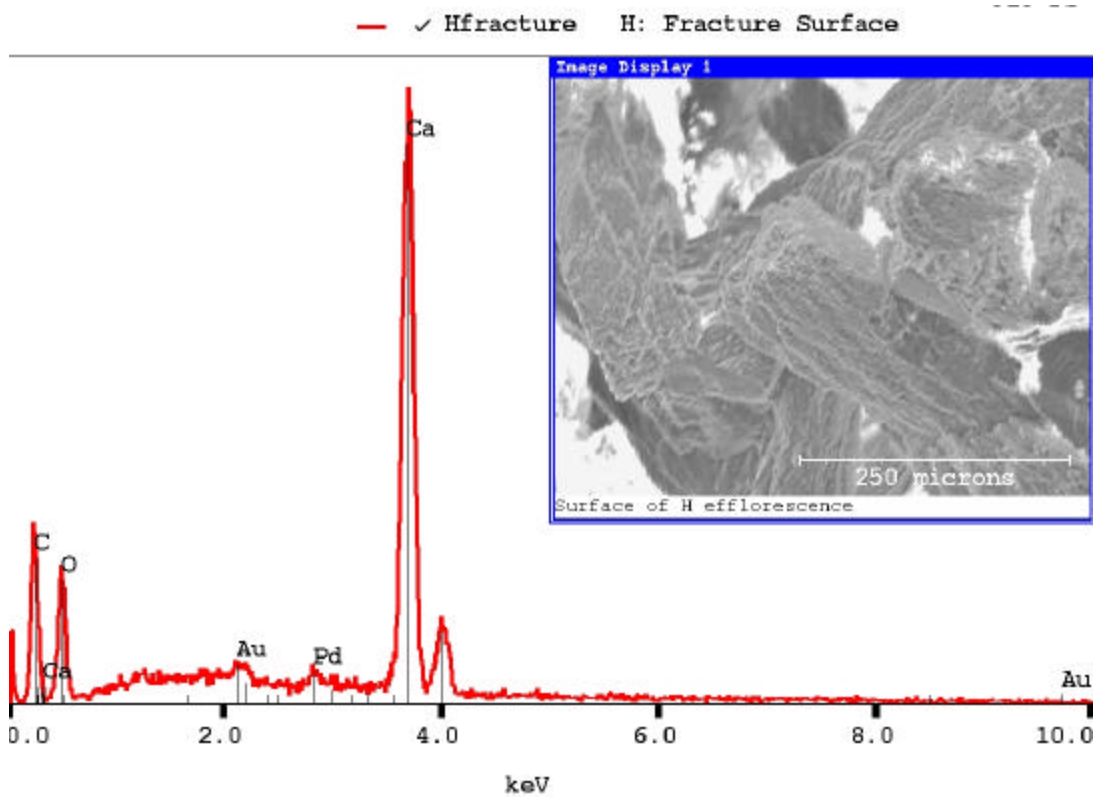


Figure 28. Secondary electron image of the surface texture and spot x-ray microanalysis of the surface of a specimen of sample H show it is composed of calcium and carbon and is probably the calcite, as observed in the XRD and HCL tests. The gold and palladium peaks are from the conductive coating necessary for imaging insulating specimens.

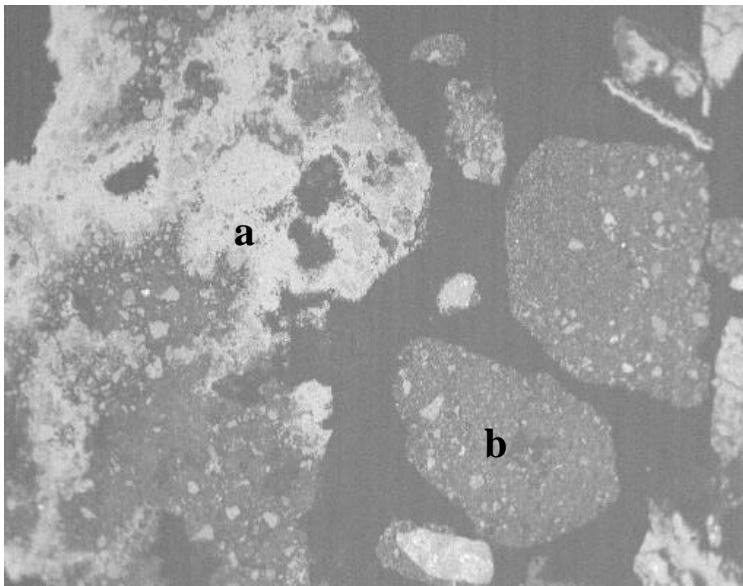


Figure 29. Sample H at 4.7 mm shows two typical textures, one of a calcium carbonate-cemented sandy material (a) and the other of a fine-grained rounded material that appears to be a shale (b).

# H-bulk, variable slit, sedimented on ZBP

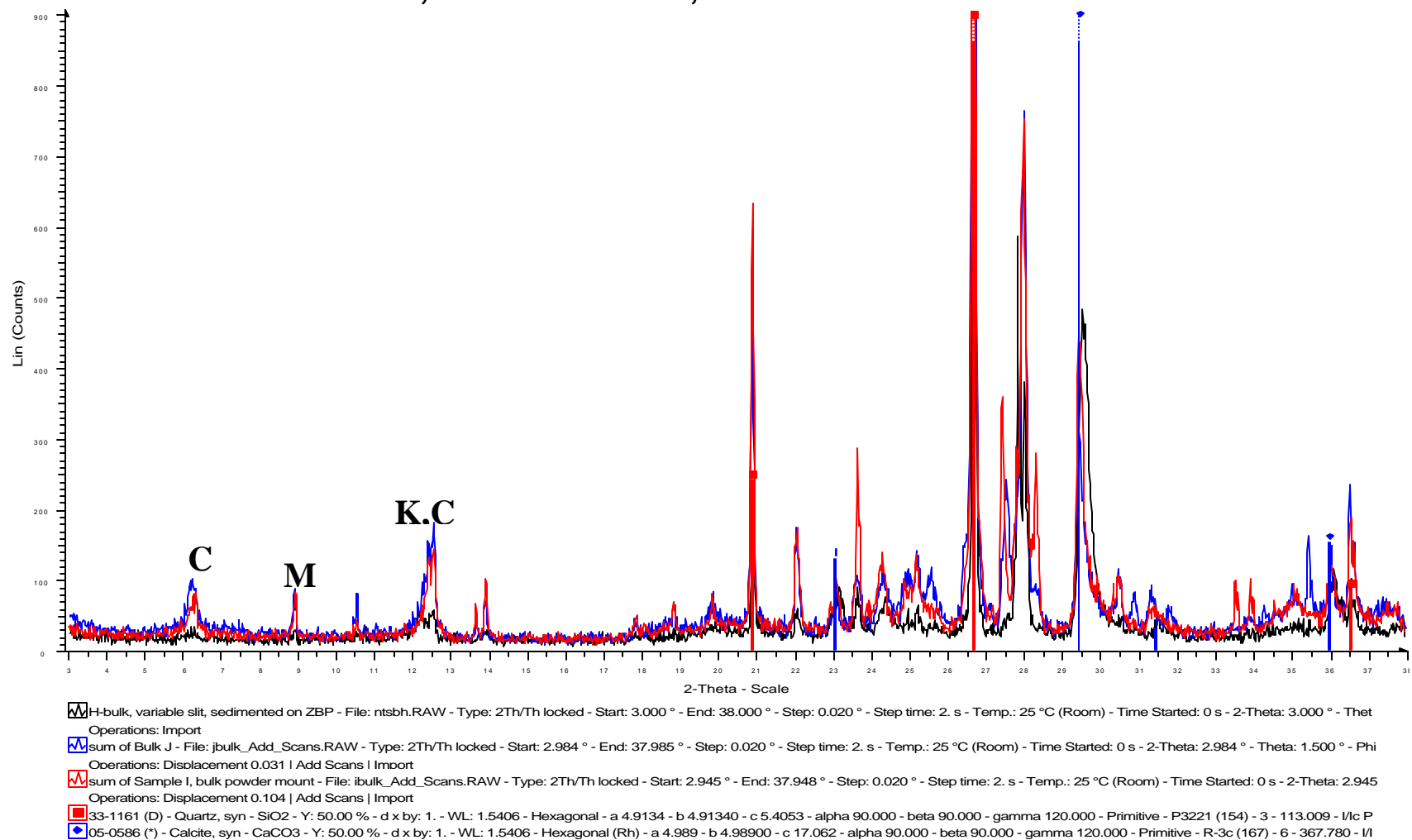


Figure 30. X-ray powder diffraction pattern of specimen H (black), I (red), and J (blue) shows the similarity to each other with quartz, calcite, mica (M), and clays kaolinite (K) and chlorite (C).

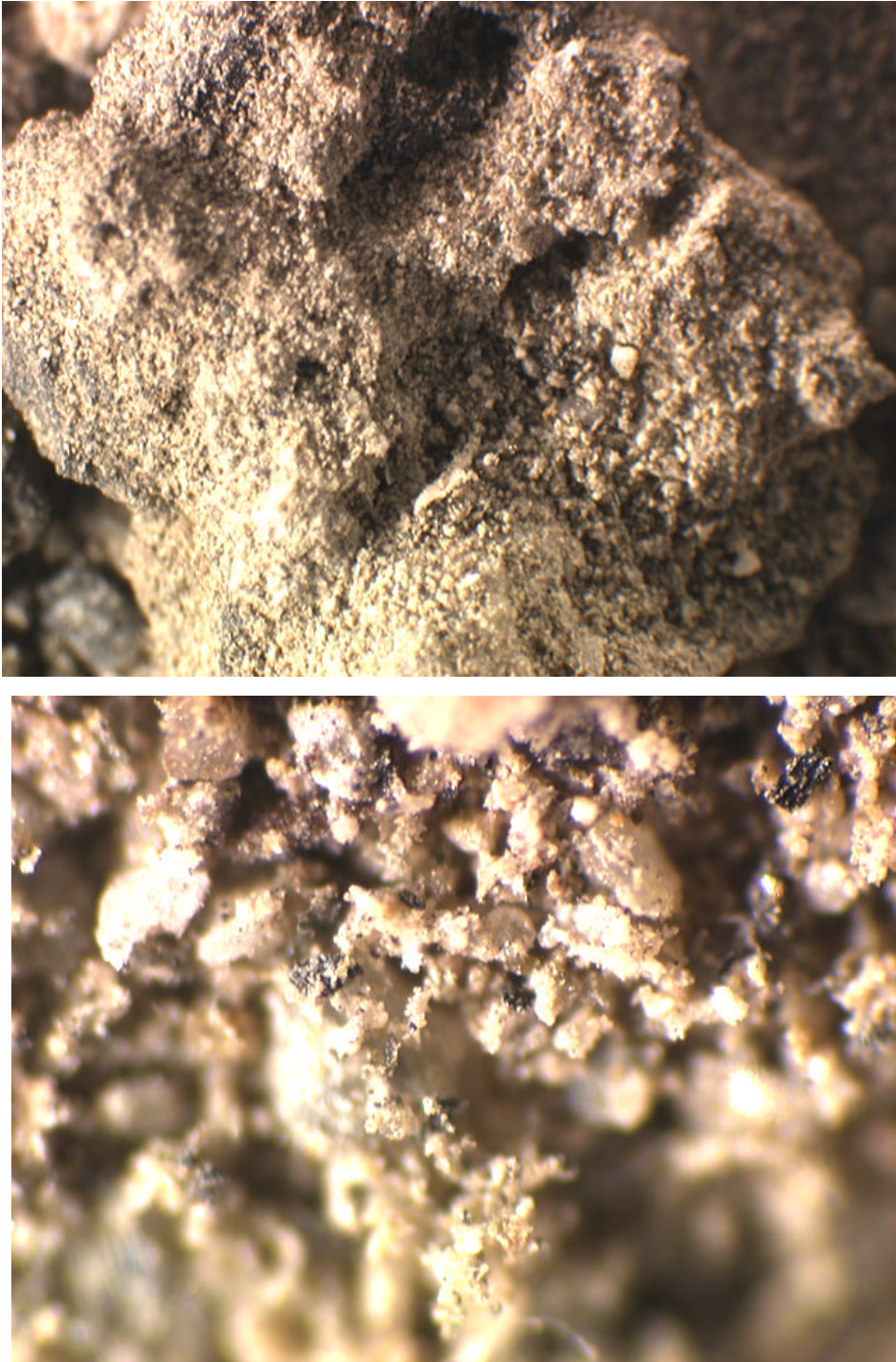


Figure 31. Specimen I with 7 mm (upper) and 1 mm (lower) field width appear similar in coloration and texture to H.



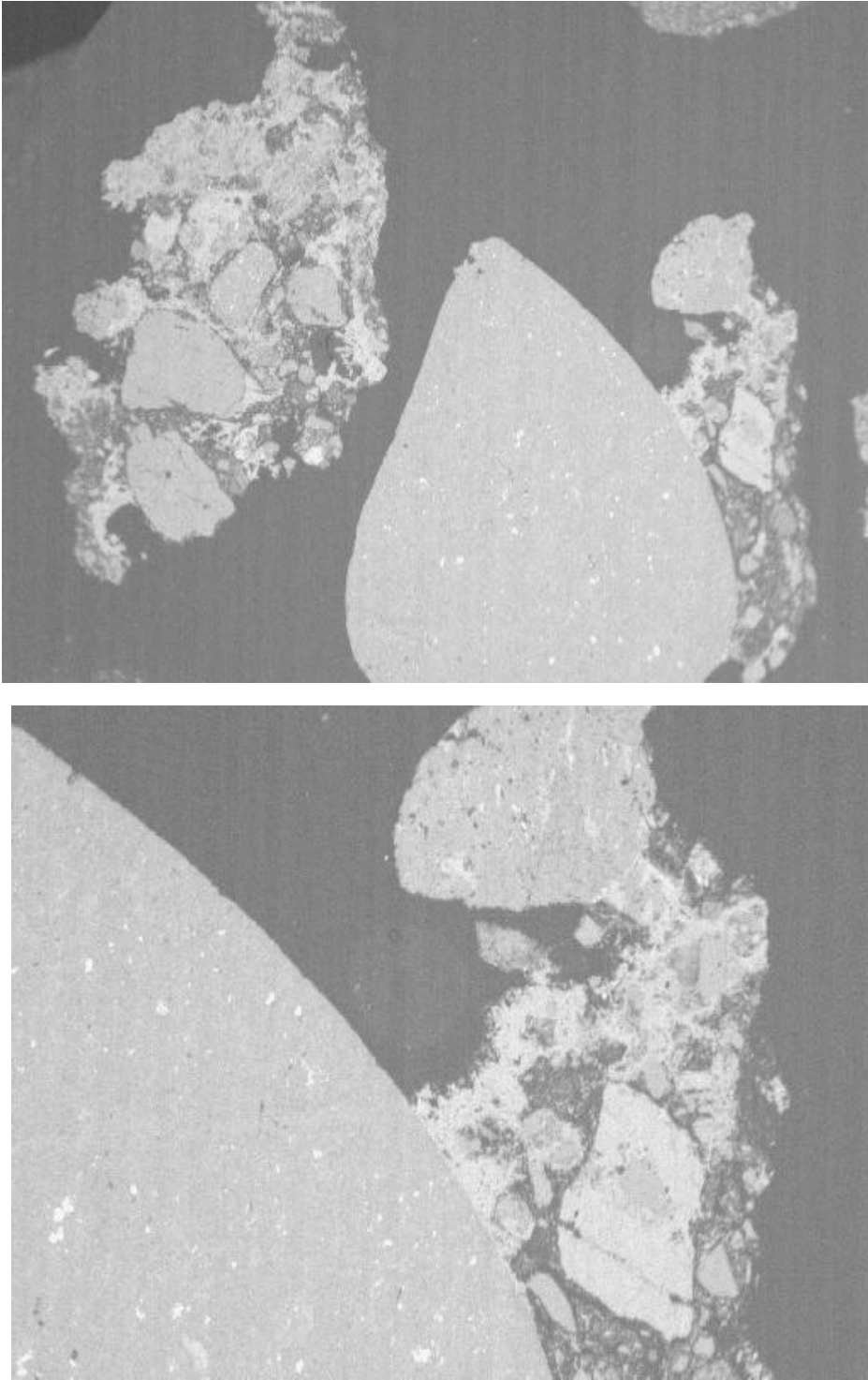


Figure 32. Specimen I at 6 mm (upper) and 2.5 mm (lower) field width shows cementation of the sand grains with a calcium carbonate cement. No portland cement hydration products or residual cement were observed.

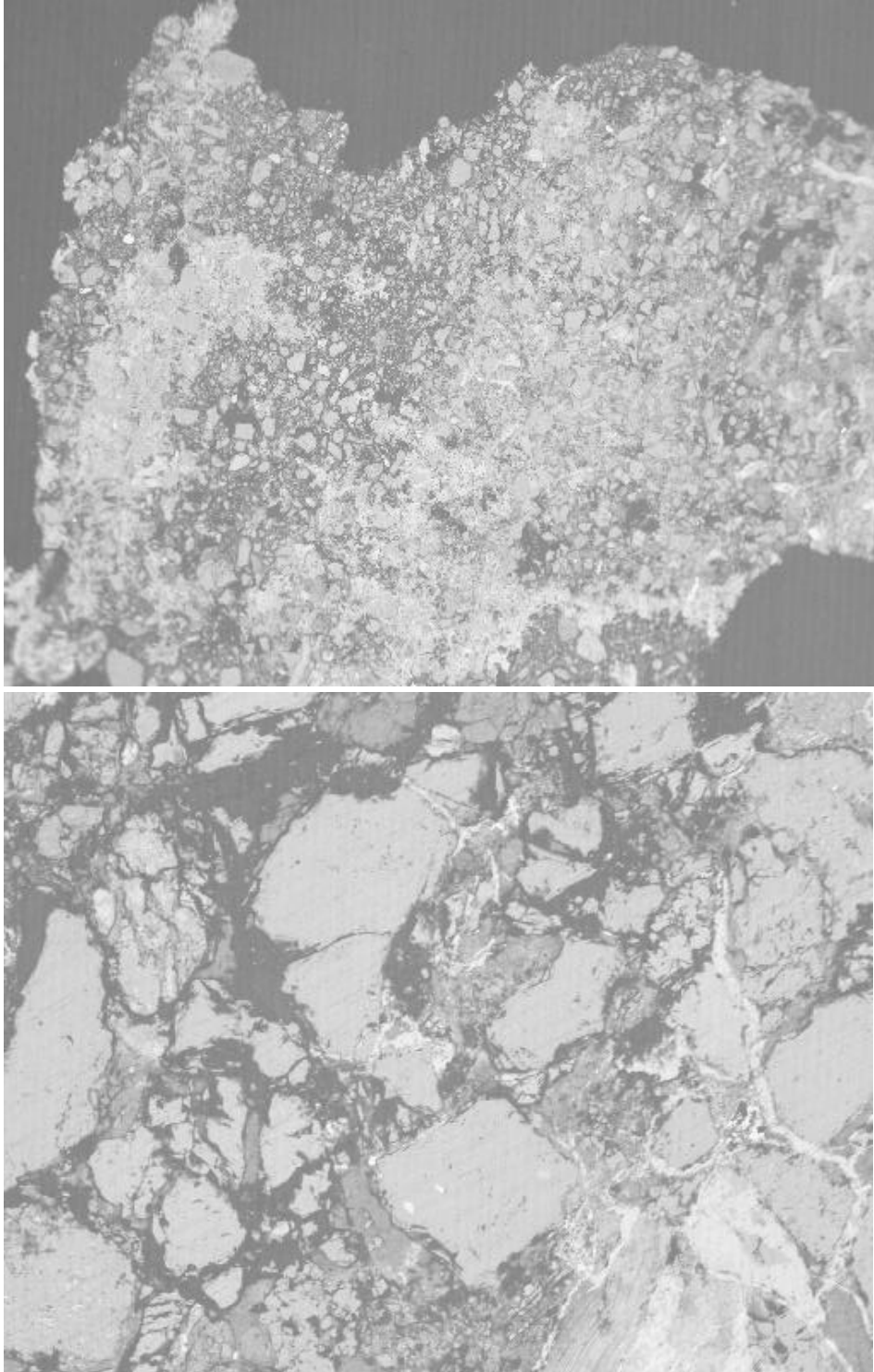


Figure 33. Specimen I at 3 mm (upper) and 490  $\mu\text{m}$  (lower) field width shows a more uniform sand size distribution but a heterogeneous distribution of porous sandy and calcium carbonate-cemented sandy regions.

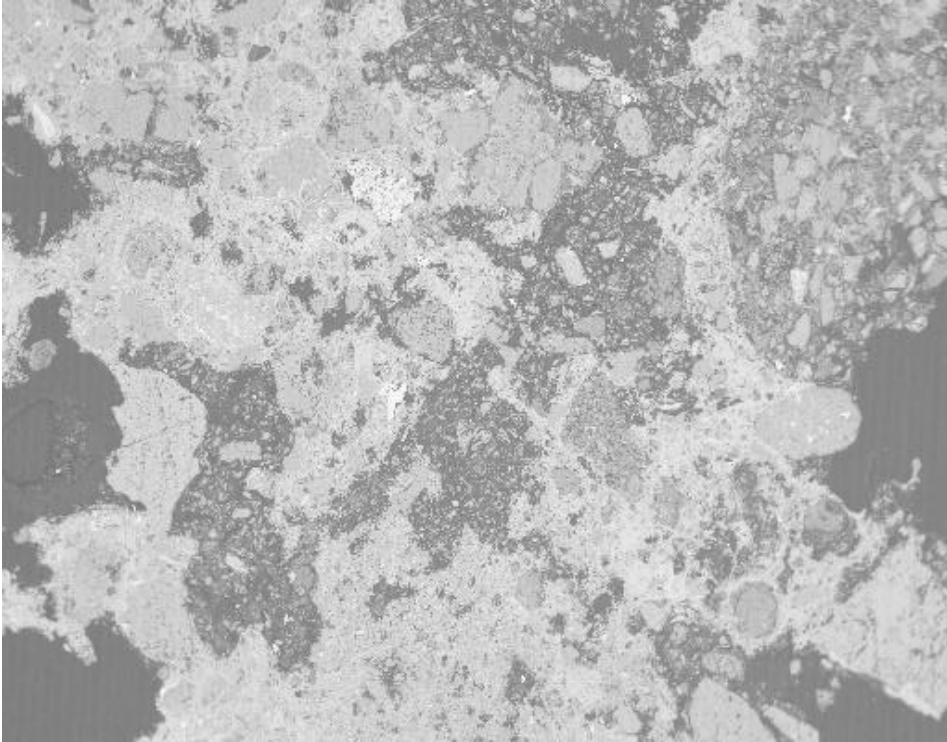


Figure 34. Another specimen from sample location I at 6 mm (upper) and 475  $\mu\text{m}$  (lower) field width shows the heterogeneous phase distribution and microstructure distinctly different from that of the concretes.

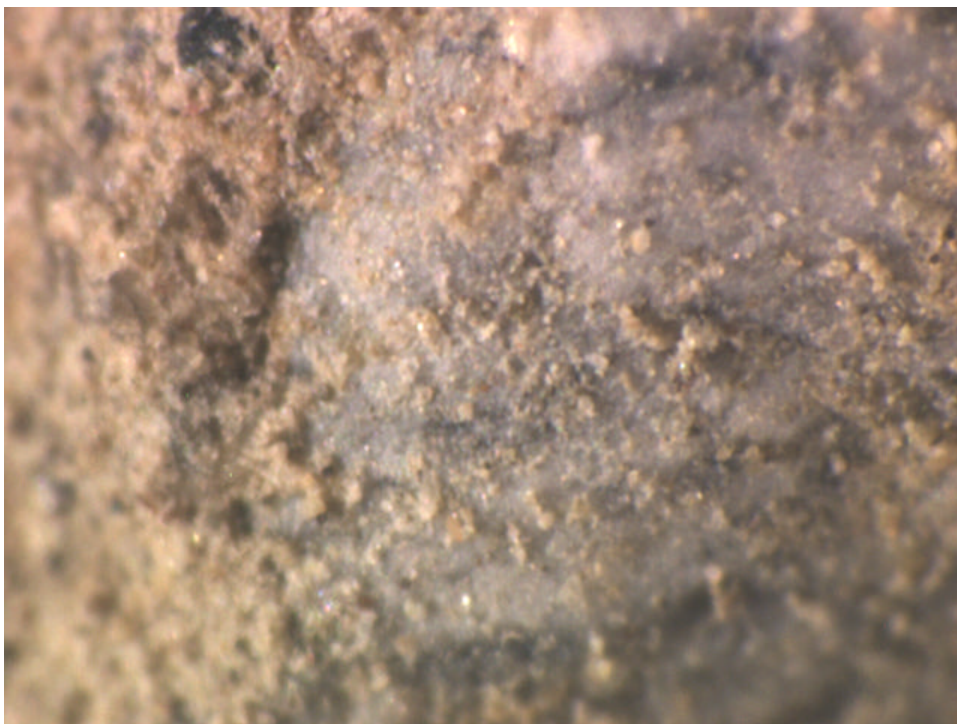
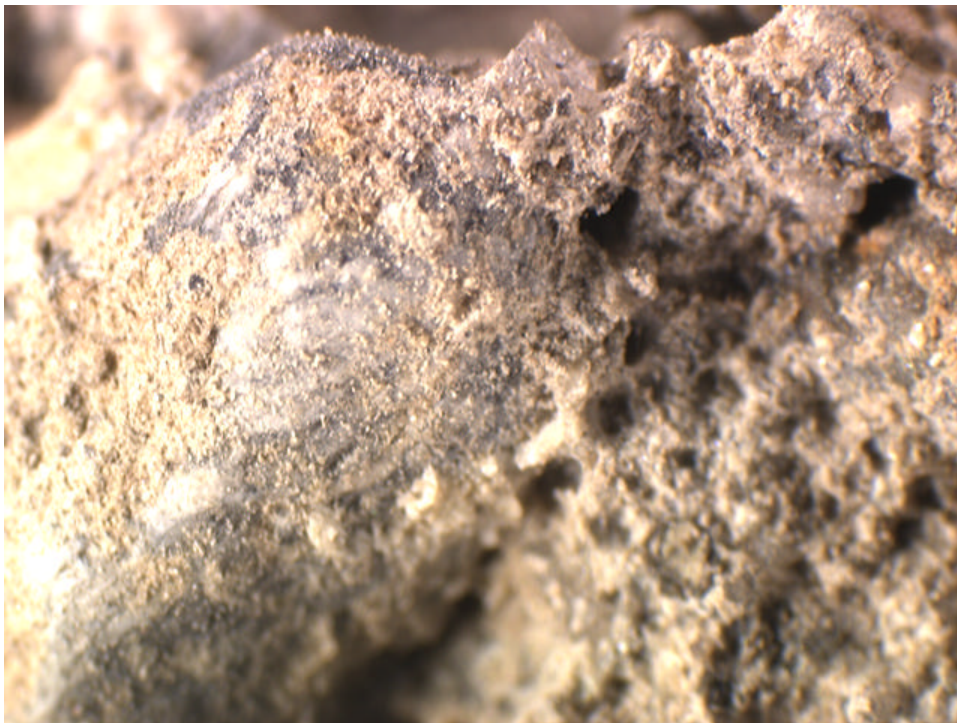


Figure 35. Specimen J at 7 mm (upper) and 1 mm (lower) field widths appears similar to that of H and I.

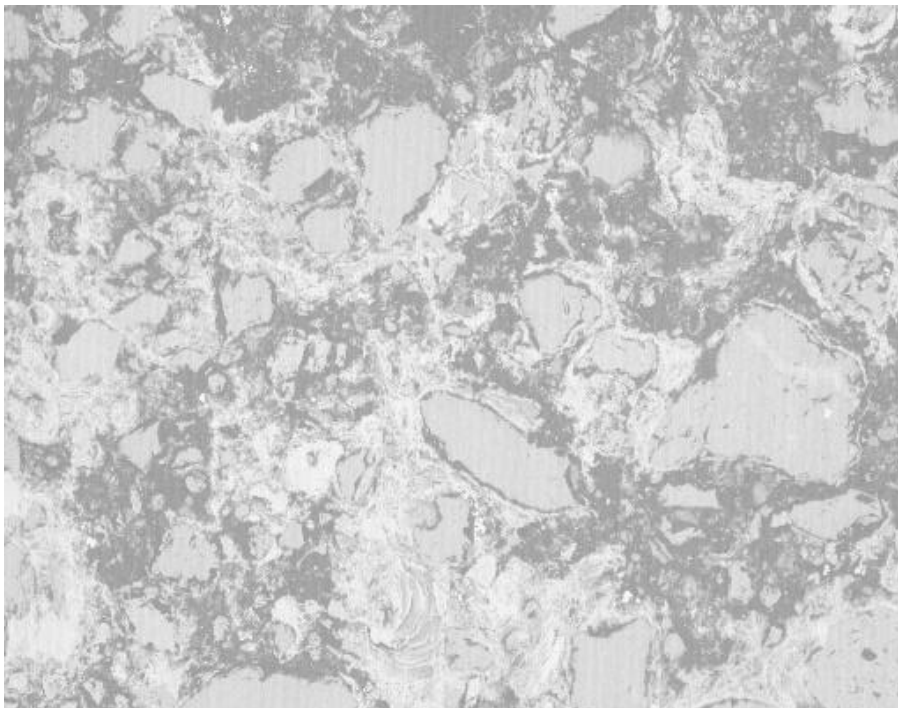
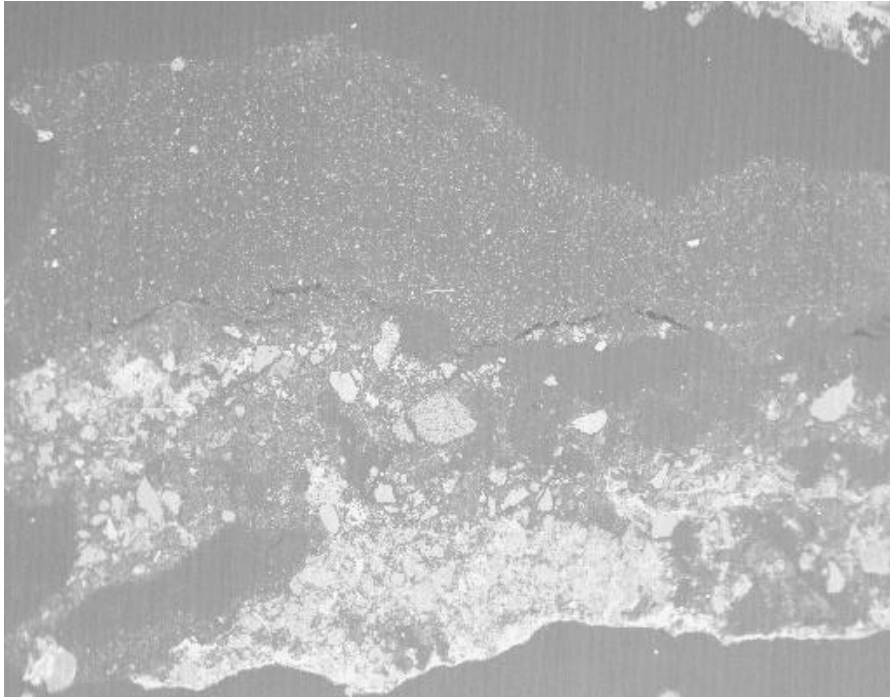


Figure 36. Specimen J at 3 mm (upper) and 490  $\mu\text{m}$  (lower) field widths has a sandy, calcite-cemented microstructure. The dark region with bright inclusions appears to be a coating with pigment and perhaps is the black coating from the pipe.

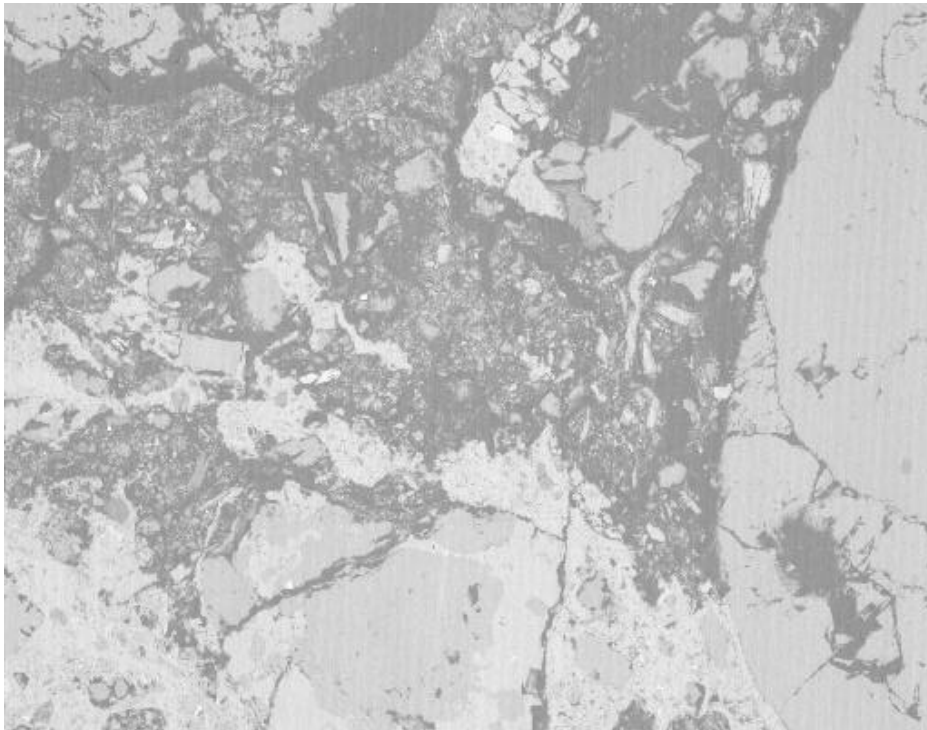
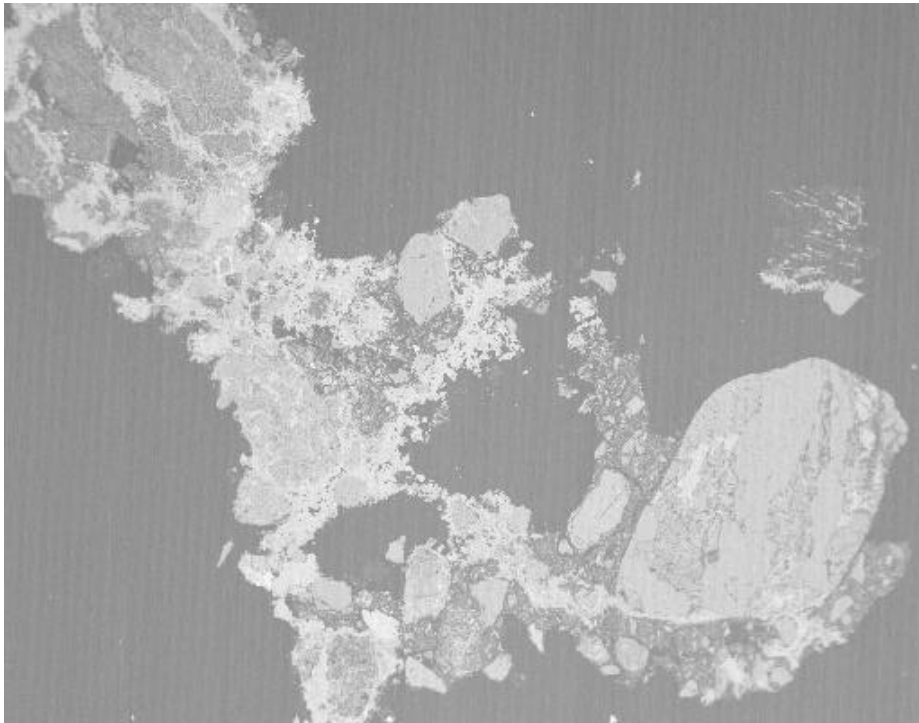


Figure 37. Specimen J at 3 mm (upper) and 490  $\mu\text{m}$  (lower) field widths showing a wide range of sand sizes and heterogeneous distribution of the calcium carbonate cement. This fragment appears to be a soil.

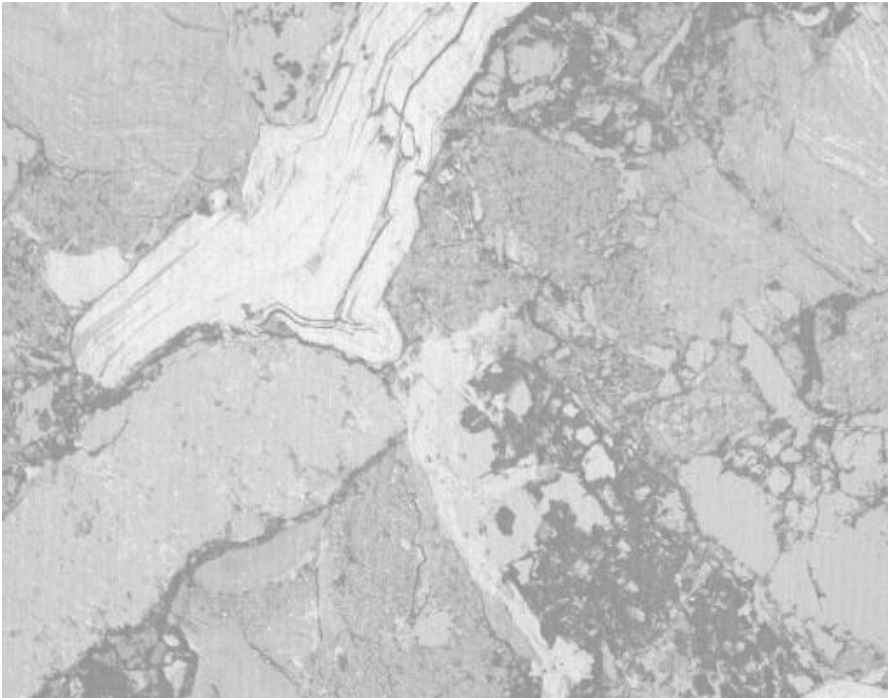
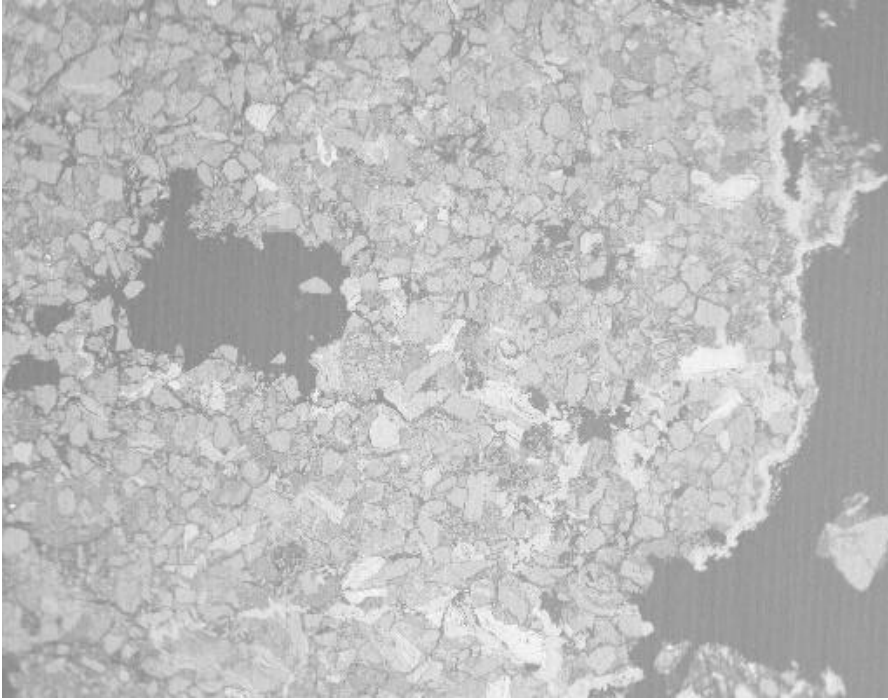


Figure 38. Specimen J fragment exhibits a more uniform sand size and a matrix similar in texture to that of the fill material and also shows evidence of the heterogeneously-distributed calcium carbonate. Upper image 3 mm and lower image 490  $\mu\text{m}$  field width.

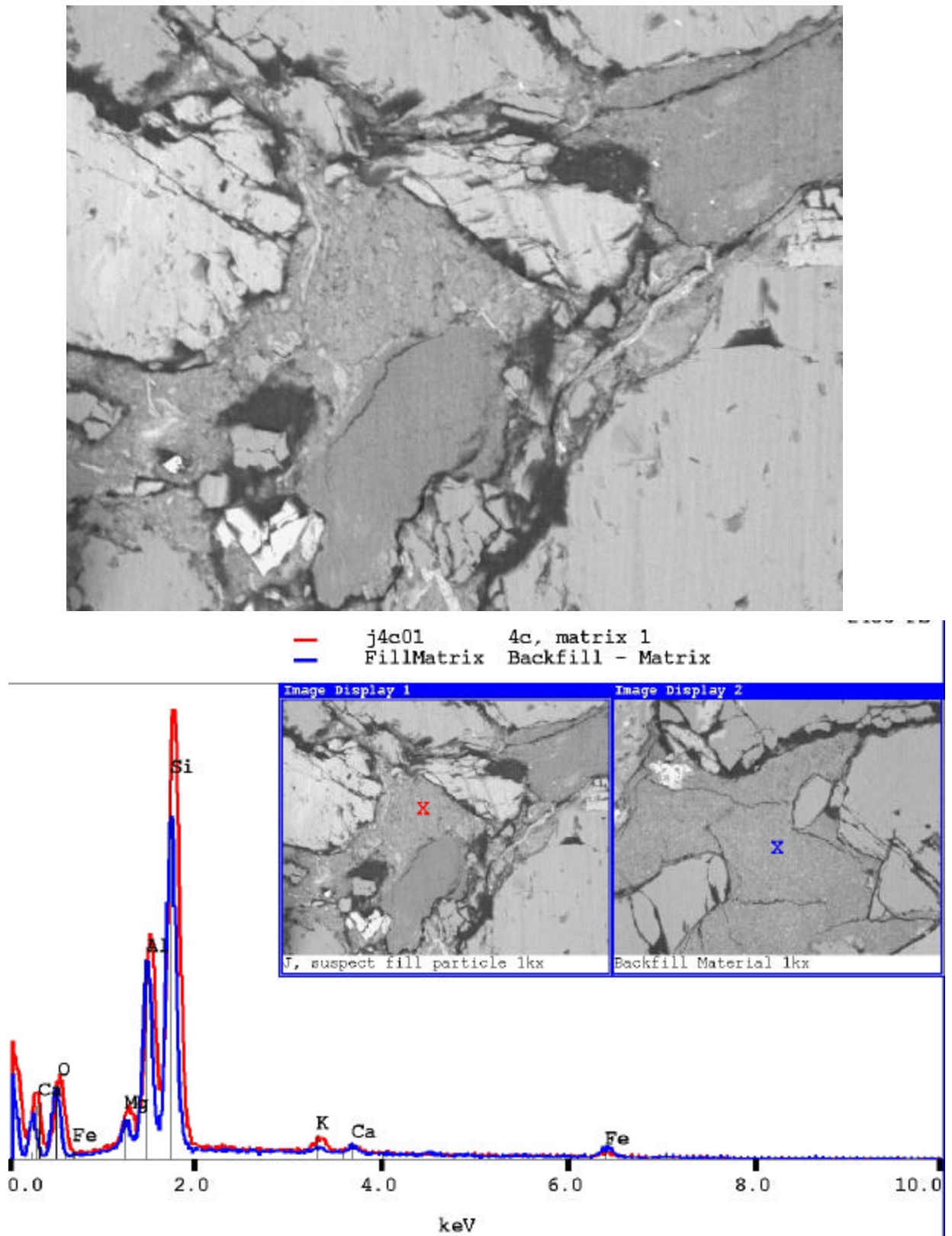


Figure 39. SEM image (upper, 150  $\mu\text{m}$  field width) shows a uniformity and texture of the matrix similar to that of the backfill. Spot EDS spectra from specimen J (left image, red spectra), and backfill (right image, blue spectra) appear similar as well.



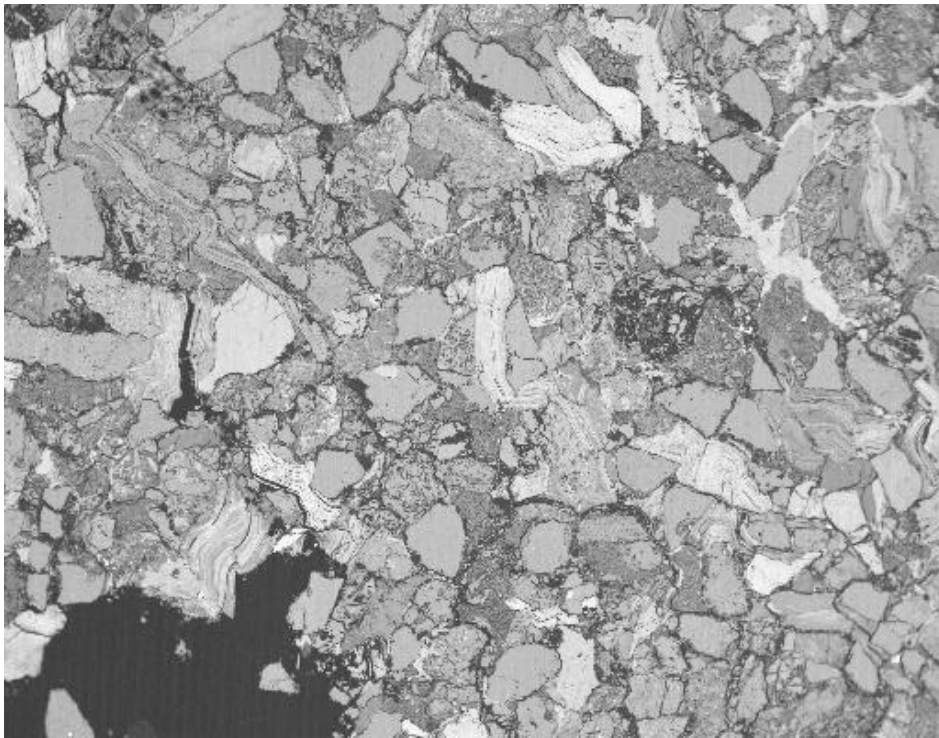
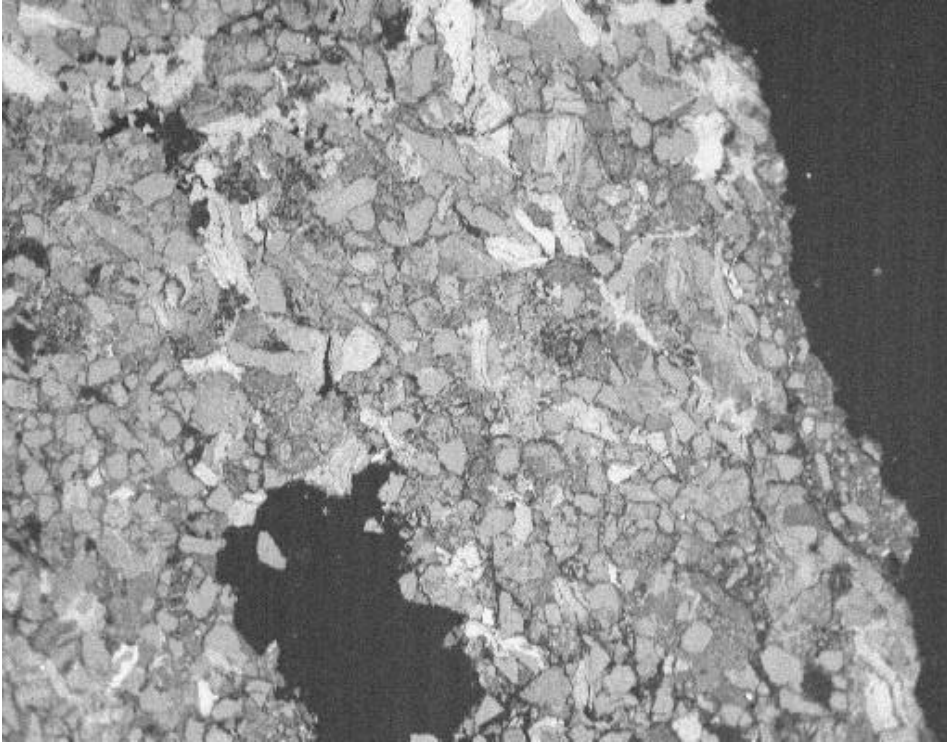


Figure 40. Specimen J fragment II showing a microstructure similar to that of the backfill material. Uniform sand size and matrix appear similar to the backfill. Upper image 5 mm and lower image 2.5 mm field widths.

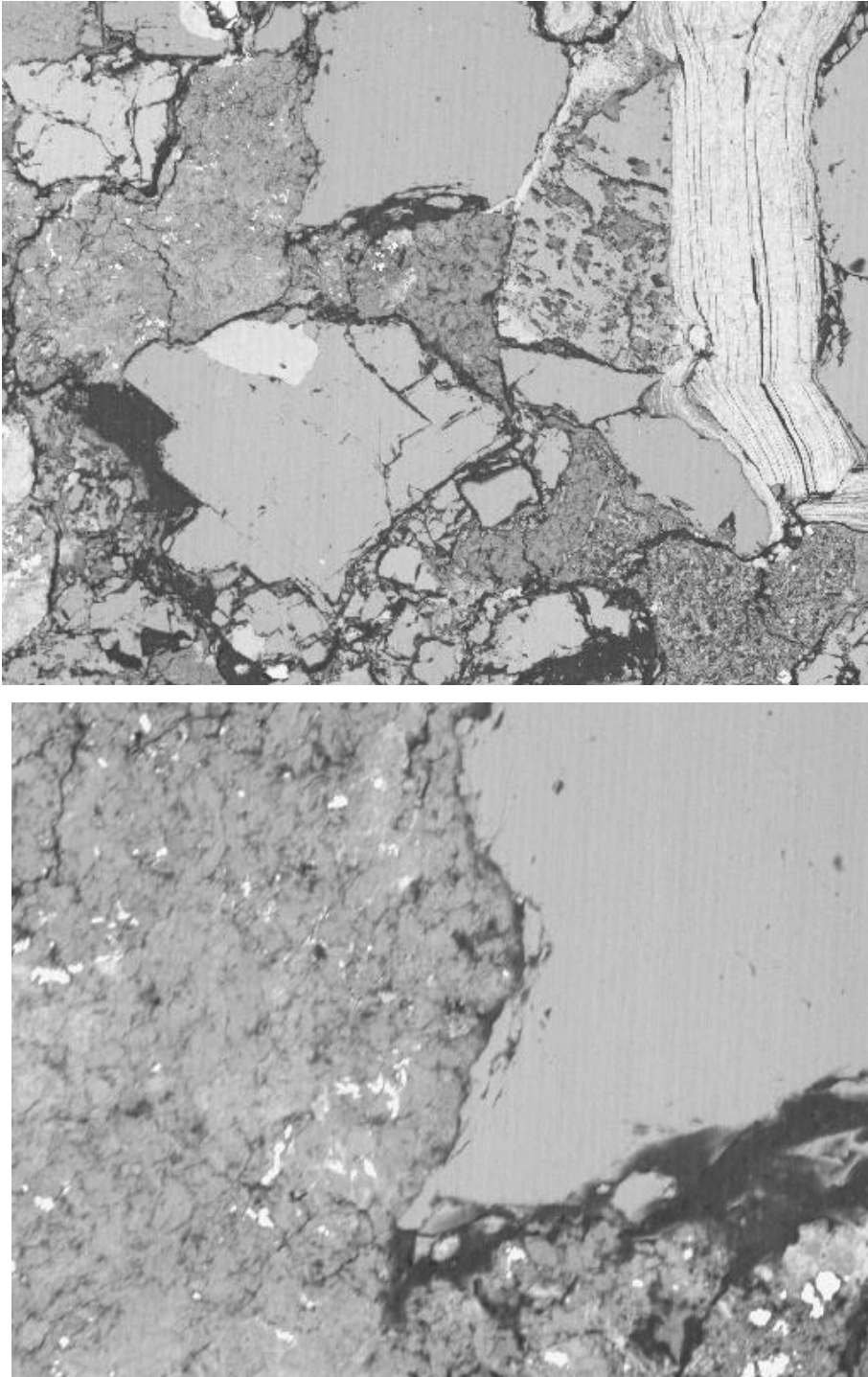


Figure 41. Fragment III of specimen J showing microstructure similar to that of the backfill material with a uniform-textured matrix. Upper image 490  $\mu\text{m}$  and lower image 150  $\mu\text{m}$  field widths.

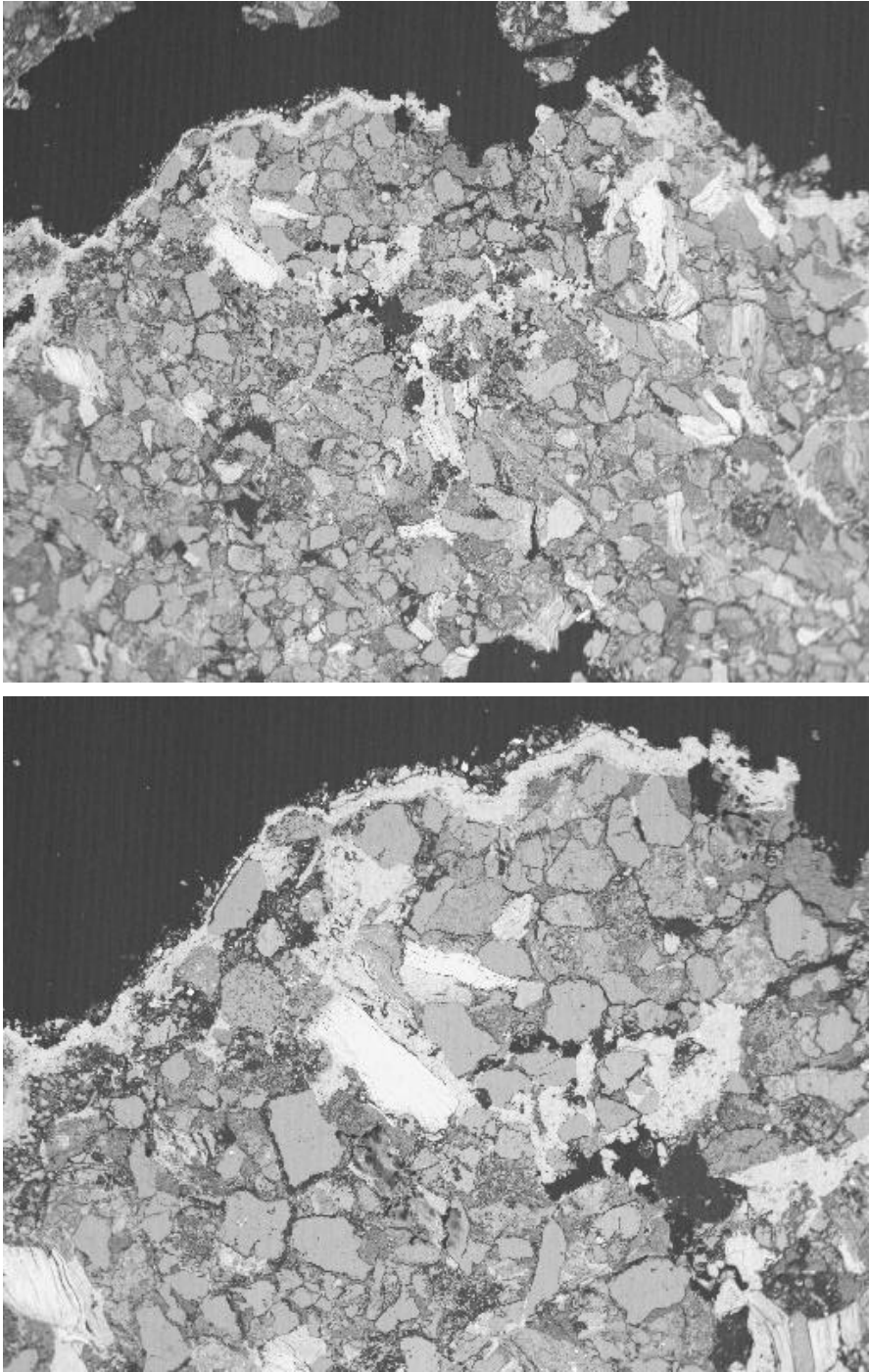


Figure 42. Specimen J exhibiting a microstructure similar to that of the backfill and also a band of secondary calcium carbonate around part of its perimeter and irregularly distributed within the fragment matrix. Upper image 5 mm and lower image 2.5 mm field widths.

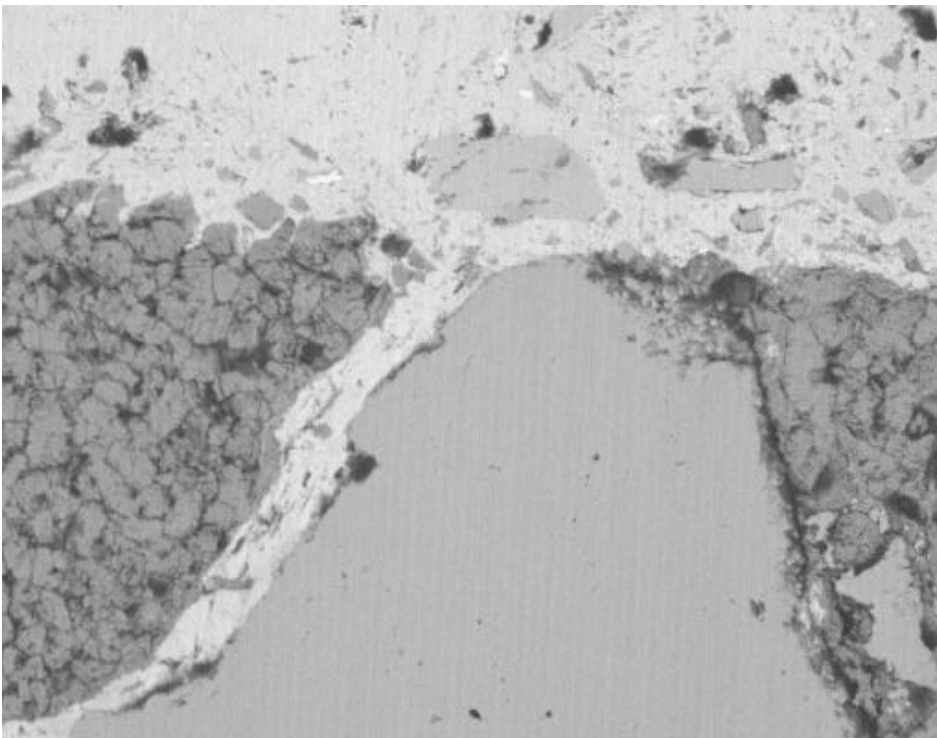
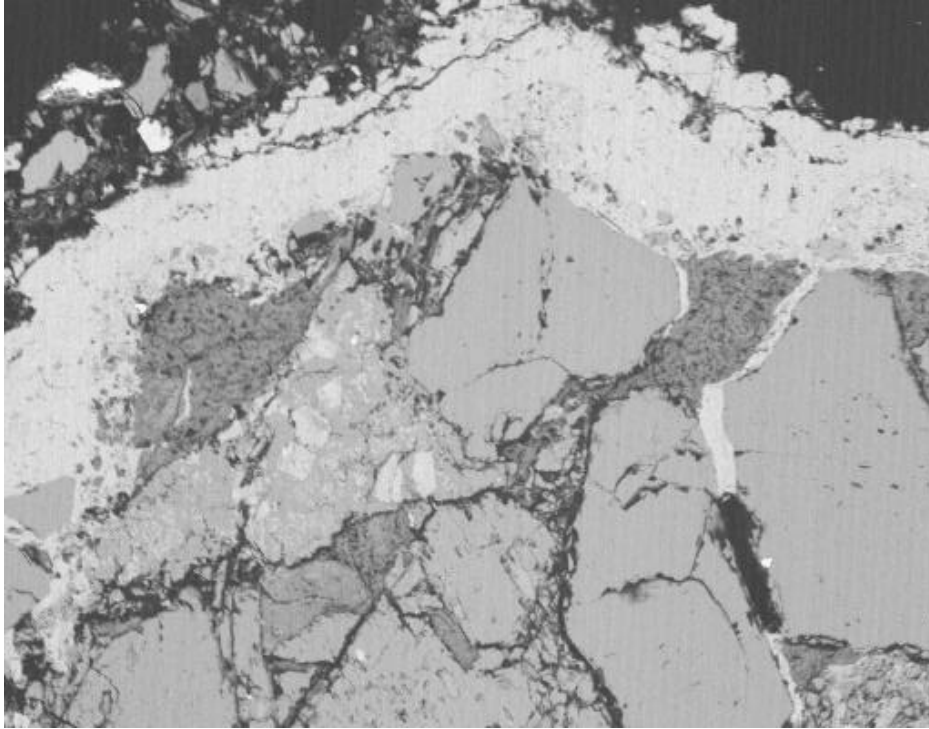


Figure 43. High-magnification SEM images of specimen J showing the calcite cement around the edge and the uniform-textured matrix. This texture is similar to that of the backfill material. Upper image 490  $\mu\text{m}$  and lower image 150  $\mu\text{m}$  field widths.

## 7.0 Summary

The NTSB provided a set of specimens, that had been adhered to a section of 40.6 cm gasoline pipeline, for microstructure evaluation. The pipeline signs of mechanical gouging and had experienced a rupture in service. The gouges were partly filled with a partially indurated material of undetermined origin.

The following conclusions were made after the laboratory examination:

1. The materials removed from the pipe are not portland cement-based materials. They do not exhibit compositional or microstructural features typical of a portland cement paste, mortar, or concrete.
2. The specimens removed from the pipe appear to be comprised of soil containing sandy mono- and poly-mineralic grains, clay, and mica cemented by calcium carbonate that appears to be in the form of the mineral calcite. This form of cementation appears to be natural resulting from the precipitation of calcium carbonate. The calcite is irregularly distributed with some regions extensively filled and some containing only isolated masses. Iron-bearing minerals were common in the extensively cemented areas and appear to be either corrosion products from the pipe, the natural mineral pyrite, or a deterioration product of pyrite, melanterite.
3. Specimens I and J contain some fragments with textures similar to those observed in the backfill specimen. The uniform sand size distribution and homogeneous matrix appear similar for some of the fragments within these specimens.
4. The backfill material contains a well-graded sand and dense, uniform clay matrix. These features make this specimen unique from the others examined in this study,

The microstructure of the concrete samples contains a portland cement paste comprised of calcium-silicate-hydrate gel, calcium hydroxide, ettringite, and residual cement grains comprised primarily of calcium aluminoferrite, or  $\text{Ca}_2(\text{Fe,Al})_2\text{O}_5$ . These phases are typically found in concrete pastes and serve as indicators of the presence of a portland cement-based material. In addition, an entrained air-void system is present and is unique to this subset of specimens. The air void system is a mass of bubbles ranging in size from about 1 mm to about 10  $\mu\text{m}$  that serves to protect the concrete from freeze-thaw cycling damage and improve the flow properties of the plastic concrete. None of these microstructural features were observed in any of the other specimens.

## Appendix A. Imaging and X-ray Microanalysis of Selected Specimens Backfill, I, and J

A second examination of selected specimens was requested by NTSB staff to collect additional images of specimens I and J to better be able to classify fragments as being soil, backfill, or other. The examination continued with Mr. Frank Zakar present on 27-April, 2001. The following image sets and comments are from that examination.

### Backfill material

The backfill material appears to be composed of medium-grained sand with a fine-grained matrix (Fig. 44, 45). The matrix appears different from the other specimens being very uniform and fine-grained with a foliated (layered) texture. This matrix appears to be a mixture of clay minerals, or clays and micas as the texture of platy minerals is visible in the microscope. The spot X-ray microanalysis (EDS) spectra indicates a magnesium- aluminum-silicate composition (Fig. 46). This is in keeping with the XRD observation of the fines of the backfill being predominantly clays such as chlorite and kaolinite. The texture and relative EDS peak intensities will be used to determine if a fragment is consistent, is similar, or is not consistent with the backfill material. The four images below were taken from arbitrarily selected fields (1.2 mm field width) and show the relative uniformity of the microstructure.

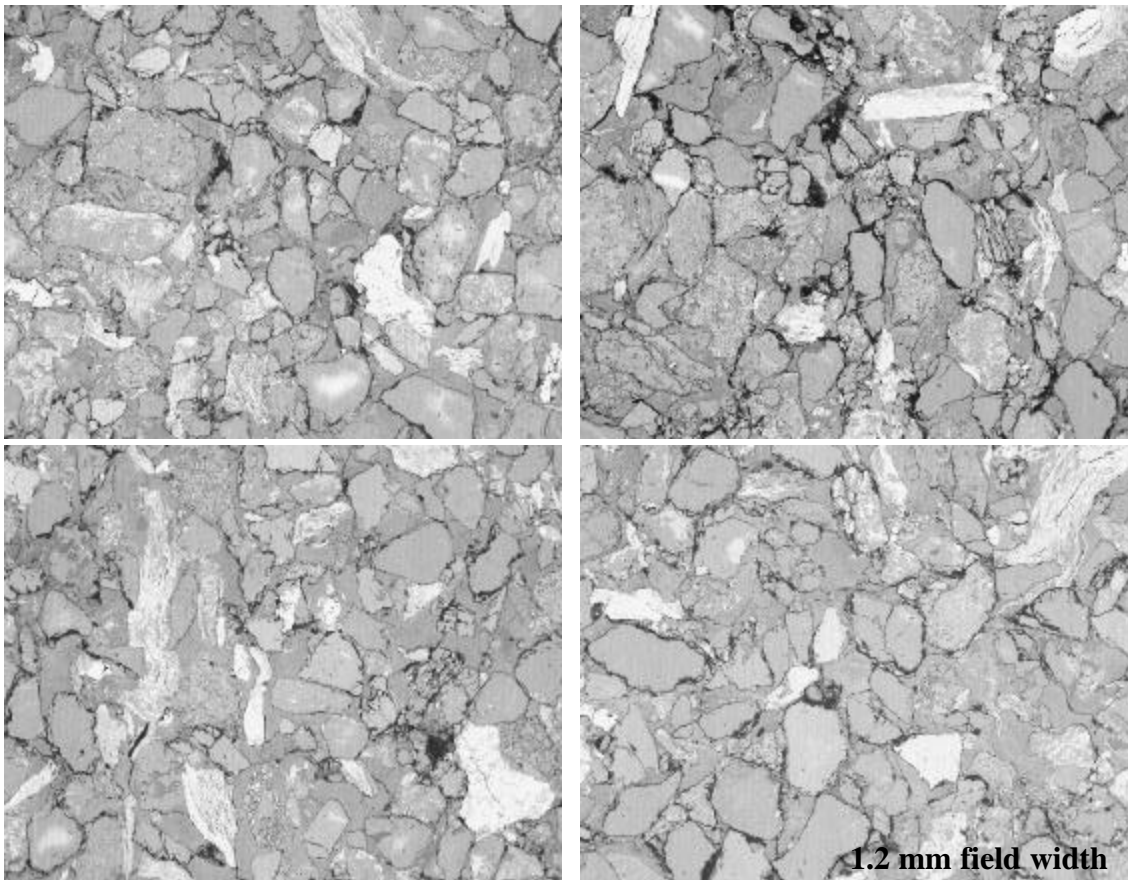
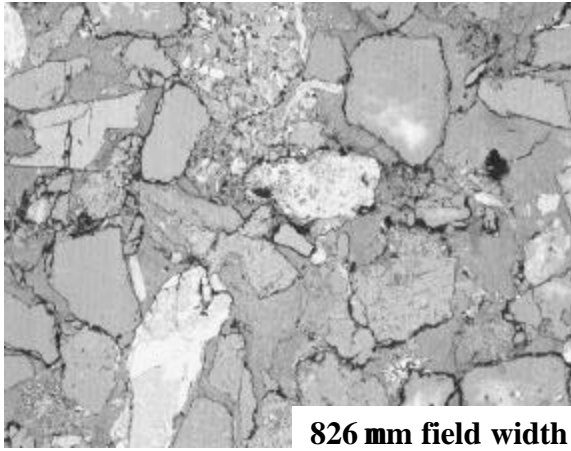
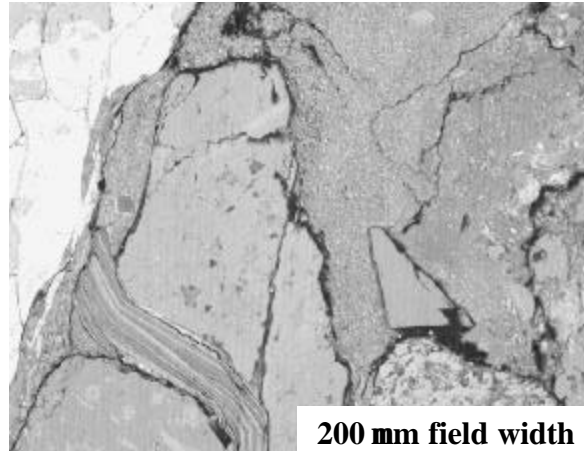


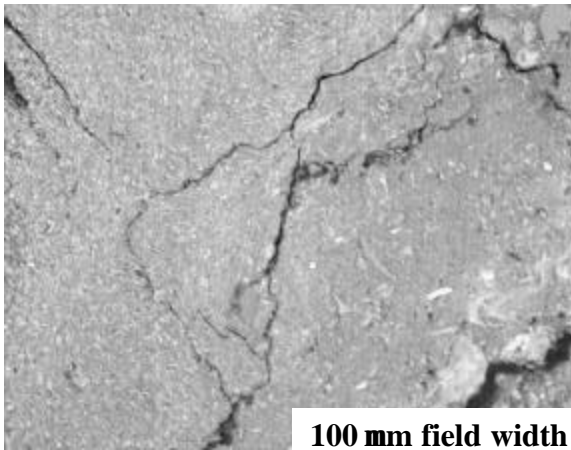
Figure 44. Four separate, arbitrarily-selected fields of the backfill microstructure at 1.2 mm field width each show the uniformity of the sand and matrix.



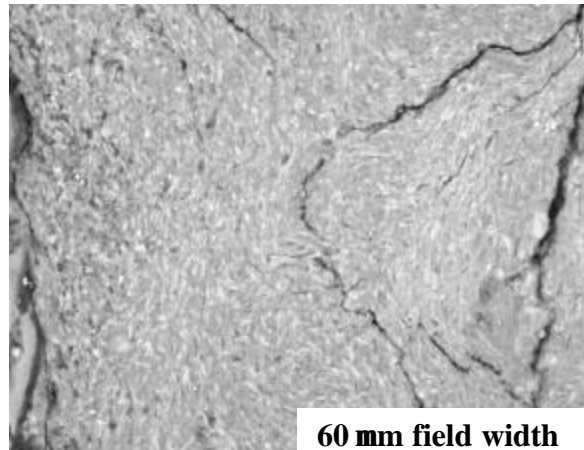
**826 mm field width**



**200 mm field width**



**100 mm field width**



**60 mm field width**

Figure 45. Higher magnification images of the matrix show the uniform-texture and the cracking both features that serve to distinguish the backfill from the soil specimens.

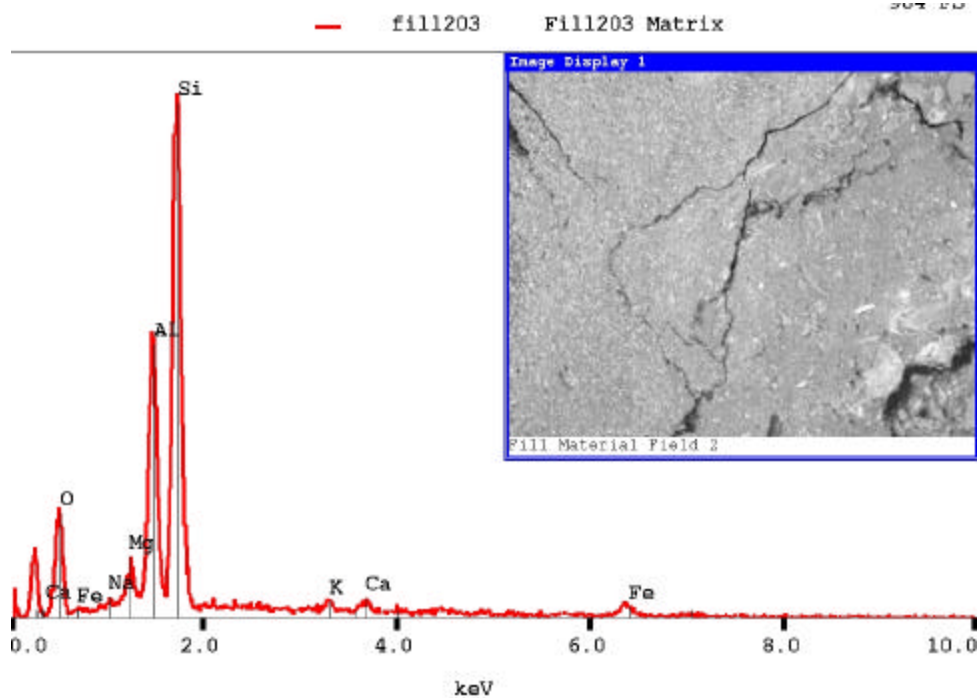
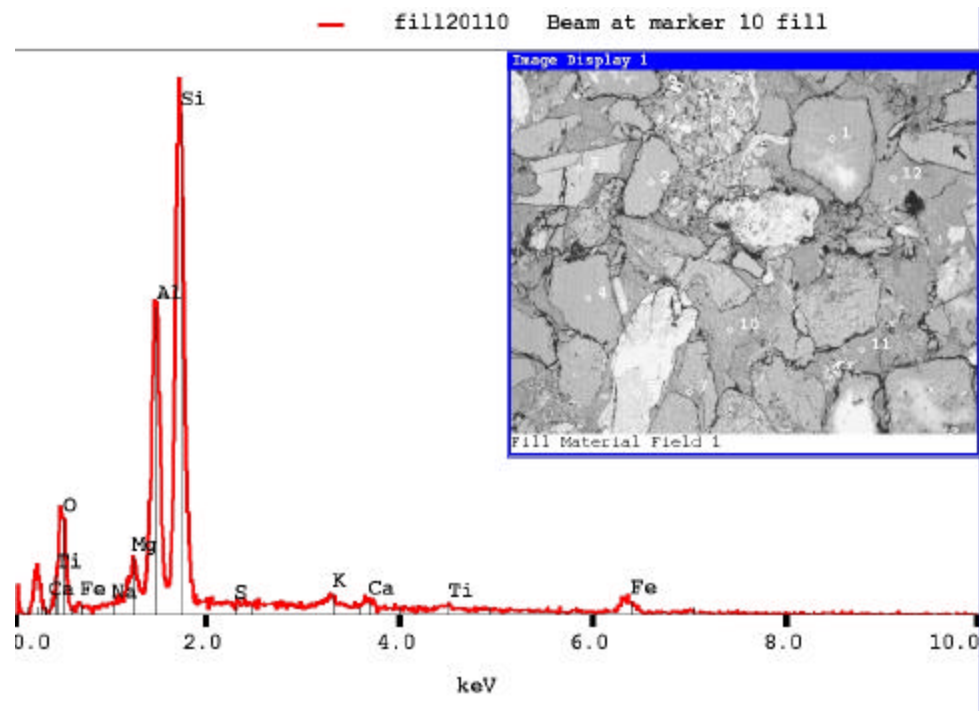


Figure 46. Spot X-ray microanalysis of the matrix indicates a magnesium - aluminum - silicate composition with minor iron, calcium, sodium, and potassium. A set of three spectra provided the following peak intensities that will be used for comparison. The ratio of the magnesium and aluminum peaks to silicon were about 0.10 and 0.57, respectively. The values of the replicate spectra were Mg : 0.11, 0.09, 0.11 and Al: 0.57, 0.56, and 0.59.



## Specimens I and J

Figures 47 through 50 show individual fragments from specimen I. These fragments exhibit a medium-grained, multi-phase matrix with heterogeneous calcite cement as well as large shale grains. Figure 49 however, shows a grain with a texture similar to that of the backfill. In this fragment, the textures are more heterogeneous than the backfill with both a clay-rich (Figure 49 B,C) and a highly porous (Figure 49 D,E) matrix as well as a calcite cement similar in texture as found in the soil. The two distinct textures suggest that this fragment may be a composite of the backfill and soil. Figure 49 F shows a details of the fine-grained matrix that exhibits a texture consistent with that of the backfill matrix. Spot X-ray analysis shows a chemical composition consistent with that of the backfill matrix (Figure 50). These data suggest that this fragment is consistent with the backfill specimen.

Specimen J is presented in Figures 51-54. In Figure 51, fragments of J appear consistent with the soil because of their porous nature, heterogeneous calcite cement, and multi-phase sand grains. Figure 52 shows a fragment that appears similar to the backfill but exhibits a matrix texture distinct from the backfill in that it is less uniform. Spot X-ray microanalysis (Figure 54) is different as it lacks magnesium, has a stronger aluminum and weaker silicon peak intensities. This fragment is similar to the backfill but, not consistent with the backfill. Another fragment, shown in Figure 53, exhibits a texture and chemical composition (Figure 54) consistent with the backfill material.

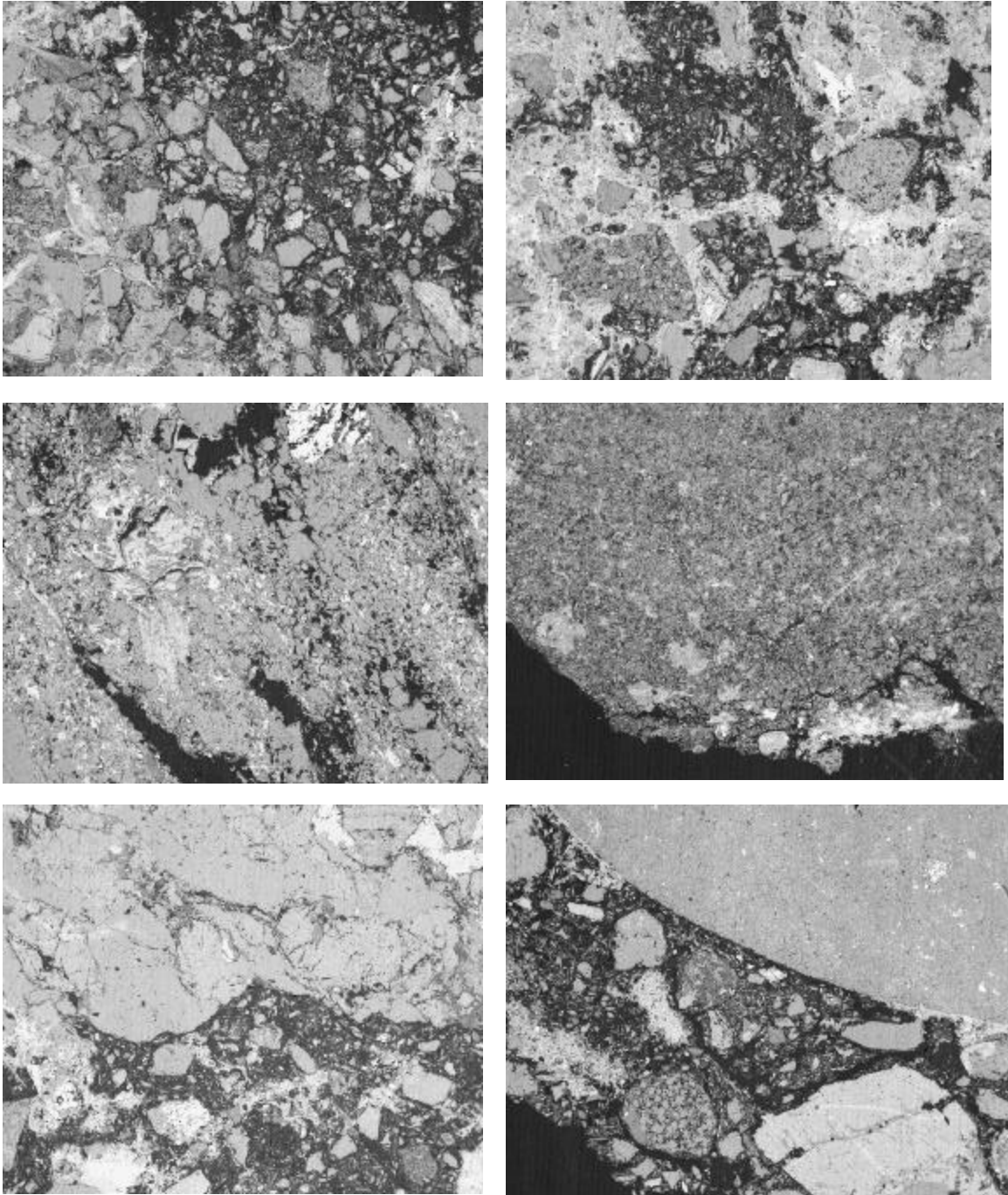


Figure 47. Fragments from specimen I in images appear consistent with the soil.  
Image field widths: 1.2 mm.

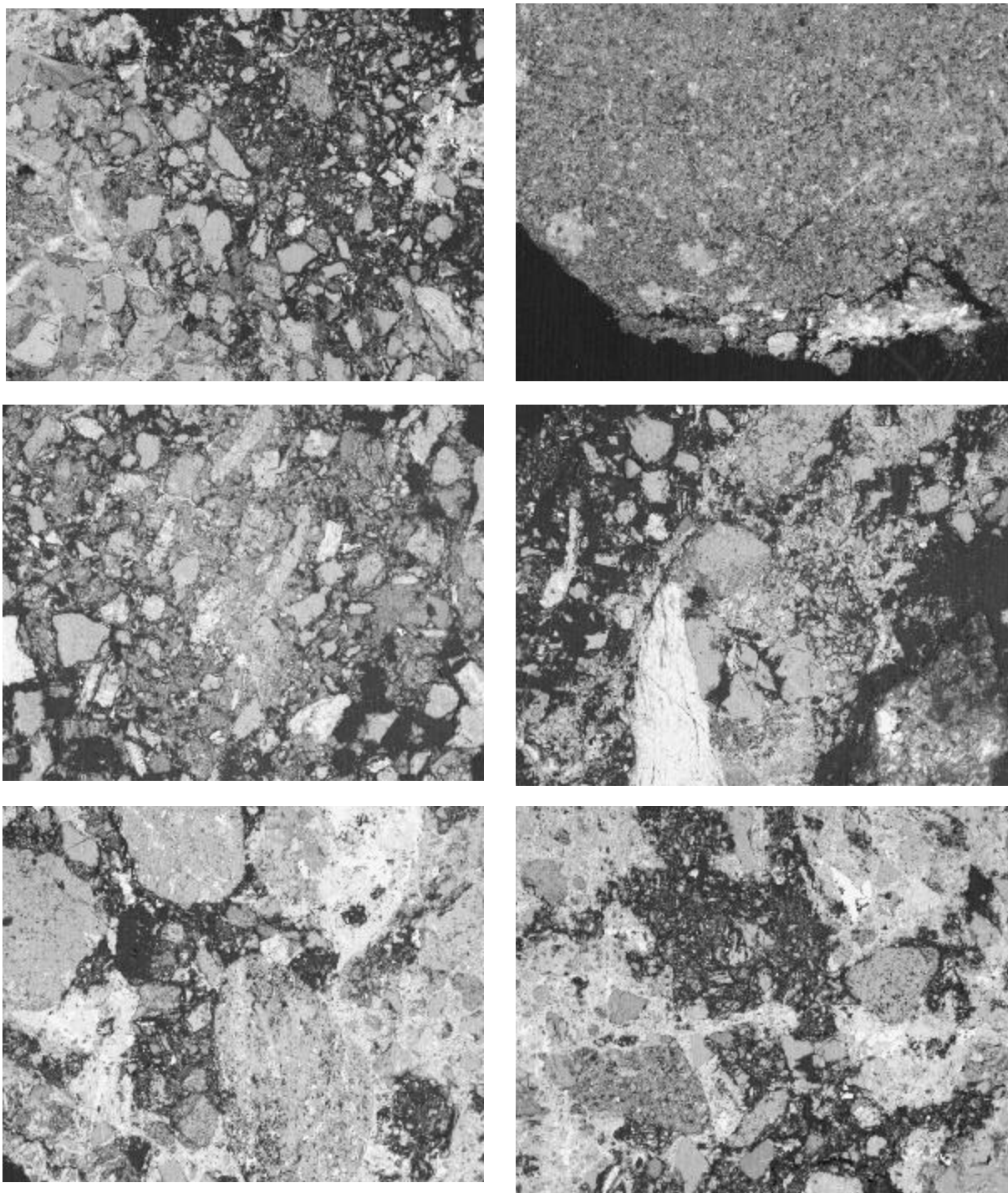
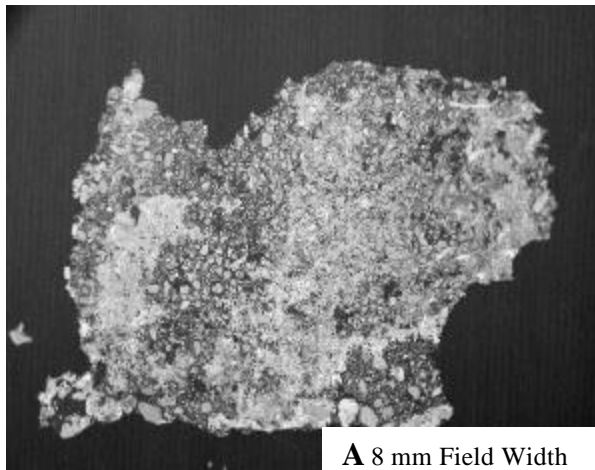
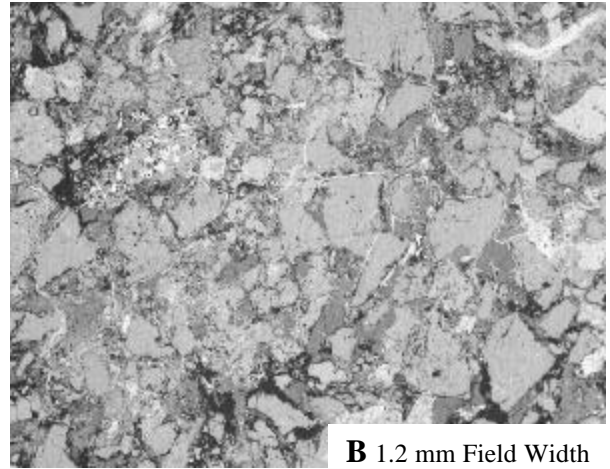


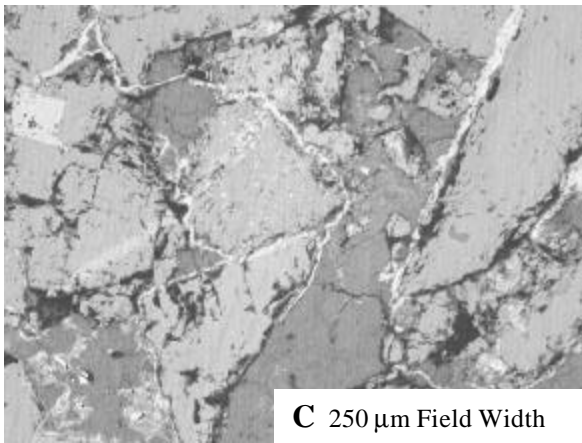
Figure 48. Additional fragments from specimen I appear consistent with the soil.  
Image field width: 1.2 mm.



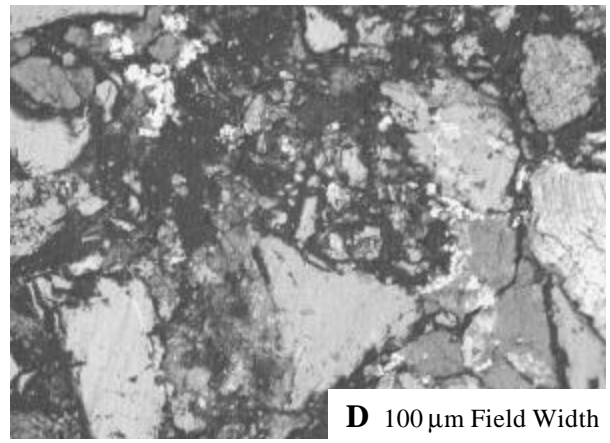
**A** 8 mm Field Width



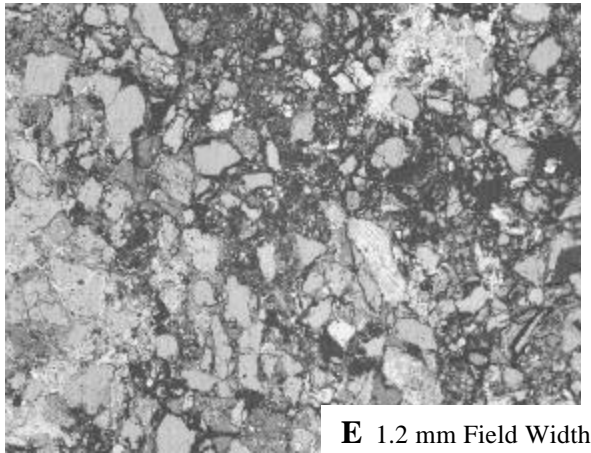
**B** 1.2 mm Field Width



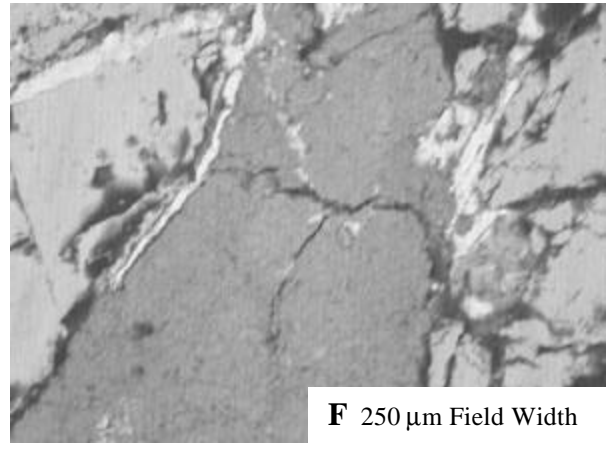
**C** 250  $\mu\text{m}$  Field Width



**D** 100  $\mu\text{m}$  Field Width



**E** 1.2 mm Field Width



**F** 250  $\mu\text{m}$  Field Width

Figure 49. Fragment 15 of Specimen I appears consistent with the backfill. Part of the fragment (images A, B, C and F) exhibits the same matrix homogeneity and cracking, as well as the chemical signature that is consistent with that of the backfill. There does appear to be some calcite cement, similar to that found in the soils. Images D and E from the other side of the fragment have more porous regions that appear consistent with the soil.

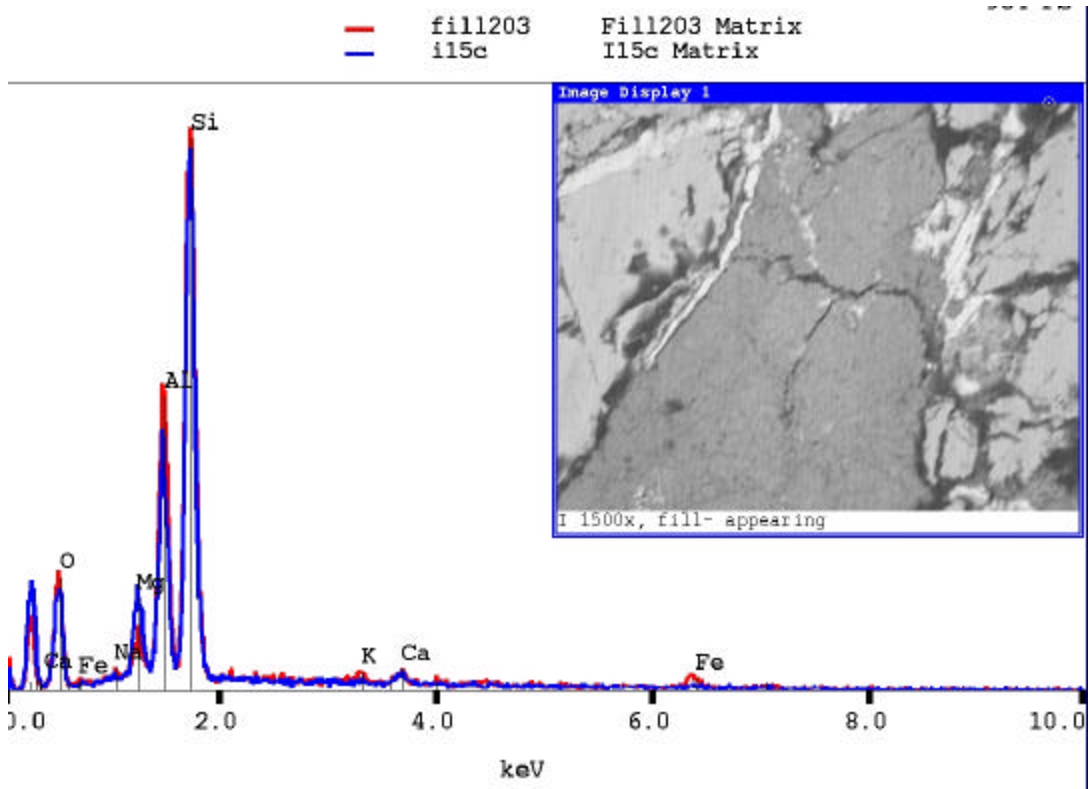


Figure 50. Comparison of the x-ray microanalysis spectra of I-15 matrix (blue) to that of the backfill material matrix (red) illustrates the similarity in composition.

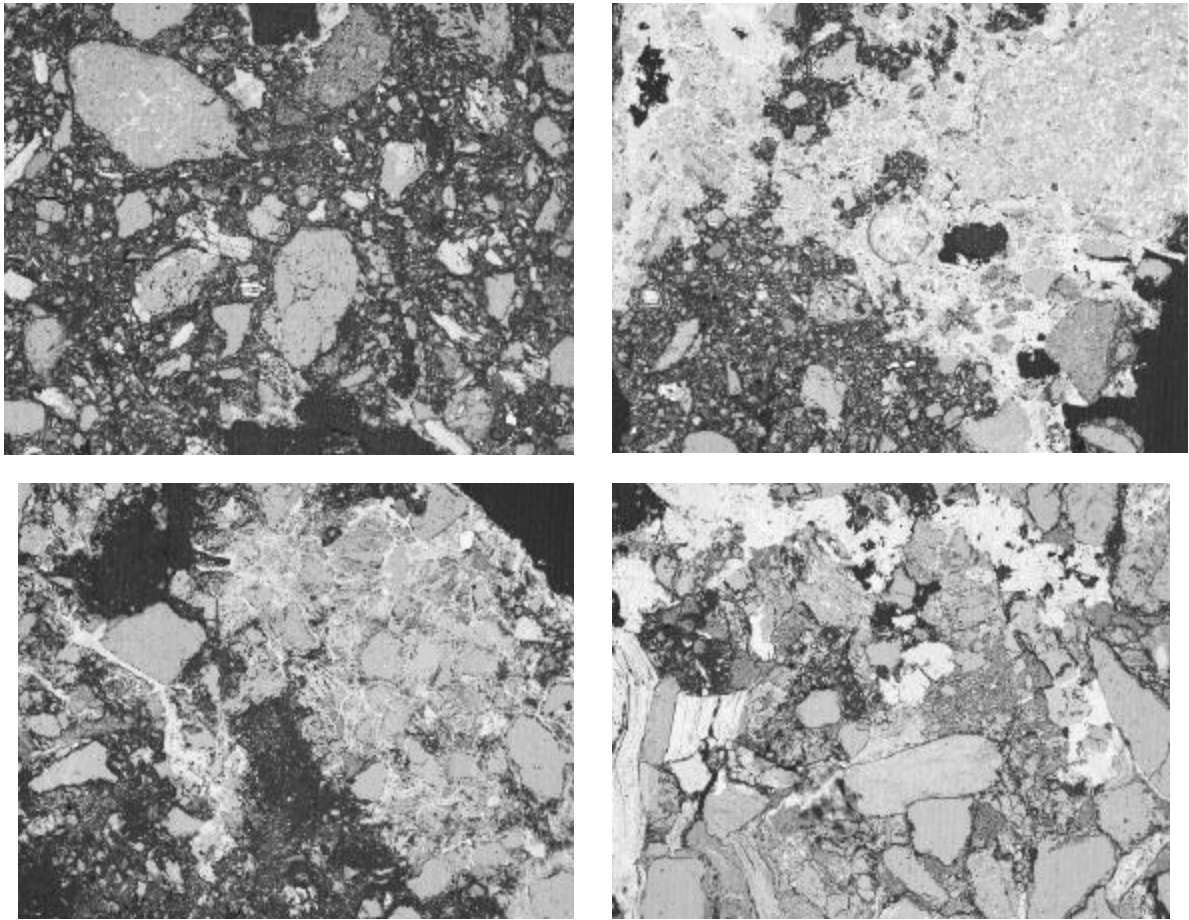


Figure 51. Specimen J fragments 1 - 4 appear to be consistent with the soil as they have a porous matrix and calcite cement.

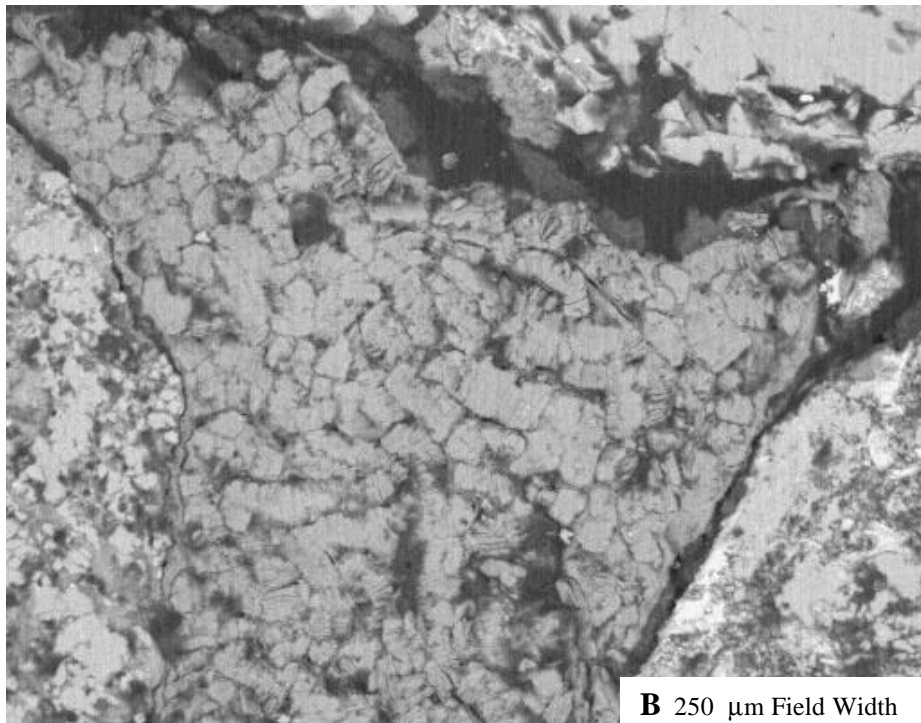
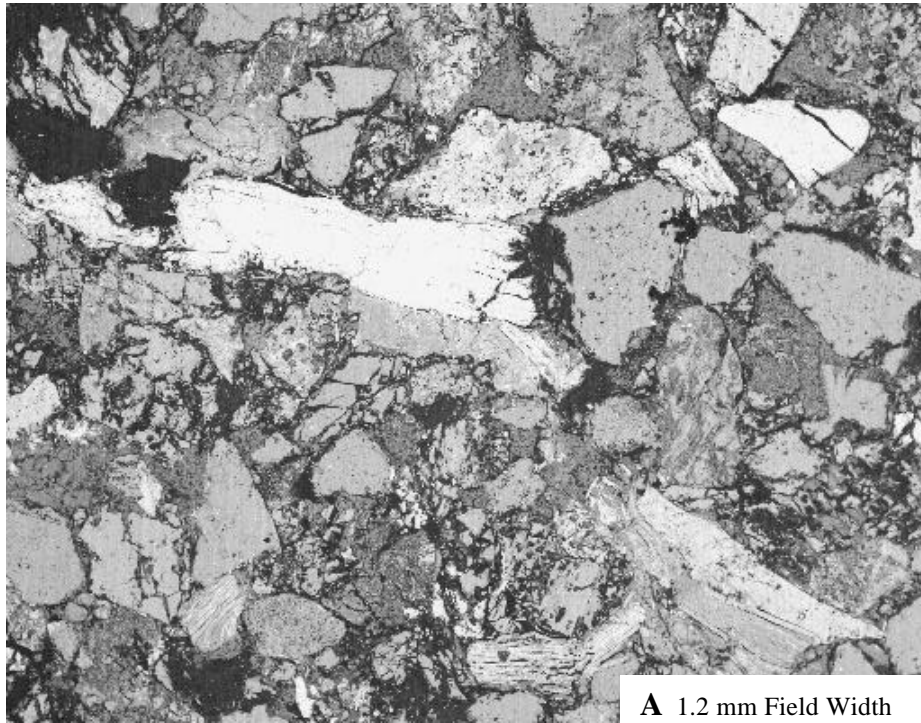
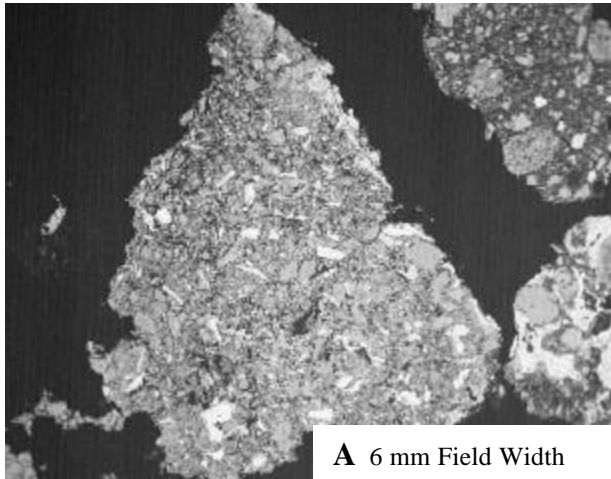
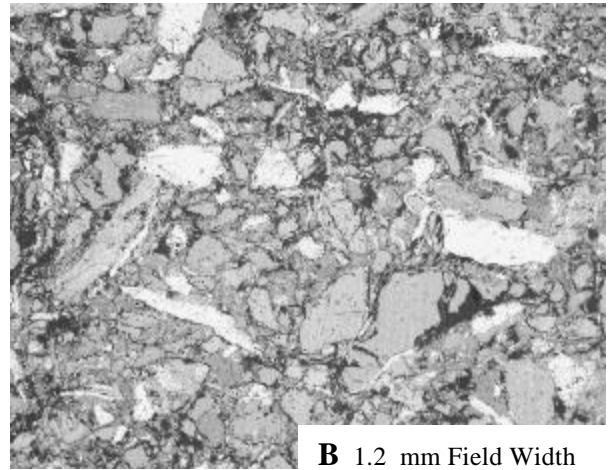


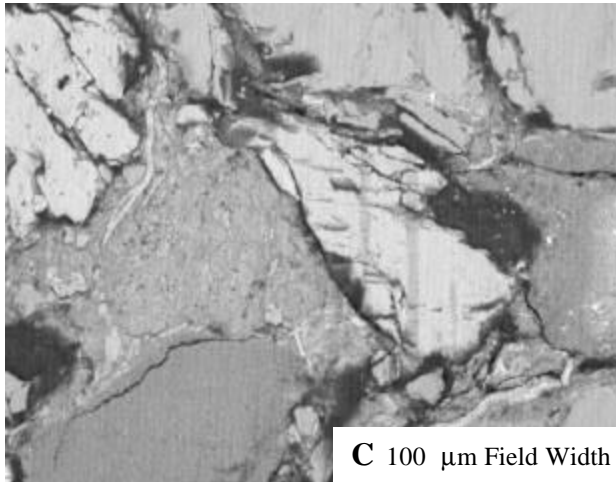
Figure 52. Specimen J fragment 7 appears similar to that of the backfill but the matrix texture and chemical composition are different.



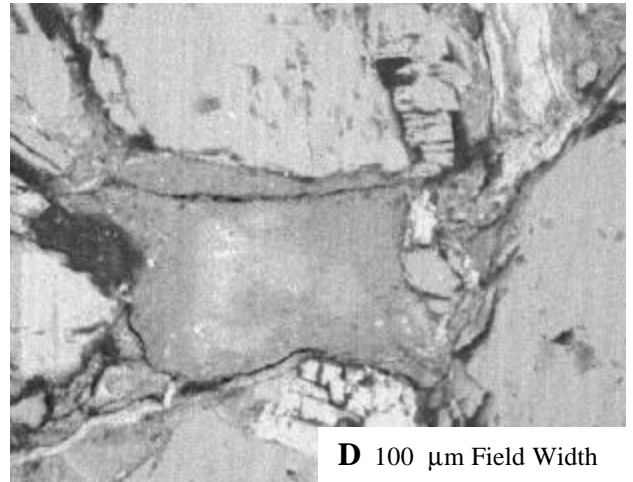
**A** 6 mm Field Width



**B** 1.2 mm Field Width



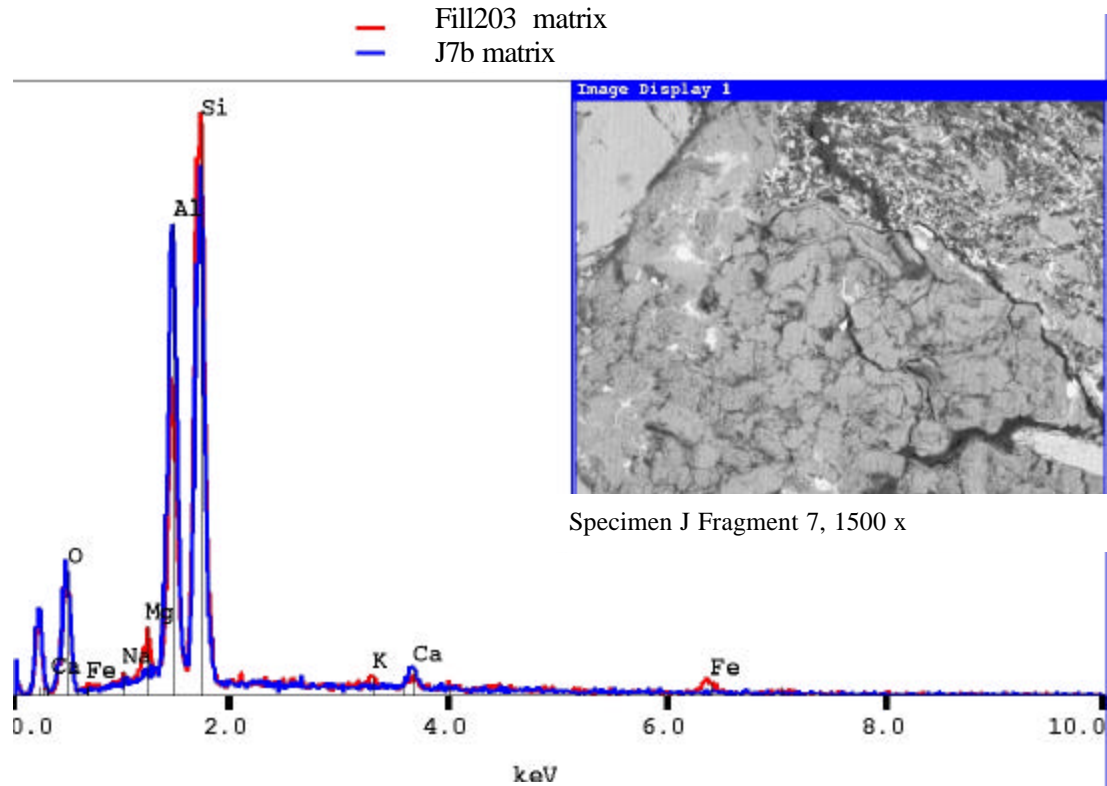
**C** 100  $\mu\text{m}$  Field Width



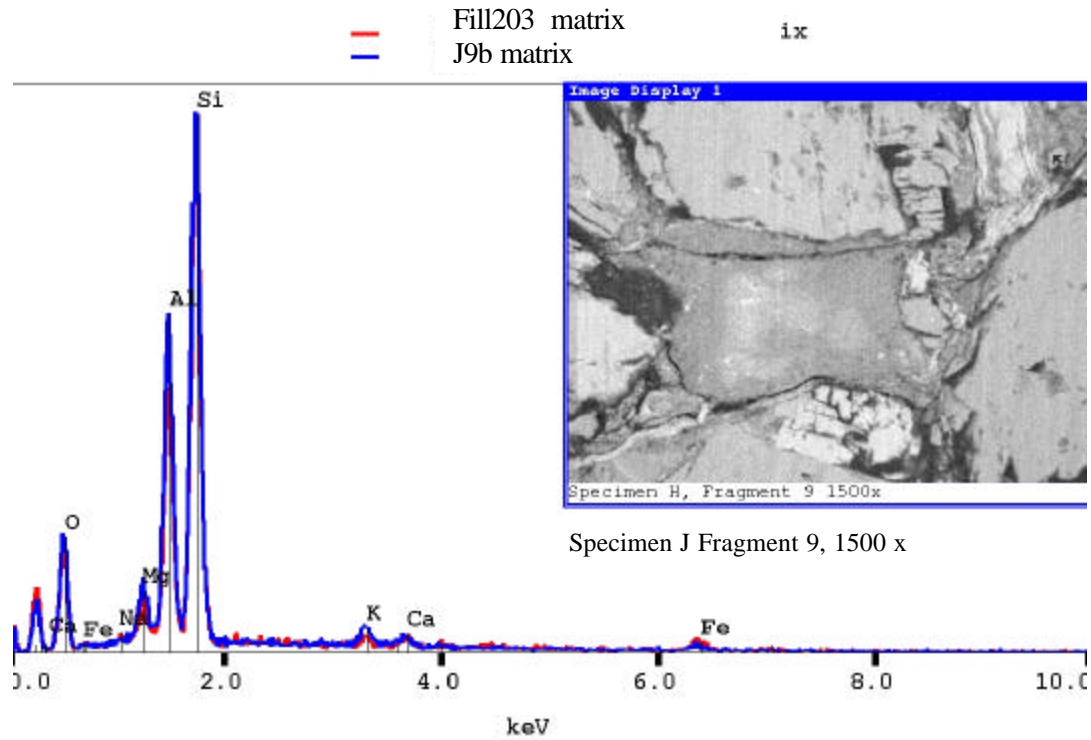
**D** 100  $\mu\text{m}$  Field Width

Figure 53. Specimen J, fragment 9 is consistent with the backfill with respect to matrix texture and spot X-ray microanalysis composition.





**A**



**B**

Figure 54. Image texture and spot X-ray microanalysis of the matrix material from specimen J (blue) plotted against that from the backfill material matrix (red). Fragment 7 matrix (A) is not consistent, while fragment 9 (B) appears consistent with the backfill material with respect to texture and chemical composition (test field width 1.2 mm).

---

<sup>1</sup> H.F.W. Taylor, Cement Chemistry, 2nd Edition, Thomas Telford, London 459 pp. 1997

<sup>2</sup> P.E. Stutzman and J.R. Clifton, "Specimen Preparation for Scanning Electron Microscopy," in Proc. of the 21st Internat. Conf. On Cement Microscopy, PP. 10-22, ICMA, Duncanville, Texas, April, 1999.

<sup>3</sup> C. Klein and C.S. Hurlbut, Manual of Mineralogy after J.D. Dana, 20th Ed., 1977